ABSTRACT

Title of dissertation: An Analysis of the Stability, Aggregation Propensity, and Negative Cooperativity of the *Escherichia coli* Chaperonin GroEL

                         Sarah Christine Wehri, Doctor of Philosophy 2013

Dissertation directed by: Professor George H. Lorimer
                            Department of Biochemistry

Since the discovery of chaperonin GroEL and co-chaperonin GroES, there has been a deluge of literature investigating many aspects of the system. Substrate proteins are protected from aggregation through a cycle of capture, encapsulation, and release made possible through rigid body motions of the GroE system driven by a combination of allosteric controls influenced by nucleotide, potassium and denatured protein termed substrate protein (SP). This dissertation first explores the sequential transition of GroEL that maintains the rings operating in an alternating fashion. To do this, an intra-subunit, inter-domain mutant, GroEL$_{D83A}$, was created that lacks the salt-bridge that stabilizes the **T** state. Steady state ATPase assays, stopped-flow fluorescence, and gel filtration chromatography were all used to demonstrate that the *trans* ring must access the **T** state before ligands can be discharged from the *cis* ring.

The dual-heptameric ring structure of GroEL and the post-translational assembly of the protein make creating mutants with a mutation within a single subunit of a ring almost impossible, however the ability to do so opens the opportunity for a myriad of

experiments that explore the allosteric transitions of GroEL. Two potential recombination methods, acetone treatment and heat treatment, were investigated. Förster resonance energy transfer (FRET) and electrospray ionization mass spectrometry (ESI-MS) were used to study recombination facilitated by such treatments. Recombination using the acetone method resulted in a one-in-one-out subunit exchange, however aggregation complicated the exchange. Heat treatment resulted in exchange of rings.

Finally, dynamic light scattering (DLS) was used to investigate stability and aggregation on the chaperonin. It was observed that the chaperonin is stable for over 30 days while incubated continuously at 37°C in sterile buffered solution, however interesting aggregation kinetics are observed upon addition of acetone, the solvent used to strip SP from GroEL during the standard lab purification procedure. GroEL partitions into 10nm and 100nm species that are extremely stable before the appearance of macromolecular aggregates and precipitation is observed.

An Analysis of the Stability, Aggregation Propensity, and Negative

Cooperativity of the *Escherichia coli* Chaperonin GroEL

by

Sarah Christine Wehri

Dissertation submitted to the Faculty of the Graduate School of the
University of Maryland, College Park, in partial fulfillment
of the requirements for the degree of
Doctor of Philosophy
2013

Advisory Committee:
Professor George H. Lorimer, Chair
Professor Devarajan Thirumalai
Professor Nicole LaRonde-LeBlanc
Professor David Fushman
Professor Richard Stewart

Acknowledgements

Many people have had a part in making this dissertation a reality. I extend many heartfelt thanks to the following individuals…

Dr. George Lorimer, my dissertation advisor, for his continued support, patience, and above all, enthusiasm even during some seemingly bleak moments in the lab.

My committee for the time they invested to critically read and comment on this dissertation.

My collaborators, Rinat Abzalimov and Igor Kaltashov of University of Massachusetts, Amhurst, for sharing their expertise in electrospray ionization mass spectrometry. Thank you for taking an interest in GroEL, your continued hard work, optimism, and seeing the project through to the end.

My collaborators, Kirtland Linegar and Mikhail Anisimov of University of Maryland, College Park, for investing so much time and unwavering effort in dynamic light scattering experiments. Dr. Anisimov has been a true supporter and motivator; I consider myself lucky to count him as a friend.

Paulette Frazier for making life in the Biomolecular Science Building just a little more bearable. She is one of the most peaceful, happy, and supportive people I have ever met, not to mention competent and always ready to listen.

My lab mates, Asha Acharya, Yu Yang, Nitya Shivaprasad, and Elena Jouravleva for their company, collaboration, support, creativity, and most of all friendship. I am so

Contents

Figures

LIST OF ABBREVIATIONS

α-lac	α-lactalbumin, bovine isolate
ADP	Adinosine Diphosphate
ATP	Adinosine Triphosphate
DLS	Dynamic Light Scattering
ESI-MS	Electrospray ionization mass spectrometry
FRET	Fluorescence resonance energy transfer
	or Förster resonance energy transfer
$GroEL^D$	Fluorescent donor labeled GroEL
$GroEL_{IAX}$	GroEL mutant with intra-subunit salt-bridge D83/K327 changed to Cysteine
$GroEL_{IRX}$	GroEL mutant with inter-subunit salt-bridge R197/E386 changed to Cysteine
$GroEL^A$	Fluorescent acceptor labeled GroES
GroES*	GroES fluorescently labeled at residue 98
LDH	Lactate dehydrogenase
NADH	Nicotinamide Adinine Dinucleotide
PBP	Phosphate binding protein
PCR	Polymerase Chain Reaction
PEP	Phosphoenol pyruvate
PK	Pyruvate kinase
R_h	Hydrodynamic Radius
SP	Substrate protein
TIRFM	Total internal reflection fluorescence microscopy

Chapter 1: An Introduction to GroEL

1.1: What is the GroE system structurally and functionally?

At the most basic biological level, GroEL is a protein: a molecule composed of amino acid building blocks that together accomplish some function in a cell. It is classified as a chaperonin: a protein that assists nonnative proteins into functional folded states in an ATP dependent fashion. Chaperonins are divided into type I and type II varieties. Type I chaperonins are found in bacterial cytoplasm as well as eukaryotic cellular organelles thought to be evolutionarily derived from eubacteria. Type II are found in archaebateria and eukaryotic cytosol. Because GroEL is a product of *Escherichia coli*, it falls into the former category.

The two families also vary structurally. Type I chaperonins employ an independently expressed co-chaperonin to assist encapsulation of non-native protein. In the case of the GroE chaperonin system, GroEL couples with the co-chaperonin GroES to trap non-native proteins. Type II chaperonins encapsulate nonnative protein using a built-in flange as a lid; an example is the thermosome from the archea *Thermoplasma acidophilum*. (2)

GroEL is composed of two heptameric rings set back to back (Figure 1a); one could imagine two doughnuts stacked upon one another. Each ring has a central seven-fold axis of symmetry (Figure 1b). A GroEL monomer is 57 kilodaltons (kD), and composed of three structurally and functionally unique domains termed apical, intermediate, and equatorial.

The equatorial domains of each ring, colored red in the renderings below, forms an interface such that the apical domains, colored green and yellow, face out from either end toward the surrounding environment. The apical domain is mainly responsible for

binding substrate protein and GroES *via* hydrophobic regions in helices H and I (colored yellow) that line the central cavity when GroEL is in its resting state. (3)
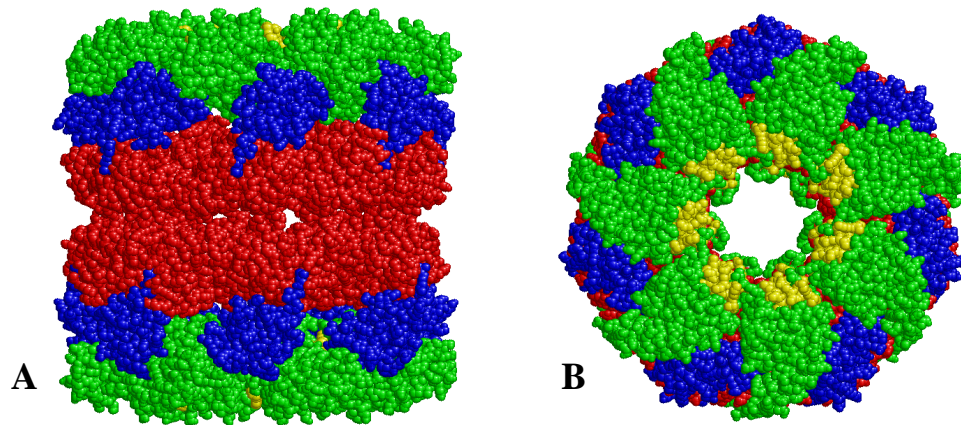
Figure 1: A spacefill model of GroEL in the resting state. A) a side view, and B) top view. Red: equatorial domain, blue: intermediate domain, green: apical domain, yellow: Helicies H and I of the apical domain responsible for binding substrate protein and GroES. Figure was created using PDB 1KP8 (4).

The intermediate domain is a connecting region between the mobile apical domain and the equatorial domain. It facilitates the rigid body motion associated with the **T** (Figure 2A) to **R'** (Figure 2B) allosteric transition. Ring expansion to the **R'** state is accomplished by the intermediate domain extending upward upon binding of ATP to the equatorial domain as shown for a visually isolated monomer in Figure 2. The structural changes, and implications thereof, will be discussed in more detail in later sections.

The equatorial domain (red region in Figure 2) is responsible for the majority of the inter-subunit and inter-ring interactions. It is composed of two helical subdomains of 4 helices each that form a pseudo dyad passing through the ATP binding site. (5) Residues involved in the binding and hydrolysis of ATP are conserved throughout GroEL homologes. (6) The secret to allosteric control of the GroE cycle is thought to lie in this

domain because it contains the ATP binding site, a K^+ binding site, and the ring-ring interface. In fact, recent structural work implicates helix M as the gate keeper to the nucleotide binding site requiring a 22° upward rotation for nucleotide to evacuate the pocket. (7) Interaction between the plates of the equatorial domains change slightly when converting between the **T** and **R'** structures. This implies a structural component is involved in the negative cooperativity of the system. This is discussed further in the following sections. (8)

A   **B**
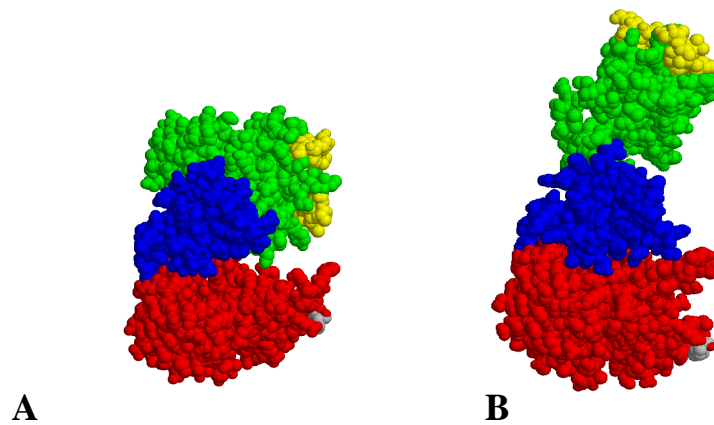
Figure 2: A monomer of GroEL in the T state (A) and the R' state (B). In B, the co-chaperonin GroES is bound but not shown. Color coding is the same as in Figure 1. Figure prepared using PDB 1AON (9).

The co-chaperonin, GroES, is a much smaller complex that serves as a lid for GroEL (Figure 3). (9) It is composed of seven identical subunits (Figure 4) with a mass of ~10 kD each; ~70 kD for the entire GroES protein. (10) There is evidence from fluorescence and equilibrium sedimentation experiments that sub-micromolar concentrations of GroES cause the monomer:heptamer equilibrium to strongly favor the monomeric state(11). The monomeric state observed in *in vitro* experiments is biologically insignificant since the cellular concentration of the GroES heptamer is ~5 μM. (12)

Residues 19-27 of GroES compose a flexible, hydrophobic mobile loop region. (13) The bullet shaped GroEL-GroES 'asymmetric complex' is formed when the mobile loops of GroES interact with the hydrophobic binding pockets that line the apical domain of GroEL. Formation of a stable asymmetric complex in the absence of SP requires four or more mobile loops to bind to GroEL. In the presence of SP, five mobile loops are required for encapsulation to occur meaning only one or two sites are available to interact with SP. (14) Once GroES is secured, the complex is committed to the hydrolysis of ATP and completion of the cycle. (15)

The two central cavities formed by the rings of GroEL serve as a hydrophilic folding environment for encapsulated substrate protein (SP). (15) Encapsulated SP is less prone to aggregation because it is contained within an infinitely dilute environment. In addition, confinement of SP reduces the total possible conformational states the protein can sample. (16) There is speculation that the many negatively charged side chains that

5

interface the folding chamber favor productive folding of the nonnative encapsulated protein by making it energetically unfavorable for hydrophobic residues to be exposed. (2) More research is required to investigate this possibility, but for substrate proteins that approach the maximum size for encapsulation within the GroEL-GroES complex, about 33Å for a molten globule protein, only one or two layers of water molecules could exist between the SP and inner wall of the chaperonin. Considering the close proximity, the character of the folding chamber may confer a distinct benefit upon SP folding. (17)

Although it appears that the central cavities of the two rings are conjoined, encapsulated SP is unable to migrate from one cavity to another. AFM tapping experiments performed on the equatorial face of the ring at ~1 nm resolution were unable to consistently resolve the expected pore into the central cavity. (18) It is proposed that the 23 residue unstructured C-terminus of GroEL blocks transmission of SP to the opposite cavity, but because the region lacks defined structure, it is simply invisible to crystallographic analyses.(19) Interestingly, truncation of the flexible C-terminus region diminishes ATPase activity to about half of wild type GroEL, whereas extension promotes ATPase activity.(19,20) The same activity modulation is not observed in the single ring variant of GroEL implying the unstructured C-terminus may play an important role in mediating inter-ring contacts.
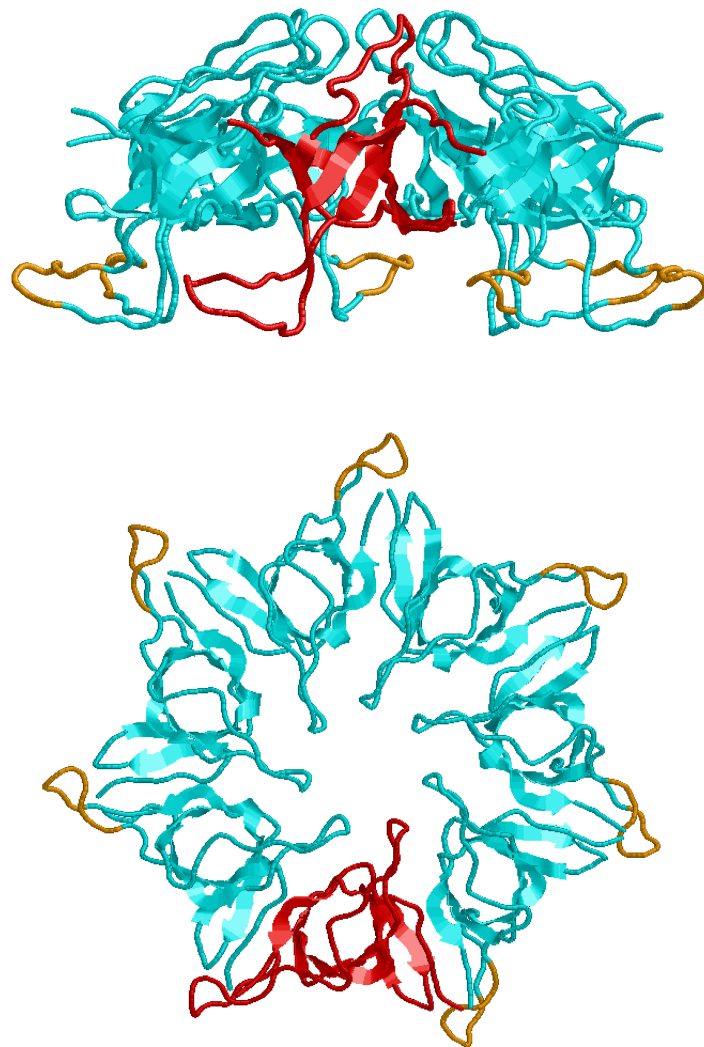
Figure 4: The co-chaperonin, GroES: A side view (A) and a top view (B). One monomer is colored red for reference. The mobile loops of each subunit that interact with the hydrophobic binding pocket of GroEL are colored orange. Figure prepared using PDB 1AON (9).

1.2: An Important Player in Cellular Biology

Why is study of the GroE system important? As a chaperonin system, the two multimeric proteins are responsible for rescuing misfolded, unfolded, or incompletely folded SP *via* a cycle of capture, encapsulation, and release. This cycle rescues SP from a fate of aggregation and proteolysis. It is specifically this function that has made the

GroE chaperonin system essential for cell viability. (15,17) In fact, homologs have been identified in almost every species. (15,21) The complexity of the system touches on several biochemical topics including allosteric control of multidomain proteins, protein folding, and aggregation.

Allosteric proteins are key players in signal transduction and regulation. Beginning with hemoglobin, the quintessential allosteric protein, the unique abilities of allosteric proteins have captured the interests of biochemists. Several models have been developed to describe the unique allosteric character of GroEL. For a discussion of those models, see section *1.4: An "Iterative Annealing Machine"*.

The mechanism by which GroEL and GroES rescue substrate protein promises insight to disease pathways that are consequences of misfolded or aggregated proteins. The way in which the environment of the encapsulation chamber favors rescue and folding of non-native protein or the effect it has on a protein folding landscape will improve understanding of protein folding dynamics.

1.3 The Role of GroEL in Protein Folding

Anfinsen asserted that all the information a protein needs to fold to its native state is encoded in the primary amino acid sequence.(22) Most proteins are able to fold productively in a crowded cellular environment with only this sequence driven information as a guide, but not all proteins are capable of this feat. Particularly in situations where cells are exposed to a stress, information from the primary structures alone fails to produce a functional protein. (15)

Protein folding is often conceptualized as a three-dimensional energy landscape funnel with each position on the surface of the landscape representing a unique conformer. An unfolded protein can occupy astronomically large number of conformations at the top of the funnel. (23) The natively folded protein occupies the lowest free energy position at the bottom of the funnel and is described by a limited number of conformation states. For an unfolded protein to populate the native state, it must successfully traverse the energy landscape without entrapment in local energy minima. Unfortunately for many proteins, the landscape is often rife with such traps that may result in an unproductive intermediate or misfolded structure (Figure 5). (23) Thermal fluctuations are adequate to assist some proteins in overcoming the local energy barriers. Such proteins move further down the funnel toward the global minima, but proteins unable to overcome the traps are often left with exposed hydrophobic regions that are prone to aggregation. (24,25) GroEL is able to recognize and interact with these trapped proteins to facilitate their movement through the local minima.

The GroE system rarely accelerates the folding of protein substrates; in fact, the contrary is more often true. Proteins that fold rapidly in the absence of GroEL often fold more slowly in its presence. Instead, the system provides kinetic assistance to trapped SP through the consumption of ATP. Interaction with GroEL results in another opportunity for the trapped intermediate to navigate the free energy landscape to the native state. (2,23)
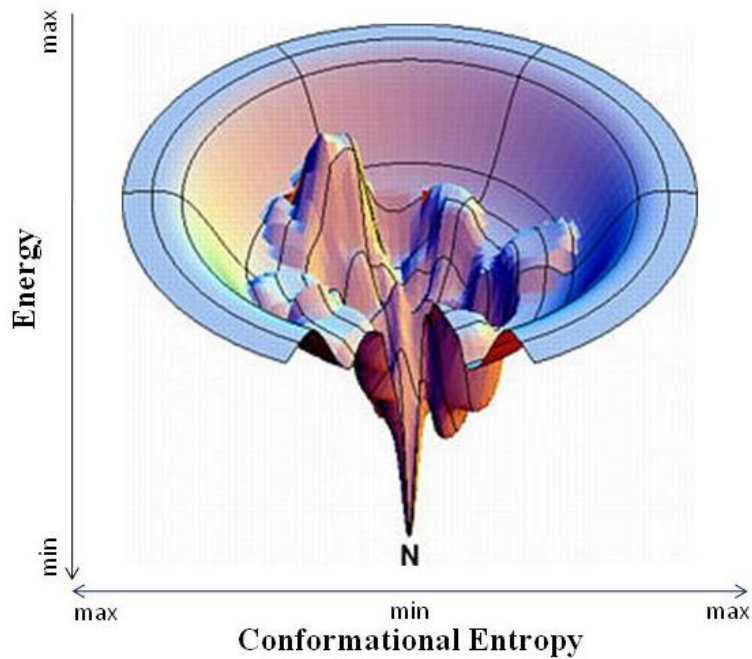
Figure 5: An example of a protein folding landscape. The landscape through which an unfolded protein must travel to reach the native state 'N' is littered with energetic barriers and kinetic traps. Figures from (23).

1.4: An "Iterative Annealing Machine"

GroEL is a complex structure with positive intra-ring and negative inter-ring allosteric controls. The active ring is termed the *cis* ring, and the opposing 'resting' ring is called the *trans* ring. A single cycle of GroEL requires turnover of both rings, whereas the turnover of a single ring is referred to as a hemicycle. (17)

During a hemicycle, a ring transitions between its two basic allosteric states, the **T** state (Taut state) and the **R** state (Relaxed state). ATP hydrolysis is not required for this transition to occur, only binding of ATP to the *cis* ring. (26,27) The **T** state is characterized by high affinity for SP and low affinity for ATP. Capture of SP is shown as step 1 of Figure 6, where the bracketed GroEL ring is the starting point of the hemicycle.

10

In step 2 of Figure 6, binding of ATP to the *cis* ring causes a slight upward expansion and 25˚ counterclockwise rotation of the apical domain countered by lowering of the intermediate domain. (17,27)
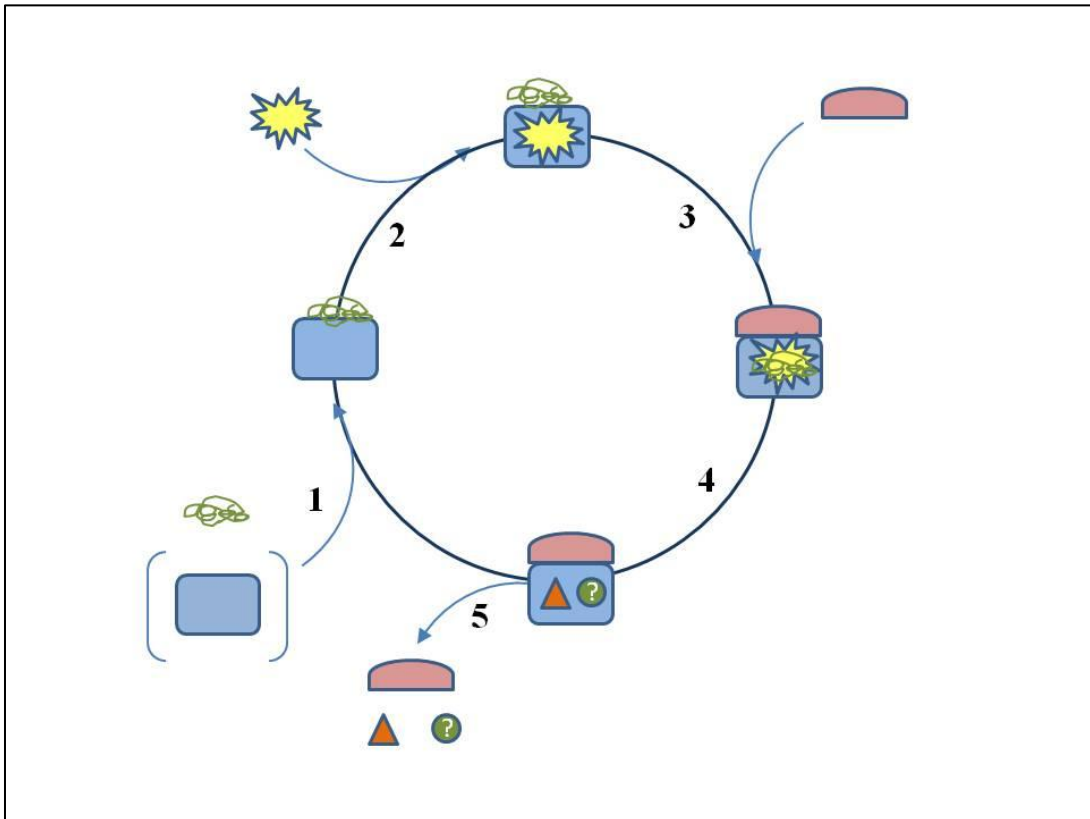
Figure 6: The events of the hemicycle. Only the *cis* ring is shown for clarity. *In vitro*, GroEL (blue rectangle shown in brackets) is introduced stripped of SP. 1: capture of SP (green squiggle), 2: binding of ATP(yellow starburst), 3: encapsulation by binding of GroES (red dome), 4: hydrolysis of ATP resulting in ADP (red triangle) and SP has the opportunity to fold in an infinitely dilute environment (green circle with '?'), 5: release of GroES, ADP and SP. In steps 4 and 5, the conformational state of the SP is known, thus the SP symbol is shown with a '? .

The addition of GroES (step 3) triggers the **R** to **R'** transition. It is characterized by further movements of the apical domain including an upward 60˚ and 115˚ clockwise rotation, as well as a 20° downward compression of the intermediate domain. The

11

movement of the intermediate domain locks ATP in the binding pocket while strategically positioning residues involved in ATP hydrolysis near the ATP. At this point, ATP is committed to hydrolysis. (9)

Once the [GroEL-GroES-ATP] asymmetric complex is formed, the *cis* ring of the complex is committed to hydrolyzing seven ATP molecules, releasing inorganic phosphate (step 4 in Figure 7). The resultant ADP remains trapped in the active site along with SP. Decomposition of the complex, along with release of ADP, occurs only after ATP binds to the opposing ring (steps 5 in Figure 7). It is suggested that a change in the tilt of the equatorial domain interface upon ATP binding may play a role in the negative cooperativity responsible for maintaining the out of phase operation of the ring, and thus the release of ES from the *cis* ring. (9)

Crystallographic work proposed that strengthening or weakening inter-ring salt-bridge Arg452-Glu461 is responsible for the negative cooperativity between the rings. (28) A more in-depth discussion of negative cooperativity is available in section 1.5. The presence of SP on the *trans* ring accelerates the decomposition of the *cis* complex. (17,29,30) The hemicycle is complete upon release of GroES. It remains unclear whether the ring undergoes an **R'→R**, **R'→T**, or **R'→R→T** transition after release of ligands.

Although these transitions are generally well accepted, the residence time GroEL occupies each step of the cycle remains debated. Cycle time depends on several factors such as ATP, K^+, SP, and GroES. (17,31-34) Failure to fully appreciate this fact has resulted in publication of many poorly controlled experiments. Lifetimes for the bullet

complex have been quoted between 8 and 15 seconds in the presence of substrate protein. (17) In the absence of SP, the bullet has a cycle time of about two minutes. (30) With so many factors influencing the cycle, it is no wonder such a great variation of residence times have been reported.

A complete cycle of the GroE system requires a hemicycle to occur in each ring of the tetradecamer. The question remains whether GroEL must release GroES from the first ring before it can bind GroES to the second ring, or if there is some time during which both rings are occupied by GroES before release from the first ring. Figure 7 A, shows the asymmetric intermediate, or 'bullet' model. Here, GroEL stripped of SP during *in vitro* experiments is combined with ATP and GroES. The system completes a hemicycle ending with release of ligand from the top ring. This is followed by binding of ATP to the bottom ring. GroES is introduced. Upon completion of the hemicycle of the bottom ring, ligand is released and ATP is bound to the top ring. The cycle continues similarly, and GroES never occupies both the top and bottom rings simultaneously.

The symmetric intermediate, or 'football' model begins as for the assyemtric complex model, however, GroES binds to the bottom ring before ligands are released from the top ring (Figure 7B). To complete a full cycle, the same steps occur for the bottom ring. Before release of ligand from the bottom ring, GroES must bind to the top. Symmetric and asymmetric species have been observed experimentally, and the presence of SP plays a vital role in formation of football complexes. (35-38)
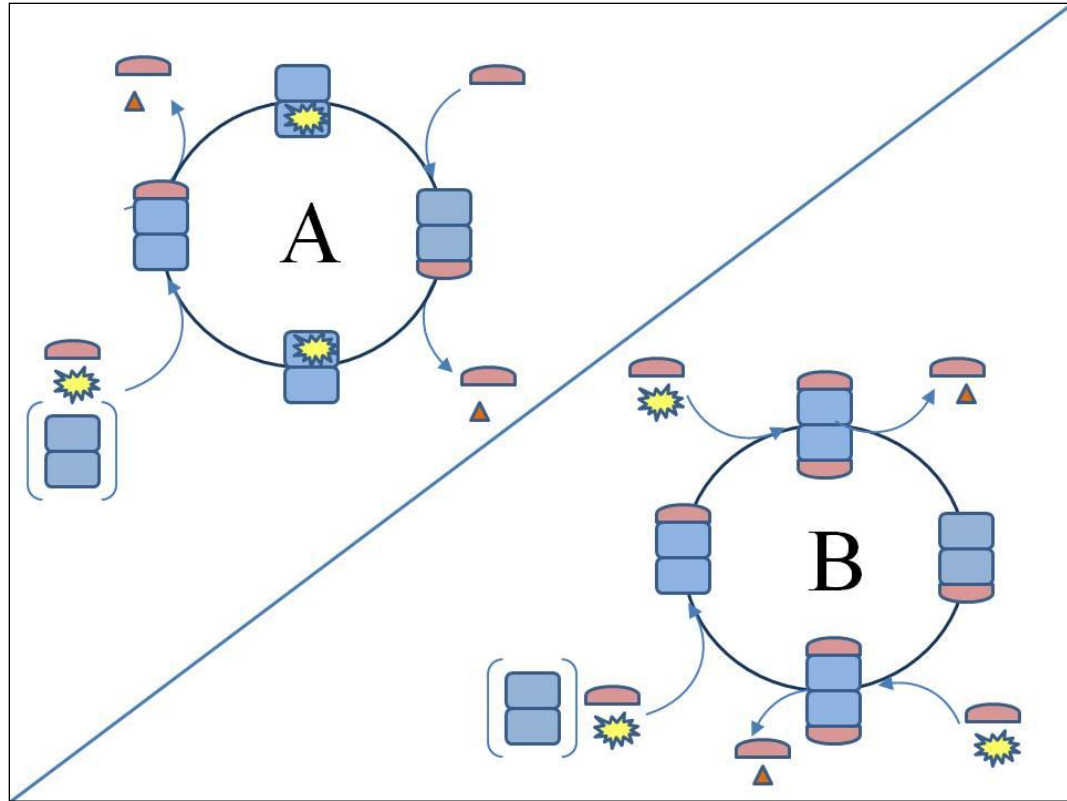
Figure 7: An Overview of the GroE cycle. The asymmetric intermediate model is shown on the top left (A). The symmetric intermediate model is shown on the bottom right (B). GroEL: blue stacked rectangles, GroES: red dome, ATP: yellow burst, ADP: red triangle

The mechanism of the GroE cycle is still debated. Followers of the Anfinsen Cage model interpret the GroEL/GroES complex as a passive observer of SP folding that assists solely by providing an isolated, hydrophilic folding environment. (39) Because encapsulation offers the peptide an infinitely dilute environment through sequestration from other proteins, it is proposed that this would result in a smoother energy landscape with fewer energetic traps as mentioned previously. Such a landscape makes it easier for the peptide to find the global energy minima incident of the native state.

This model seems logical since preventing SP-SP interaction between unfolded peptides in turn prevents aggregation and increases the opportunity for productive

folding. The model does not explain the rescue mechanism for misfolded SP upon incubation with GroEL, but supporters of this model assert that thermal fluctuations due to transient binding and release to GroEL may be adequate to overcome the energy barrier required for the unfolding of misfolded species.

The alternative model empowers GroEL as an active component in unfolding. Rather than simply providing a folding environment, GroEL forces the substrate protein to unfold by doing work on SP. In the active unfolding model, GroEL, fueled by ATP, forces the substrate protein to stretch between two substrate binding sites before discharge of a now less folded SP into the folding cavity. (40) This gives SP another opportunity to partition to the native state.

This model is based on the concept that the SP binding pockets of the apical domain move apart during the **T→R→R'** transitions. The force exerted on a protein would be contingent upon how tightly the SP is bound to the hydrophobic patches of the apical domain. This pulling motion breaks interactions that may be preventing the substrate protein from reaching its native conformation. (41) Here the substrate protein is given a small window of opportunity to navigate to the native state in an entropically favorable hydrophilic environment before ejection from GroEL. (17) The length of the folding window is still debated because of experimental inconsistencies as mentioned previously, but recent work has started to shed more light on the topic. (30,33,34,42)
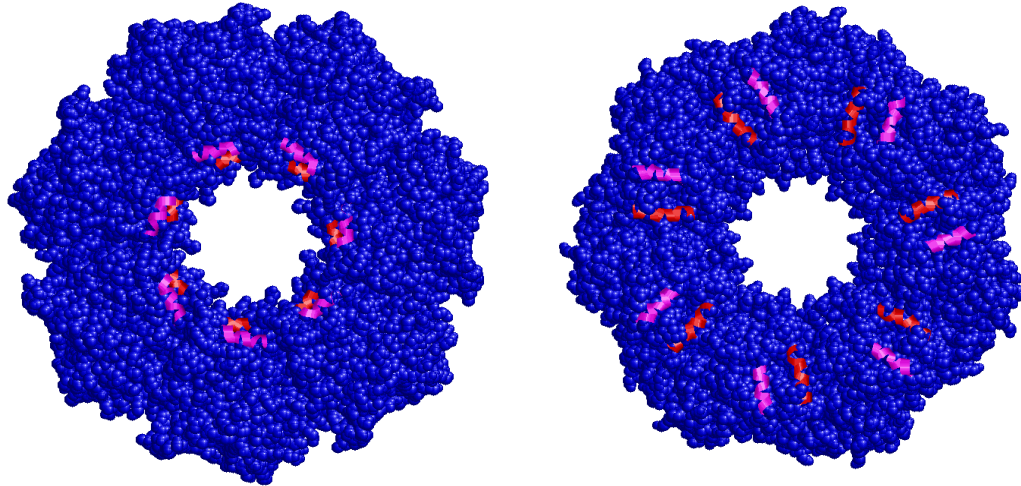
Figure 8: Movement of the Hydrophobic SP Binding Sites During the T to R' transition. GroES is not shown for clarity. Residues 234-243 composing helix H, and residues 257-269 composing helix I are color coded magenta and red respectively. On the left, helices involved in SP binding line the hydrophobic cavity. On the right, the helices move away from the cavity in the R' state. This movement causes release of captured SP into the cavity. The figure was prepared using PDB 1AON (9).

1.4.1 The Timer

Characterizing the window available for SP folding, and eventually the residence time GroEL occupies each stage of the hemicycle, depends on understanding the timing mechanisms that govern the basic GroEL/GroES interaction. The GroE hemicycle is often thought of as a 'single step' timer mechanism governed by a single rate constant. This means, assuming excess SP, ATP, and GroES are available in solution, all of the mechanical processes of the hemicycle through SP release into the cavity are assumed to take place immediately (<1 second), meaning steps 1-4 in Figure 7 are essentially instantaneous with the complex lingering at step 5. According to ensemble research, the average hemicycle lasts 4 to 6 seconds. (42)

By examining GroES occupancy with single molecule total internal reflection fluorescence microscopy (TIRFM), Taguchi et al. were able to identify two steps in the

16

GroE cycle to support a 'two step' mechanism (42). The on-time histogram failed to display the exponential decay expected in the case of a single timer leading to the proposition of an intermediate step in the hemicycle, described by the equation:

$$[GroEL - GroES] \xrightarrow{k} [GroEL - GroES]^* \xrightarrow{k'} [GroEL] + [GroES]$$
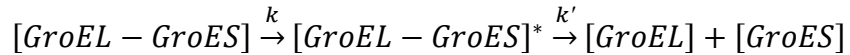
Where the transition to the [GroEL-GroES]* state is governed by k and the second transition to the individual constructs is governed by k'. (42)

The two step model is a composite of a three second period where GroES is tightly bound to GroEL, and SP folding is arrested, followed by a period of 5 seconds where GroES leaves GroEL. ATP hydrolysis resulting in the release of SP into the folding cavity is thought to occur after the three second delay. This correlates to a ~5 second folding window for encapsulated SP. (42,43)

Stopped-flow experiments using fluorescent phosphate binding protein (PBP) to monitor production of P_i do not support the delayed ATP hydrolysis proposed in the 'two-step' timer mechanism. With ADP absent from the *trans* ring, the asymmetric complex was challenged with ATP. The traces show an instantaneous burst of increased fluorescence correlated with production of ~6 moles P_i per mole of $GroEL_{14}$. (30,33,34) Were there a delay in ATP hydrolysis as proposed by the Taguchi group, the increase in fluorescence should also be delayed.

An alternative timer mechanism was proposed by Grason et al., wherein the mean residence time (MRT) of GroES on the *cis* ring is governed by the allosteric state of the *trans* ring of GroEL. (33,34) Using a combination of ATPase and stopped-flow FRET

17

experiments that monitor discharge of GroES from the asymmetric complex, it was possible to manipulate the MRT by varying concentrations ADP, SP, and K^+ (33). The asymmetric complex, composed of $^{cis}GroEL_B{}^{R'}$-[GroES]-[ADP]-$^{trans}GroEL_A{}^{R}$, is defined as the resting state for the system, and A and B are arbitrary identifiers assigned to the two rings of the tetradecamer.

At the completion of a hemicycle, GroES will occupy the opposing ring, and the resting state is expressed as $^{cis}GroEL_A{}^{R'}$-[GroES]-[ADP]-$^{trans}GroEL_B{}^{R}$. Figure 9 shows the proposed allosteric transitions that the *cis* and *trans* rings undergo over the course of the hemicycle. The MRT defines the length of the hemicycle since, as mentioned previously, no delay in ATP hydrolysis was observed in these experiments. Conditions that favor the R state lengthen the cycle. These conditions include the presence of ADP and 100mM K^+. Conditions that favor $^{cis}GroEL^{R'}$-[GroES]-[ADP]-$^{trans}GroEL^{T}$, such as the presence of SP, shorten the MRT and consequently the length of the hemicycle. The speed limit of the cycle is set by the hydrolysis of ATP

Ring A (*trans*)

GroEL-ADP

$\downarrow$ → ADP

GroEL

↓ ATP

GroEL-ATP

↓ GroES

GroEL-ATP-GroES

↓ → Pi

GroEL-ADP-GroES

Resting State #1

Resting State #2

Ring B (*cis*)

GroEL-ADP-GroES

↓

GroEL-ADP-GroES

↓ → GroES

GroEL-ADP
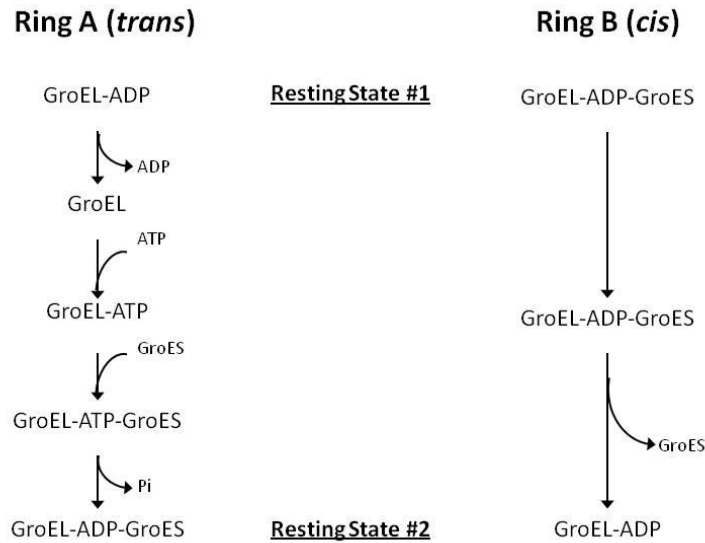
Figure 9: The timer mechanism proposed by Grason et al. alternates between two assymetric resting states labeled #1 and #2 here. It is proposed that both rings undergo allosteric changes in transition between the two resting states. (33)

1.5 Binding and Encapsulation of SP within GroEL

The **R** to **R'** transition is best summarized as an expansion of the internal cavity resulting in greater distances between SP binding sites. The internal volume of the cavity nearly doubles from 85,000 Å^3 to 170,000 Å^3. (17) Eventual burying of the hydrophobic binding residues results in release of SP into the hydrophilic internal cavity. (9,17,44)

A molten globular protein of ~58 kD is thought to be the largest SP able to be encapsulated within the fully expanded cavity; however, electron cryo-microscopy of the single ring variant of GroEL has demonstrated encapsulation of a heterodimeric assembly intermediate of mitochondrial branched-chain α–ketoacid dehydrogenase, an 86 kD

19

protein. (17,45) Accomplishing this feat requires significant distortion of the normally accepted structure of GroEL as well as stretching of GroES. The same experiment with wild-type GroEL fails to mimic encapsulation of the dehydrogenase. Nevertheless, there appears to be some flexibility in the size of SP able to be encapsulated. (45)

GroEL is promiscuous in binding substrate protein. However, an *E. coli* cell contains only enough GroEL to bind between 2 and 10% of newly synthesized proteins. (12,46) The remedy is that not all proteins are obligate. Obligate SP are unable to fold in the absence of GroEL under physiological conditions, whereas non-obligate SP are able to fold spontaneously under physiological conditions. GroEL binds to obligate and non-obligate substrate proteins as long as they meet one stringent criterion: they are not in the native state. (47,48) In a study of mutant P22 capsid proteins, it was shown that mutants in rapid equilibrium between the unfolded and native state became obligate SP for GroEL, whereas the wild-type capsid protein that has a low unfolding propensity was not an obligate SP (49). Moreover, bioinformatic analysis of known *in vivo* substrates demonstrates they have low folding propensity and high translation efficiency. (50)

There are two competing views on how GroEL identifies SP. The first is that substrate proteins are selected entirely on the basis of the presence of exposed hydrophobic residues characteristic of unfolded or misfolded proteins, rather than by a specific sequence or secondary structural motif. (51) Hydrophobic regions of substrate proteins are clearly important since SP binds to the highly hydrophobic helices H and I of the apical domain (Figure 8). However, only ~40% of denatured soluble proteins from *E. coli* are captured by GroEL. If hydrophobicity were the only requirement, it follows that a greater percentage of the denatured soluble proteins should be captured by GroEL.

A second view stipulates that SP are identified by the presence of a substrate protein binding motif (SPBM) typified by the primary sequence of the GroES mobile loop, GGIVLTGAA. Bioinformatic analysis indicates that known substrate proteins contain multiple instances of the SPBM to account for the multivalent binding of SP to GroEL. An analysis of published three dimensional structures of known SP confirms that the SPBM is buried within the native protein. (52,53)

1.6: Allostery in the GroE system

A detailed description of a hemicycle is provided above, but the entire story of GroEL cannot be understood without careful consideration of the interactions both within a single ring, and between the rings of a tetradecamer. Maintenance of an out-of-phase behavior mandates communication between the two rings, and efficiency of ATPase activity and encapsulation requires communication within a ring.

A model describing the unusual impact of ATP concentration on the ATPase activity of GroEL was first described by Yifrach and Horovitz. (54) They invoked the concept of nested cooperativity, wherein the subunits of a single ring of a tetradecamer undergoes a concerted 'all or none' MWC type transition from the **T** state to the **R** state in the presence of increasing ATP. However, when taken together, the rings undergo a sequential KNF type transition from the **TT** to **TR** to **RR** states, where each letter represents the state of a single ring in the tetradecamer. The unique shape of the ATPase curve, essentially rate of ATP hydrolysis versus ATP concentration, described by Yifach and Horovitz can be conceptualized as follows: GroEL begins in the **TT** state which is characterized by low activity. Because the initial transition to the **TR** state is governed by the all-or-none transition of a single ring, it occurs upon addition of small amounts of

ATP resulting in rapid increase of ATPase activity. Larger amounts of ATP prompt the rings to occupy the **RR** state which is characterized by lower ATPase activity than the **TR** state leading to the diminished ATPase rate at high concentrations of ATP.

This phenomenon can be understood though consideration of the relationship between the two allosteric constants $L1 = \frac{[TR]}{[TT]}$ and $L2 = \frac{[RR]}{[TR]}$. Under the influence of nested cooperativity, L2 is necessarily much less than L1, but the fact that the **R** state has a higher affinity for ATP results in an increasing L1 as ATP concentration is increased. In the presence of SP, there is a loss of the second transition in the ATPase rate curve implying a shift toward the **T** state and a concomitant decrease in L1. (54,55)

One of the assumptions of the Yifrach and Horovitz model is that ATP is unable to bind to the **T** state. This concept is referred to as the exclusive binding assumption. It forces the ring to assume the **R** state before binding ATP, thereby eliminating one possible regime regulating the allosteric interaction of a ring. This is illustrated in the pathway with the red arrow in Figure 10. Although convenient for the sake of simplifying fitting and mathematics, it is not an empirically supported assumption, and results in a less than optimal fit of ATPase data. (56)

An alternative model developed by J. Gresham maintains that the **T** state has some affinity for ATP, however it is much lower than affinity of the **R** state. (56) By allowing ATP to interact with both the **T** and the **R** state, both possible allosteric pathways shown in Figure 10 are permitted and evaluated by the model. A second assumption made in both the exclusive and non-exclusive allosteric models is that a ring in the **R** state has higher activity in **TR** versus an **R** ring in the **RR** conformation. The validity of this

assumption is unsubstantiated, but it was required for fitting. The model proposed by Grason et al. circumvents these assumptions by attributing the apparent loss of activity of the **RR** state to occupancy of the *trans* by ADP. A discussion of that model is available in section 1.4.1. (33,34)
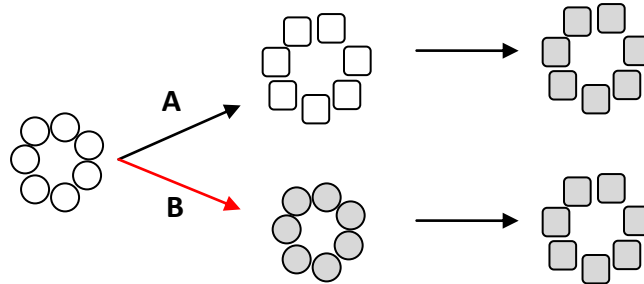
Figure 10: The sequential MWC type transition **of a single ring**
. In path A, the ligand free T state of a single ring converts to the R state,
represented by square monomer, and then binds ligand (grey squares). Path B

1.7: Research Objectives

Since GroEL was discovered in the early 1970's, significant progress has been made toward understanding the GroE reaction cycle and the allosteric transitions it undergoes; however, many questions remain. Research presented in the following chapters is intended to address several underlying questions as enumerated in the points below.

1. The ability to control the allosteric transitions of GroEL enables characterization of those transitions. Two double cysteine mutants that facilitate such control by locking GroEL in the **T** state using disulfide bonds have already been studied. Those mutants are D83C/K327C, an intra-subunit salt-bridge, and R197C/E386C, an inter-subunit salt-bridge. (30) Results of this work suggest

23

the *trans* ring must populate the **T** state before discharge of the *cis* ring occupants, but additional evidence is needed corroborate these observations. To further probe the sequential allosteric transition, a mutant containing a destabilized intra-subunit salt-bridge was developed to investigate the following hypothesis: If the t*rans* ring must occupy the **T** state before discharge of the c*is* ring substituents may occur, destabilization of the **T** state will (1) compromise the release of the *cis* ligands and (2) halt or severely retarded ATPase activity. Contrastingly, stabilization of the **T** state of the *trans* ring will facilitate rapid discharge of the *cis* ring substituents. This hypothesis was investigated with a combination of ATPase measurements and experiments probing the rate of discharge of GroES from the *cis* ring.

2. How many ATP are required for the **T→R** transition to occur? How many subunits of a GroEL ring must bind a mobile loop of GroES for the complex to be committed? These and many similar questions limit our understanding of the GroE system because of the seven fold symmetry of the ring and the dyadic symmetry of the system. Several attempts to answer such questions have been made, but have failed to adequately and reproducibly facilitate control of the system. An optimal means of investigating these questions is to combine monomers from wild type GroEL with those of a mutant in a statistically significant manner. If the wild type and mutant subunits reassemble stochastically, the composition of the mixture can be determined from the binomial distribution, but practical methods to accomplish this are lacking. To address this issue, protocols resulting in mixed species were developed, and the

efficacy of each protocol was examined using techniques including, affinity chromatography, gel filtration chromatography, and electrospray ionization mass spectrometry (ESI-MS).

3. Activity of GroEL under cellular stress is essential for successful completion of the chaperonin's SP rescue function. A logical requirement drawn from this observation is that GroEL has an innate structural stability. Acetone is a known protein denaturant, and GroEL necessarily aggregates during treatment with 45% (v/v) acetone (discussed in chapter 5). However, curious properties of GroEL, specifically recovery of functional tetradecamer after exposure to 45% (v/v) acetone spurred interest in the stability and aggregation processes of the protein. Dynamic light scattering (DLS) was used to investigate not only the stability of GroEL in buffer solution, but the aggregation process the material undergoes during exposure to varying amounts of acetone.

Chapter 2: Materials and Methods

2.1: Purification of GroEL

GroEL was purified using the method described by Grason. (30) A schematic of the major purification steps is provided in Figure 11. A more detailed description is available in the appendix. To circumvent aggregation problems associated with cysteine mutants, DTT in the buffer was increased from 2mM to 10mM.

Over-expression in LB media

↓

Cells harvested and lysed by sonication

↓

Remove DNA with Streptomycin sulfate treatment

↓

Purify on DEAE column

↓

Concentrate by ammonium sulfate precipitation

↓

Desalt on S300 column

↓

Strip residual SP with 45% acetone treatment

↓

Remove residual acetone by PD-10

↓

Quick-freeze in methanol bath and store at -80°C
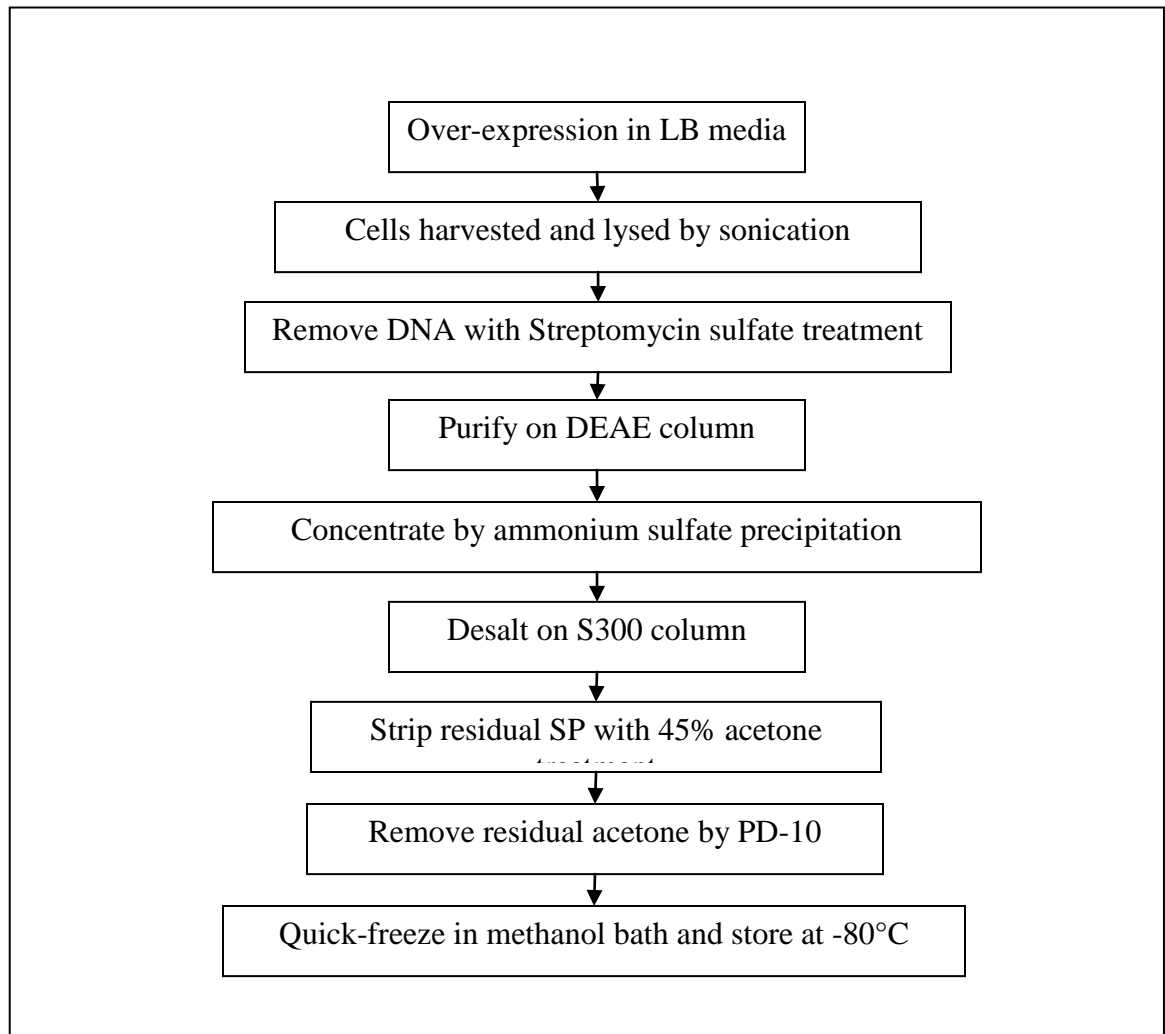
Figure 11: Overview of GroEL purification process. The major steps of the purification are summarized in the flow-chart above

2.3: Purification of GroES

   GroES was purified using the method described by Grason.   A flow chart summarizing the purification steps is provided Figure 12, and a more detailed description of the method is provided in the appendix. To prevent aggregation during purification of cysteine mutants, the DTT concentration was increased from 2mM to 10mM in all buffers.

```
┌──────────────────────────────────────────────────────────────┐
│                                                                │
│              ┌──────────────────────────────┐                  │
│              │   Over-expression in LB media │                 │
│              └──────────────────────────────┘                  │
│                            ↓                                   │
│         ┌──────────────────────────────────────┐               │
│         │  Cells harvested and lysed by sonication │            │
│         └──────────────────────────────────────┘               │
│                            ↓                                   │
│      ┌──────────────────────────────────────────────┐          │
│      │ Remove DNA with Streptomycin sulfate treatment │         │
│      └──────────────────────────────────────────────┘          │
│                            ↓                                   │
│    ┌──────────────────────────────────────────────────┐        │
│    │ Heat treatment at 72°C for 10 minutes and centrifugation │ │
│    └──────────────────────────────────────────────────┘        │
│                            ↓                                   │
│     ┌────────────────────────────────────────────┐             │
│     │ Concentrate by ammonium sulfate precipitation │           │
│     └────────────────────────────────────────────┘             │
│                            ↓                                   │
│              ┌──────────────────────────┐                      │
│              │    Desalt on G25 column   │                     │
│              └──────────────────────────┘                      │
│                            ↓                                   │
│          ┌──────────────────────────────────┐                  │
│          │  Adjust to pH 5 with sodium acetate │               │
│          └──────────────────────────────────┘                  │
│                            ↓                                   │
│          ┌──────────────────────────────┐                      │
│          │   Purify on SP Separose column │                     │
│          └──────────────────────────────┘                      │
│                            ↓                                   │
│     ┌──────────────────────────────────────────────┐           │
│     │ Concentrate with ammonium sulfate precipitation │         │
│     └──────────────────────────────────────────────┘           │
│                            ↓                                   │
│           ┌──────────────────────────────┐                     │
│           │   Desalt using PD-10 column   │                    │
│           └──────────────────────────────┘                     │
│                            ↓                                   │
│      ┌──────────────────────────────────────────────┐          │
│      │ Quick-freeze in methanol bath and store at -80°C │       │
│      └──────────────────────────────────────────────┘          │
│                                                                │
└──────────────────────────────────────────────────────────────┘
```

Figure 12: Overview of GroES purification procedure.

2.4: Over-expression of isotopically labeled GroEL

Culture of carbon 13 and nitrogen 15 labeled GroEL (^{13}C,^{15}N-GroEL) in minimal media (M9) required special supplementation with salts and trace elements for over-expression to occur. A procedure developed by Eva de Alba was adapted for this purpose. A GroEL starter culture was prepared in standard LB-Ampicilin broth and grown at 37°C shaking at 225 rpm until cloudy. The cells were centrifuged for 2 minutes at 5,000 RCF. The LB-ampicilin broth was decanted, the cells were washed with filtered, supplemented M9 media (see Table 1 for composition of supplemented M9 media) to remove residual LB-ampicilin broth, centrifuged again for 2 minutes at 5,000 RCF, and then resuspended in sterile filtered, supplemented M9 media. Incubation at 37°C with shaking at 225 rpm was resumed until an OD_{600} of about 0.8 was reached. Over-expression was induced by addition of IPTG, and 4 mL of sterile filtered glucose was added to the culture to sustain growth. Once the culture reached a cloudy consistency, the cells were harvested by centrifugation at 10,000 RCF for 15 minutes. From this point forth, the material was purified according to the GroEL purification above.

Composition of Supplemented M9 Media	
Ingredient	**Amount per 500mL**
KH_2PO_4	13g
H_2HPO_4	10g
$NaHPO_4$	9g
K_2SO_4, pH 7.2	2.7g
$CaCl_2*2H_2O$	0.04g
$FeSO_4*7H_2O$	0.04g
$MnCl_2*4H_2O$	0.007g
$CoCl_2*6H_2O$	0.005g
$ZnSO_4*7H_2O$	0.004g
$CuCl_2*2H_2O$	0.0019g
H_3BO_3	.0001g
$(NH_4)_4Mo_7O_{24}*4H_2O$	.003g
Sodium dibasic EDTA	0.03g
$^{15}NH_4Cl$	4g
Yeast Extract	0.001g
$MgCl_2$	5mM final concentration
^{13}C-Glucose	3.5g

Table 1: Composition of M9 media supplemented with metal ions for over-expression of isotopically labeled GroEL

2.5: Purification of the Single Ring Variant (SR1) of GroEL

All steps between over-expression and streptomycin sulfate treatment were performed identically to the procedure described above for GroEL. SR1 is further purified by application to a Q Sepharose FF chromatographic column run with a linear gradient between a buffer containing 50 mM Tris pH 8, 1 mM EDTA, 5 mM $MgCl_2$, and 1 mM DTT, and a buffer containing 50 mM Tris pH 8, 1 mM EDTA, 5 mM $MgCl_2$, 1 mM DTT, and 1 M NaCl. Fractions containing SR1 were identified by SDS-PAGE and pooled. The material was concentrated to between 5 mg/mL and 10 mg/mL followed by acetone treatment and storage as described for the GroEL purification.

2.6: Measuring and Discussing Concentrations

GroEL concentration was determined by measuring the absorbance of the material at 276 nanometers (nm) in the presence of 6M guanidinium hydrochloride (GHCl) using an extinction coefficient, ε, for a GroEL monomer of 9,600 $M^{-1}cm^{-1}$.

GroES concentration was similarly determined at 280 nm in the presence of 6M GHCl using $\varepsilon = 1,200$ $M^{-1}cm^{-1}$, also corresponding to a monomer.

In this dissertation, all concentrations of GroEL and GroES refer to monomer concentration unless otherwise noted.

2.7: Primer design, mutagenesis, and harvest of plasmid DNA

Introduction of mutations into the GroEL or GroES genetic sequence were made using the Stratagene Quick-Change mutagenesis kit according to the published instructions using primers designed according to the kit instructions. Mutant DNA was harvested in useful quantities using the Mini- or Midiprep kit from Qiagen. A more detailed description of these procedures is provided in the appendix. All mutant DNA was sent to University of Maryland Center for Biosystems Research DNA Sequencing Facility for complete sequencing of the gene.

2.8: Transformation of plasmid DNA

Expression of mutant protein was accomplished by transforming BL21 competent cells (Novagen) with plasmid DNA of interest according to the instructions included with the competent cells. Generally 50 µL of pre-aliquoted competent cells were dispensed into a chilled, round-bottom polypropylene culture tube and 1µL of plasmid DNA (~5 ng) was placed in the cell suspension. The material was mixed by gently swirling the tube,

followed by incubation on ice for 30 minutes. Using a water bath pre-equilibrated to 42°C, the cells were heat treated for 45 seconds with continuous swirling, and then placed on ice for an additional two minute incubation. 250 µL of SOC media equilibrated to 37°C was added to the cells, followed by immediate incubation at 37°C for 1 hour with shaking at 200 rmp. LB-ampicilin plates were streaked with 20 µL of the cell suspension and left overnight at 37°C. Resultant individual colonies are the starting point for all subsequent preparations.

2.9: Preparing denatured α-lactalbumin as substrate protein

Experiments utilizing SP were performed with denatured, carboxymethylated α-lactalbumin isolated from bovine (Sigma). α –lactalbumin is stabilized by four disulfide bonds (Cys6-Cys120, Cys28-Cys111, Cys61-Cys77, and Cys73-Cys91) and folding is dependent upon correct oxidation of the cysteines as well as the presence of Ca^{2+}. This means the material can be permanently denatured by reducing the disfulides in the absence of calcium ion, and then functionalizing them to prevent reformation of the bonds.

Permanently denatured α-lactalbumin was prepared by suspending lyophilized material in 2 mM Tris pH 7.5 buffer and first reducing the disulfides with 2 mM DTT for approximately 10 minutes. The lyophilized material purchased from Sigma is already stripped of Ca^{2+} to simplify the process. The protein was acid denatured by adding a volume equivalent of 0.2 M HCl while rapidly stirring, and was allowed to denature for 1 hour before proceeding. The material was brought to ~pH 7, and then buffer exchanged into PBS by PD-10 column. The reduced cysteines were blocked by treatment with iodoacetate. Excess iodoacetate was removed by a second PD-10 column equilibrated

with storage buffer, generally 10 mM Tris pH 7.5 10 mM $MgCl_2$. The concentration was determined by absorbance at 280 nm using $\varepsilon = 28,400$ $M^{-1}cm^{-1}$. Material was divided into aliquots and frozen at -20°C until use. (57)

2.10: Gel Electrophoresis

SDS-PAGE gels were prepared in the lab with 8 by 10 centimeter glass plates using a 20% bis-acrylamide solution from Biorad according to a previously described recipe (58,59). For SDS-PAGE, spacers of 0.75 mm or 1.0 mm were used and 10% or 12% acrylamide gel were typically run. In the case of native gels, spacers of 1.0 mm or 1.5 mm were used for the sake of making the gel more amenable to manual manipulation. The same recipe was used for the native PAGE as for SDS-PAGE with the caveat that DTT and SDS were replaced by water, and the gel contained only 4% or 5% acrylamide. Gels were run on the Hoefer 250 Mini-Vertical electrophoresis unit.

Gels were stained using PhastGel Blue and destained in a 10 parts methanol:10 parts acetic acid: 80 parts water destain solution. Gels were scanned using the densitometer, or in the case of fluorescently labeled samples, by the Storm 860. The relative intensity of the bands was determined using ImageQuant software which works by generating a graph of the band intensity and then integrating the area under the peak much like a chromatogram. In circumstances requiring accurate protein concentrations of samples containing little protein, known sample concentrations were run alongside unknown samples of interest to create a standard curve from which the unknown concentrations could be derived. For an example of this, see 2.12: Dye and Biotin Labeling.

2.11: Preparation of Cross-linked Materials

For some experiments, it was necessary to apply cross-links to lock the protein of interest in a particular conformation. Stock solutions of dimaleimide were prepared at 1M concentrations in DMF or DMSO because H_2O hydrolyzes maleimide. Stocks were stored at -80°C, and were diluted with water to a useful concentration before use to minimize the impact of the organic solvent. The cysteine residues in the protein were first completely reduced by incubation with DTT for 10 to 20 minutes. Removal of the DTT was accomplished by passing the material through a PD-10 column equilibrated in the desired buffer in the absence of DTT. The eluent was collected and treated with the desired cross-linking reagent. (60) Previous work done in our laboratory demonstrated that the cross-links form very rapidly, well within a minute of reagent addition. Previous work demonstrated that the extent of cross-linking could be manipulated by varying the ratio of cross-linking reagent to GroEL monomers. (30)

2.12: Dye and Biotin Labeling

Any protein that was covalently modified with dye or biotin in this work was made using a maleimide conjugate containing the modifier of choice (*i.e.*: fluorescent dye or biotin). Maleimides react selectively with the thiol group of cysteine (Figure 13) by creating a thioether, have a half-life of fifteen minutes in aqueous solutions since maleimides are easily hydrolyzed by water. (61) To maintain the efficacy of the label, stocks were prepared in DMSO or DMF and stored at -80°C.

Maleimide   Thioether
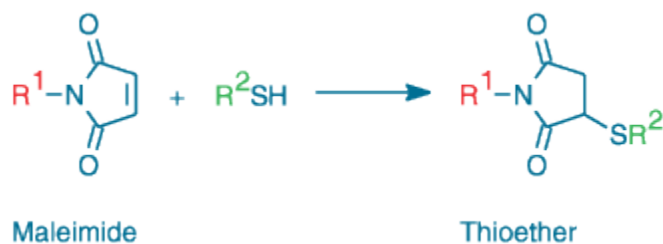
Figure 13: Conjugation with fluorophores or biotin: Fluorescent and biotinylated proteins were created using a maleimide functionalized fluorophor or biotin represented by the species on the far left. The label is represented by the red R^1. Maleimides react selectively with thiol groups (the R^{2}SH species where R^2 represents the protein) yielding a thioether (far right species). Figure from Molecular Probes Handbook, Invitrogen, ©2008. (61)

To prepare the protein for modification, the material was reduced with a final 5mM DTT for about 30 minutes at room temperature. DTT was removed by PD-10 desalting column equilibrated with 10 mM Tris acetate pH 7.2, 10 mM magnesium acetate buffer. Following collection of the desalted protein, the maleimide label was added at a concentration twice that of the possible labeling sites. Additional aliquots of material were added every 15 minutes. This process was repeated as needed to obtain the desired labeling efficiency. Then the reaction was quenched with excess DTT.

Free dye was removed by concentration and dilution followed by a PD-10 column. The final protein concentration was determined using a quantitative SDS-PAGE gel in the case of dye labeled protein. Standards of known concentrations and the unknown samples were loaded at several dilutions for comparison (Figure 14). A standard curve was prepared based on the band density of the standards, and the equation derived from the linear regression was used to calculate the concentration of the unknown samples (Figure 15).
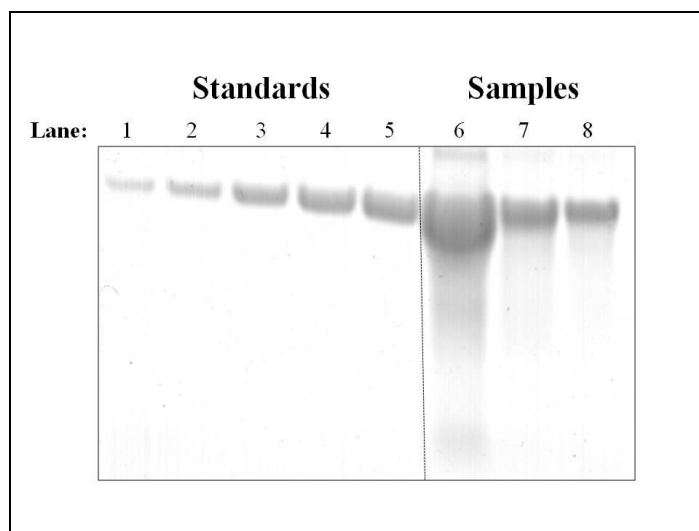
Figure 14: An example quantitative SDS-PAGE. Standards occupy lanes 1 to 5, and the labeled sample occupies lanes 6, 7 and 8. Note the sample lanes have varying band density because three different dilutions were loaded on the gel. In this example, lane 8 was used for quantitation as the area of the band fell within the area of the standards.
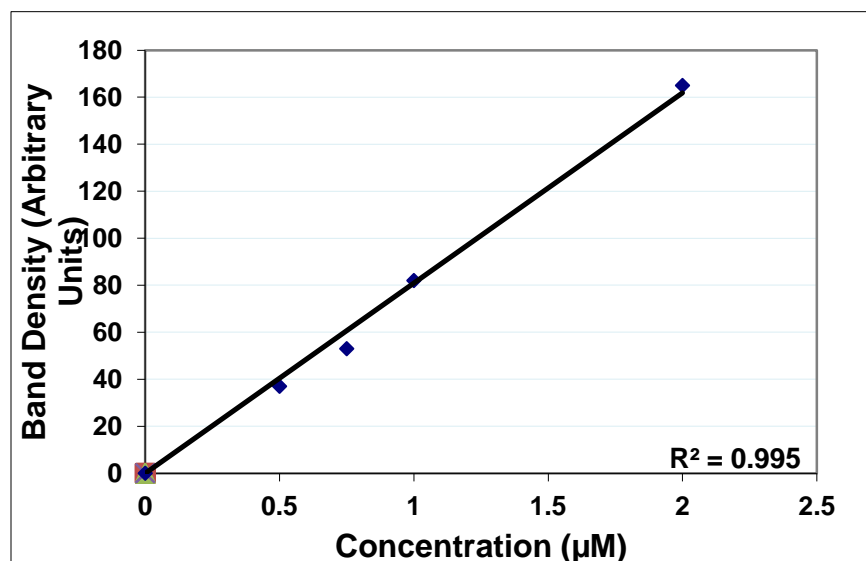
Figure 15: An example standard curve derived from a quantitative PAGE. Standard concentrations were plotted against band volume (density) and fitted by linear regression. The goodness of fit (R^2) is shown at the bottom right of the figure. The resulting equation was used to calculate the concentration of unknowns.

For biotinylated material, the protein concentration was measured at 280 nm in guanadinium hydrochloride according to the standard laboratory procedure described

above. Final dye concentrations were obtained by measuring the absorbance at the appropriate wavelength and calculating the concentration using the appropriate extinction coefficient. The extent of biotinylation was determined using a HABA based biotinylation quantitation kit from Pierce. Labeling efficiency for fluorescent or biotin labeled material was calculated as:

$$\% \ Labeling = 100 * \frac{[dye \ or \ biotin]}{[protein]}$$

2.13: Preparation of ATP & ADP

ATP and ADP were prepared by dissolving the disodium salt purchased from Sigma in milli-Q H_2O. The material was adjusted to approximately pH 7 using $NaHCO_3$, then filtered with a 0.22µm syringe filter. Concentration was determined by measuring the absorbance at 260 nm using $\varepsilon = 15,400 \ M^{-1}cm^{-1}$. During the preparation of ATP, contaminating ADP was removed by treatment with pyruvate kinase and phosponenolpyruvate for 30 minutes at 37°C. The mechanism responsible for the regeneration is discussed in the section below describing the ATPase assay. Pyruvate kinase was removed by ultracentrifugation with a centricon YM-3. The flow through was collected and ATP concentration measured as described above.

2.14: ATPase Assay

Non-equilibrium kinetics of GroEL were measured using a coupled enzyme assay that spectrophotometrically measures the conversion of NADH ($\varepsilon_{340nm} = 6220 \ M^{-1}cm^{-1}$) to NAD^+ ($\varepsilon_{340} = 0 \ M^{-1}cm^{-1}$) in real time. When GroEL turns over, ADP and P_i are released as products. The ATPase assay utilizes the coupling enzyme pyruvate kinase (PK) to consume the released ADP in combination with phosphoenolpyruvate (PEP) to

37

yield pyruvate. The second coupling enzyme, lactate dehydrogenase (LDH), uses pyruvate and NADH to generate lactate and NAD^+ resulting in a net decrease in absorbance over time. This experimental setup is extremely robust since hundreds of data points are collected over the course of a single run. Linear regression was used to determine the fitness of each run, and runs with an R^2 of less than 0.99 were discarded. The samples were prepared as described in Table 2. The rate of ATP consumption per minute can be calculated by the equation

$$\frac{\Delta[ATP]}{minute} = \left(\frac{Slope\ (sec^{-1})}{6.22mM^{-1}}\right)\left(\frac{60\ sec}{1\ min}\right)\left(\frac{10^6\ nmol}{1\ mmol}\right)(0.0009L)$$

and then converted to turnovers per minute by the equation

$$Turnover = \left(\frac{\Delta[ATP]}{min}\right)\left(\frac{1}{nmol\ GroEL_{14}}\right).$$

The assay is designed such that the coupling enzymes are in excess, and ATP hydrolysis by GroEL is the rate limiting step. A detailed description of the ATPase assay is described by Grason. (30)

Component	Concentration
$GroEL_{14}$	2 µM
KOAc	100 mM
MgOAc	10 mM
PEP	0.2 mM
NADH	0.2 mM
PK	5 Units
LDH	4 Units

Table 2: Sample concentrations used in ATPase assay.
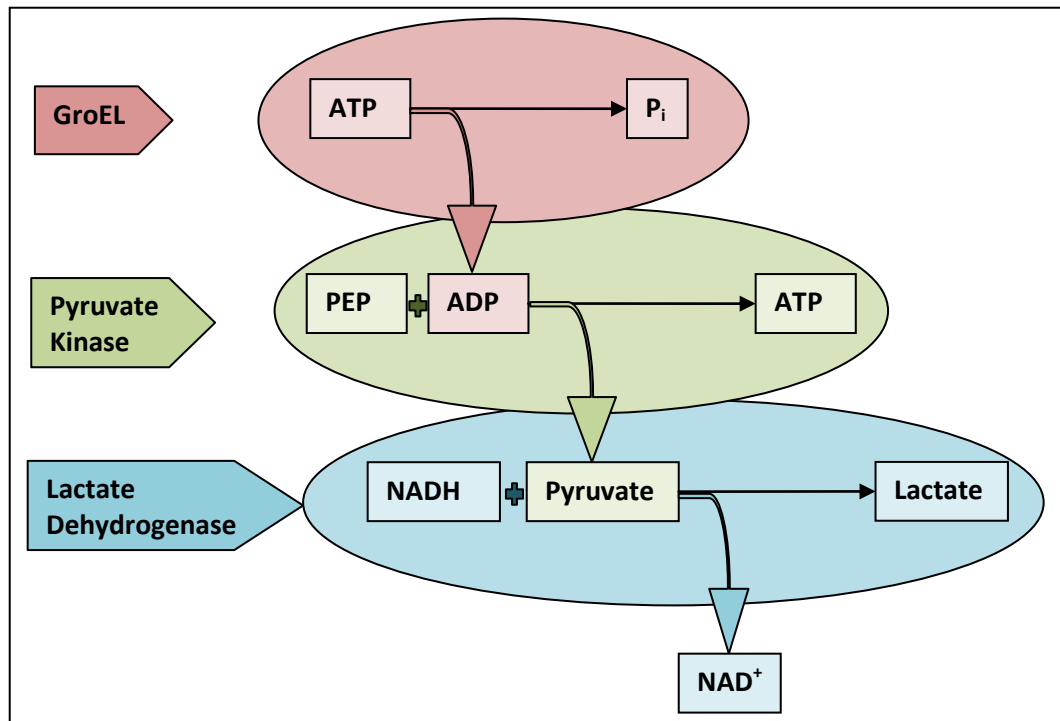
Figure 16: The ATPase Assay:

A graphical representation of the steps that take place during the ATPase coupled enzyme assay. The steps are color coded to make correlating the enzyme responsible for the reaction easier. The responsible enzyme is listed in an arrow box on the left, and to the right are the steps that each enzyme is responsible for completing. Any materials passed on to the next step carry the color of the originating

Chapter 3: The Consequences of Destabilizing the T-state-stabilizing Inter-domain Salt-bridge

3.1 Introduction

The dual heptameric rings of GroEL and co-chaperonin GroES constitute a nano-machine responsible for rescue of non-native substrate proteins (SP) from aggregation and proteolysis. SP rescue occurs through a cycle of capture, encapsulation, and release in an ATP dependent fashion. GroEL exhibits nested cooperativity, whereby, turnover of the machinery is regulated by positive cooperativity within a given ring, but negative cooperativity between the stacked rings (17,54,62,63). A simplistic explanation of the sequential transition characteristic of nested cooperativity exhibited by GroEL is illustrated in Figure 17. Nucleotide prefers to occupy a ring in the **R** state, thus the presence of ligand drives the allosteric state of the tetradecamer to the **RR** state. Substrate protein binds preferentially to the **T** state because of interaction with exposed hydrophobic surfaces that are accessible only in the **T** state. This results in increasing amounts of substrate protein driving the equilibrium toward the **TT** state. The nested
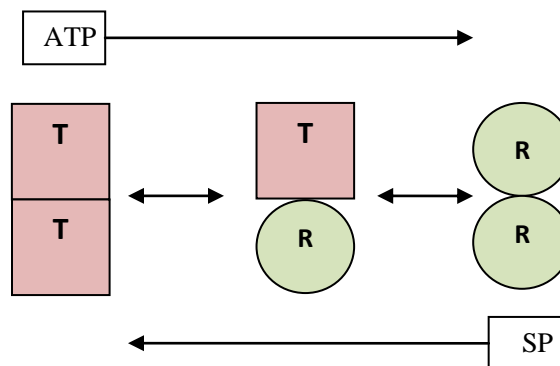
Figure 17: :A basic diagram of the KNF type sequential allosteric transition of GroEL.
Addition of ATP drives the equilibrium toward the RR state, whereas, SP drives it toward the TT state.

cooperativity model requires the **TT** conformation to be considered the resting state of GroEL in the absence of ligand. (8)

It is commonly believed that in the absence of SP is that GroEL binds only one GroES at a time forming an asymmetric complex, binding GroES on one ring, termed the *cis* ring, while the alternate *trans* ring remains fallow. The *cis* ring must hydrolyze ATP and release bound GroES from the asymmetric complex before the alternate ring may bind GroES. In the presence of SP, an alternative model involving symmetric complex has been proposed (64,65). A symmetric complex, or 'football', is created when both rings of GroEL are occupied by GroES at the same time.

The turnover of a single ring is called a hemicycle and a complete cycle of the GroE system requires turnover of both rings. The mean residence time (MRT) of the GroES heptamer on GroEL is controlled by the concentrations of K^+, nucleotide, and SP (33,34,54). Multiple allosteric states have been evoked to characterize the GroE hemicycle, but previous work largely focused on the transitions of the *cis* ring. Because the rings work in concert, we here explore the impact of allosteric transitions occurring in the *trans* ring. Grason et al. proposed a detailed scheme reflecting allosteric states of both the *cis* and *trans* rings during a hemicycle as illustrated in Figure 18.
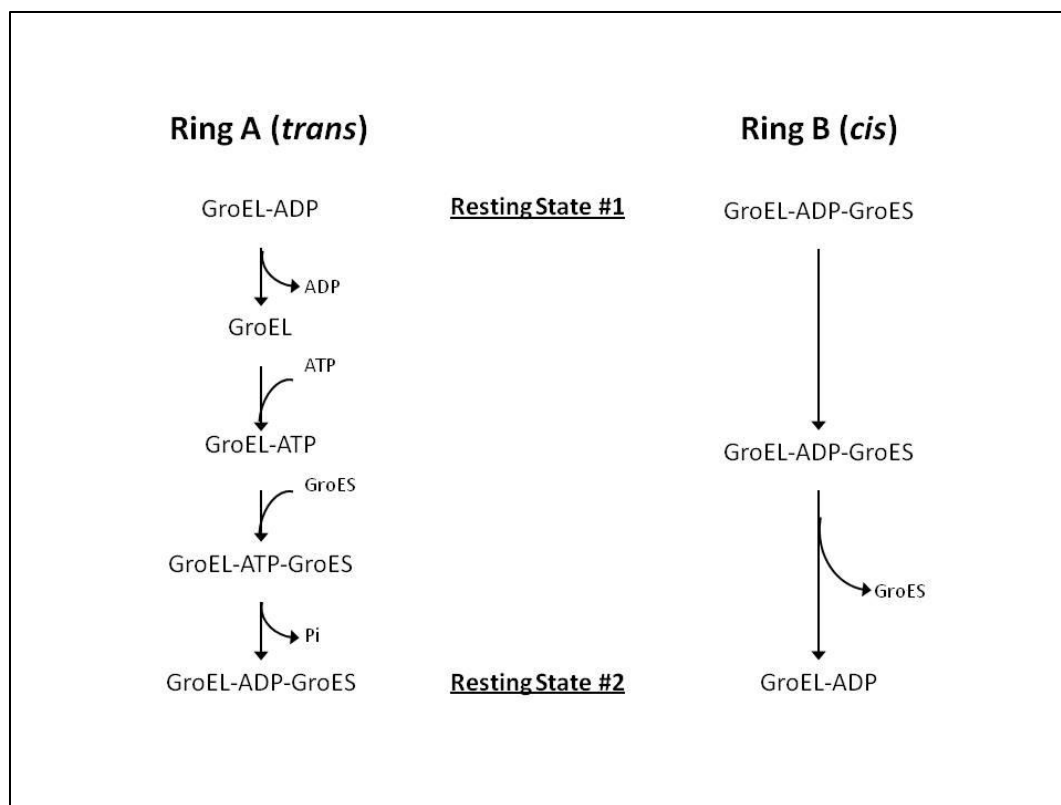
Figure 18: Grason et al. proposed that a GroEL hemicycle required allosteric transitions to occur in both the *cis* ring and the *trans* ring for continuous viability of the chaperonin.

In this work, we investigate the allosteric transitions of the *trans* ring. We ask whether it is necessary for the *trans* ring to access the **T** (taut) state, the state with the greatest affinity for SP, before the cycle can continue. We explore the likelihood of three possible pathways (Figure 20). The first possibility is that the *trans* ring of the $EL_R \bullet ADP$ resting state adopts the **R** (relaxed) state, and that it undergoes ADP/ATP exchange without visiting the **T** state . If the **T** state is an obligatory step in the GroE cycle, as proposed by Grason et al. (30,34), equilibration between the **T** and **R** states is necessary. In this instance, two pathways are possible since the discharge of ADP from the *trans* ring may come before or after the conversion of the ring to the **T** state. Schematics of the possible pathways are shown in Figure 20

The **T** state is stabilized by several salt-bridges; one in particular is an intra-subunit salt bridge between D83, located in the apical domain, and K327, located in the equatorial domain as shown on the left in Figure 19. The α-carbons of these residues exist only 9Å apart, locking the apical domain in place and exposing helices H and I that function as SP binding sites. Apical domain expansion facilitated by binding ATP drives the α-carbons of D83 and K327 to 37Å apart abolishing the **T**-state stabilizing salt bridge as shown on the right in Figure 19 (66).
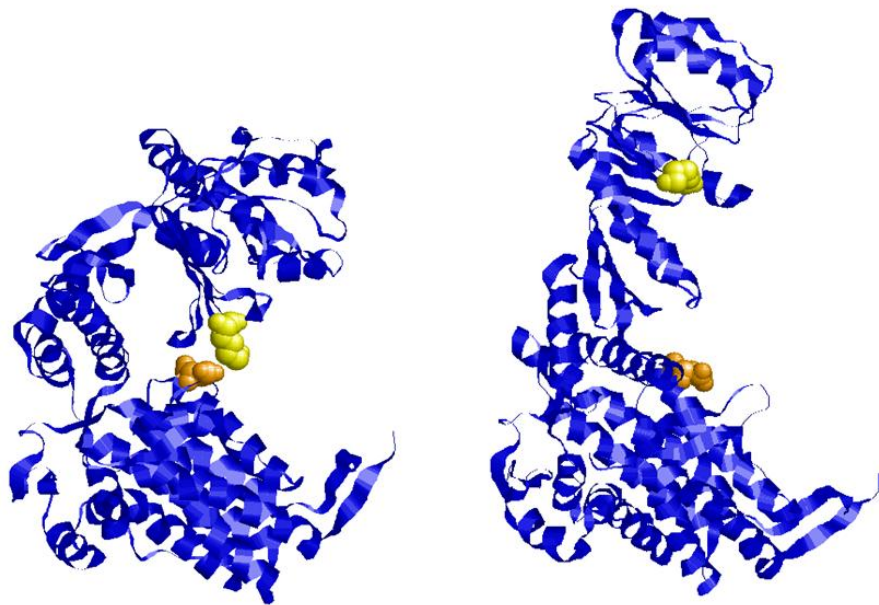
Figure 19: Structures highlighting the location of intra-subunit interactions governing the T to R transition. In A, the T state (left) and R state (right) of the D83 (orange spacefill) and K327 (yellow spacefill) intra-subunit salt- bridge. A single subunit is shown for clarity. Structures were constructed using PDB file 1AON (9).

The ability to create a homogenous population occupying a desired allosteric state by manipulation of the properties of rings is an extremely attractive proposition. Selectively forcing or preventing the population of an allosteric state interrupts the normal GroE cycle, and creates an opportunity to test the proposed allosteric models and coincident

44

regulation. Through selective mutagenesis of intra-subunit salt-bridge residues, it is possible to lock the ring in the T state, or alternately shift the equilibrium in favor of the R state.

Murai et al. constructed a D83C/K327C mutant that, upon oxidation becomes covalently cross-linked in the **T** state. They found that inhibiting the expansion of the apical domain eliminates the ability of GroEL to bind GroES (66). Conversely, a mutant GroEL lacking the intra-subunit salt bridge, creating by replacing the D83 residue with alanine, is expected to destabilize the **T** state. Here we explore the properties of the D83A mutant. A destabilized **T** state is expected to impair the chaperonin cycle if either scheme 2 or 3 are correct (Figure 20). Conversely, turnover of the GroEL machinery will not be impacted in the case of scheme 1.
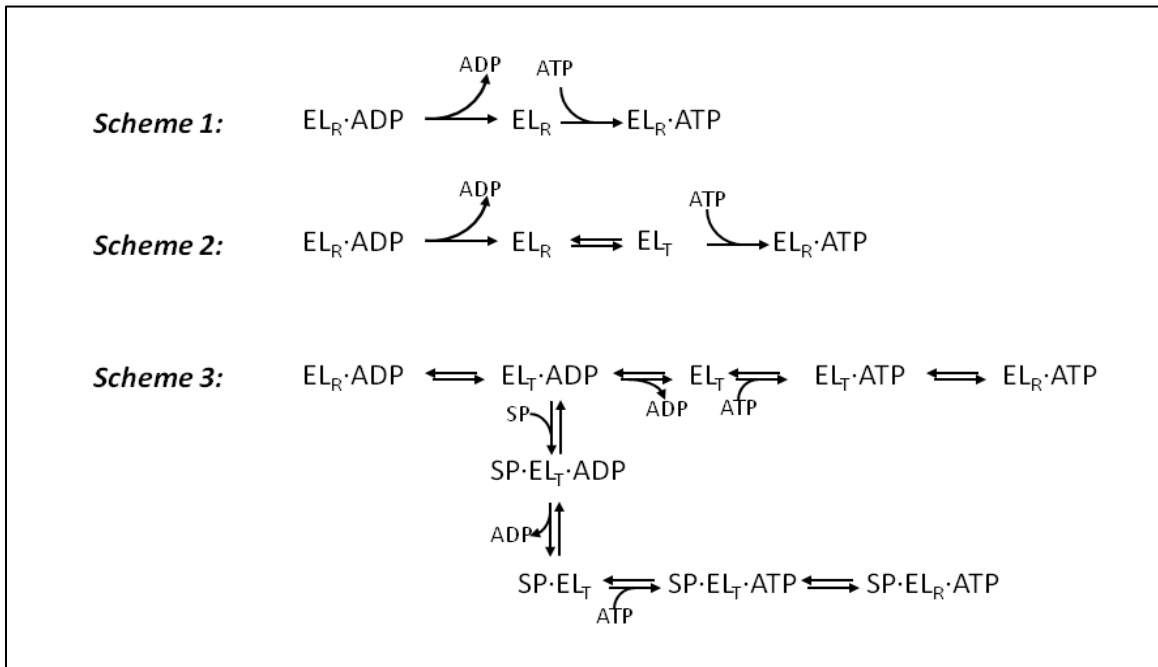
Figure 20: Three possible models of the allosteric transitions that occur upon release of product ADP from GroEL. In scheme 1, upon release of the product ADP, GroEL occupies the R state and is able to bind ATP. In

scheme 2, there is an equilibrium between the T and R states only in the absence of nucleotide. Scheme 3 allows for transition to the T state with nucleotide still bound to the *trans* ring. This possibility presents a unique pathway to explain the increased rate of ATP hydrolysis that occurs in the presence of SP.

3.2 Additional Methods

3.2.1 Design of the GroEL$_{D83A}$ Mutant

Primers for a destabilized intra-subunit mutant were designed by Dr. Asha Acharya. The GAC to GCA change at GroEL codon 249 underlined in the Figure 21 modifies the aspartic acid residue to an alanine, and also creates a blunt end PvuII restriction site used to identify plasmids containing the mutation of interest by agarose gel electrophoresis. Mutagenesis and protein purification was carried out as described previously in the materials and methods chapter.

EL WT: 5'-GCC TCT AAA GCA AAC <u>GAC</u> GCT GCA GGC GAC GGT ACC-3'

EL D83A: 5'-GCC TCT AAA GCA AAC <u>GCA</u> GCT GCA GGC GAC GGT ACC-3'
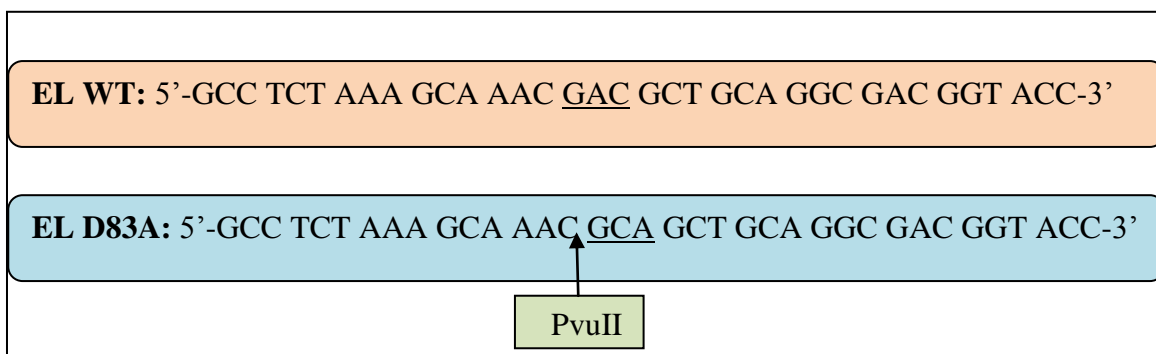
PvuII

Figure 21: The sequence of WT EL (top) and the primer sequence used to create mutant D83A (bottom). Codon 249 where the sequence was changed from aspartic acid to alanine is underlined. The PvuII restriction site is highlighted in red with the position of the cut shown by the arrow.

3.2.2 Capping Free Thiol Groups

Experiments using GroEL$_{D83C/K327C}$ mutant developed by Murai et al. require treatment of the material with an oxidizing agent such as diamide to cross-link the disulfides. This presents a technical problem for discharge experiments because the fluorescently labeled GroES$_{98C}$ retains a population of free thiol groups. Upon oxidation

of the GroE complex, aggregates appear. To minimize aggregate formation, fluorescently labeled GroES$_{98C}$ was treated with a molar equivalent of NEM to cap the free thiols as shown in part A of Figure 22. GroEL$_{D83C/K327C}$ was reduced and fluorescently labeled as well (part B of Figure 22). GroEL•GroES complexes were formed by addition of ATP. The complex was desalted by PD-10 column and then the *trans* ring was locked in the T state by oxidization using either diamide or dimaleimide (part C of Figure 22).

Efficient binding of the fluorescently labeled, NEM capped GroES to GroEL was confirmed by observing the shift of the fluorescence elution of samples run on a TSK-4000 column. Both samples contained the labeled, capped GroES, wild-type GroEL, 100mM K$^+$, 10mM Mg^{+2}, and 50mM Tris, pH 7.5. One sample was incubated for 30 minutes in the presence of 50µM ATP whereas the other lacked ATP. In the absence of ATP, no fluorescence co-eluted with the GroEL peak, but in the presence of ATP, all the fluorescence eluted with the GroEL peak (chromatogram not shown).
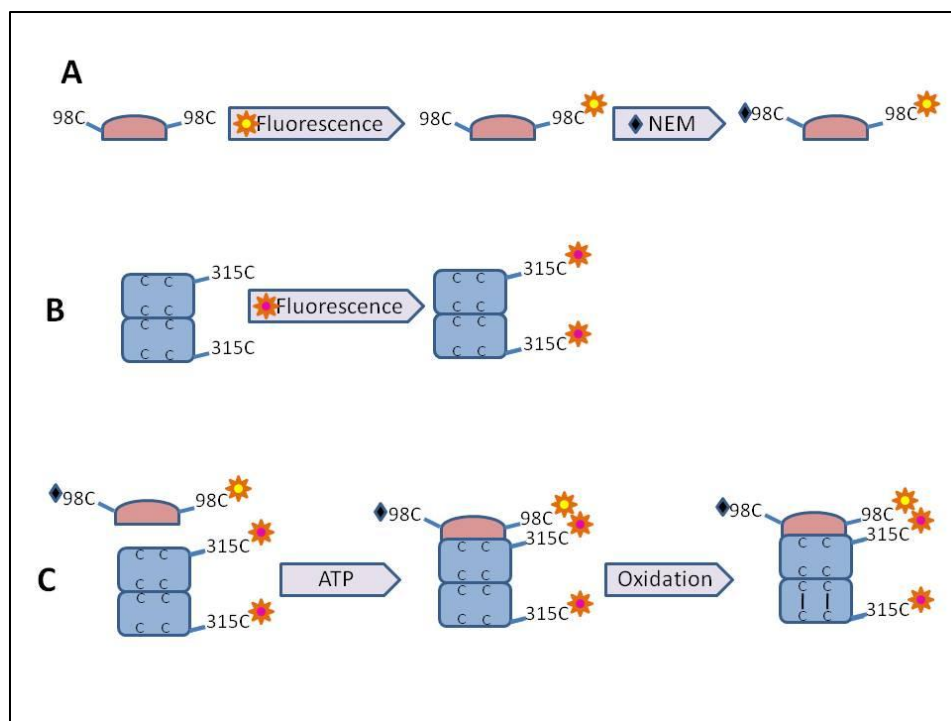
Figure 22: Capping free thiols to prevent aggregation during GroES discharge experiments. In A, GroES98C was first fluorescently labeled and then treated with NEM to block free thiol groups. The GroEL is also fluorescently labeled as shown in B. To create the cross-linked complex, the two proteins were combined and treated with ATP. The *trans* ring was locked in T state through oxidation to create a disulfide bridge between the 83C and 327C positions.

3.3 Results

3.3.1 Comparing the ATPase activity of wild type GroEL to GroEL$_{D83A}$ in the presence of 100mMK$^+$

ATPase activity of EL wild-type and EL$_{D83A}$ were measured between 0 and 1500μM ATP in the presence of 100mM K$^+$. Wild type GroEL exhibits maximum ATPase activity at approximately 40 μM ATP, but removal of the inter-domain, intra-subunit salt-bridge shifts the peak ATPase rate to 10 μM ATP as shown in Figure 23 A & B. The rapid rise in ATPase activity exhibited by the mutant is a hallmark of lost cooperativity. (67)

Additionally, activity for GroEL$_{D83A}$ is about half that of wild type at the point of maximum ATPase activity and only one third that of wild type at high ATP concentrations. The mutant exhibits a decrease in affinity for ligand in the **R** state with a concomitant increase in affinity for ligand in the **T** state.
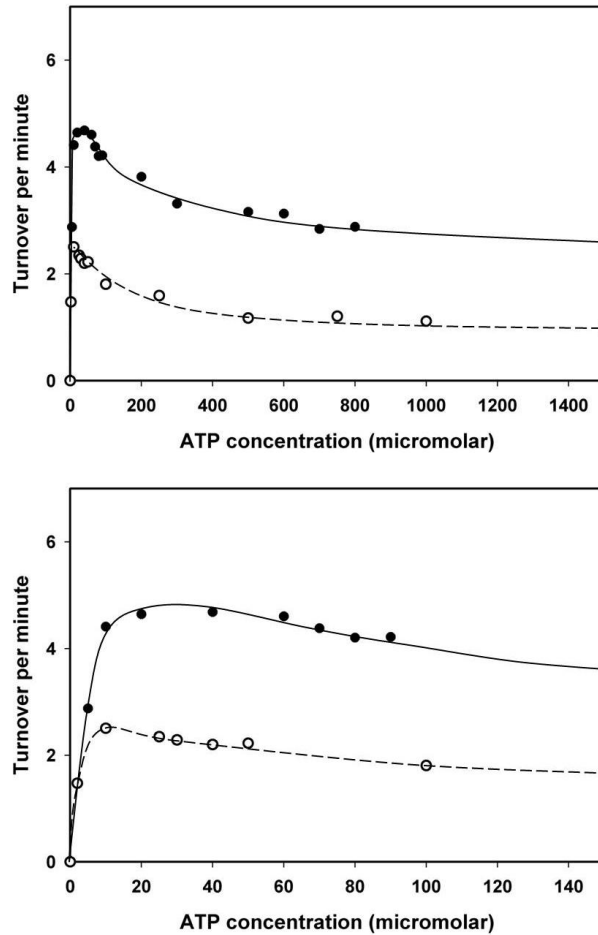
Figure 23: Turnover/minute of GroEL WT (black circles) versus GroEL$_{D83A}$ (open circles) at 2μM GroEL$_{14}$ and 100mM K$^+$. The full scale is shown on the top and an expanded version is on the bottom to show the rapid rise in ATPase activity of the EL$_{D83A}$ mutant. Traces were drawn by hand to assist in comparison of the plots.

Potassium is a known allosteric affector of GroEL. (34) As potassium concentration is increased, the affinity of GroEL for nucleotide also increases, therefore product nucleotide (ADP) remains bound to the active site for longer times resulting in slower

49

turnover of the system. (34) This dose-response aspect is a way to regulate the duration of the hemi-cycle. The alternate aspect is also true: as K^+ is decreased the affinity for nucleotide diminishes and ADP is discharged from the ring more rapidly resulting in faster turnover at low K^+ concentrations.

ATPase assays were performed on the $GroEL_{D83A}$ at 1mM K^+. In this environment $GroEL_{D83A}$ recovers the cooperativity of the first transition as demonstrated by the increase of sigmoidocity at low ATP concentrations. The maximum rate of ATP hydrolysis is shifted to 60 µM ATP compared to 10 µM at 100mM K^+ as shown in Figure 24 A and B. Compared with wild type GroEL, the first transition of the D83A mutant occurs more rapidly in the presence of 1mM K^+ and the maximum rate of turnover is 3.5 turnovers per minute versus 6.5 per minute for wild type.
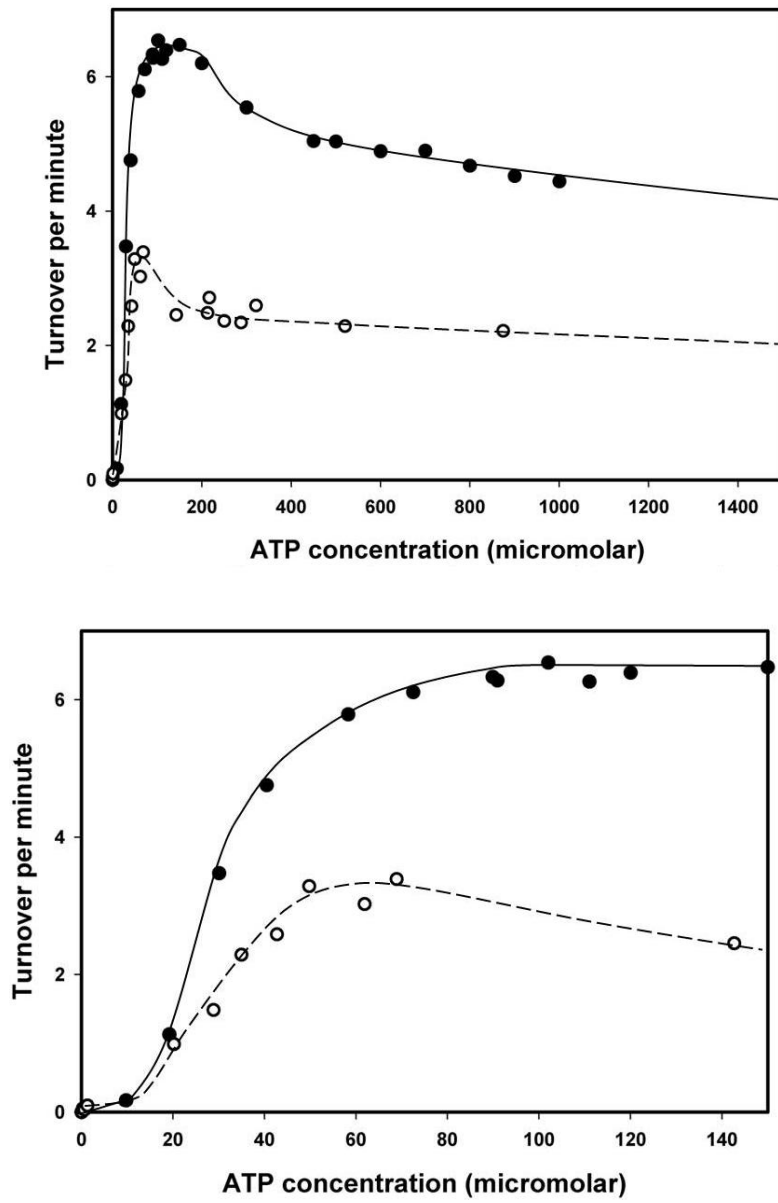
Figure 24: ATPase activity of WT and 83A mutant in the presence of 1mM K$^+$. Full scale is shown on top and an expanded scale is shown on the bottom. Traces were added by hand to help the viewer follow the plots.

3.3.2 Exploring the effects of GroES and substrate protein

Upon addition of GroES, ATPase activity of SP free wild type GroEL in the presence of 1mM ATP and 100mM K^+ slows to about 0.5 turnovers per minute. Addition of SP to the asymmetric complex greatly stimulates ATPase activity and loss of the second transition is observed (top of Figure 25). In the case of GroEL$_{D83A}$, addition of GroES halts ATP hydrolysis except at very low ATP concentrations (between 0 and 50 μM) where minimal turnover in the range of 0 to 0.3 turnovers per minute is observed (bottom of Figure 25). The stalled ATPase activity is reversible upon addition of substrate protein. Turnover is resumed at a rate three times greater than that of GroEL$_{D83A}$ and ATP alone. .
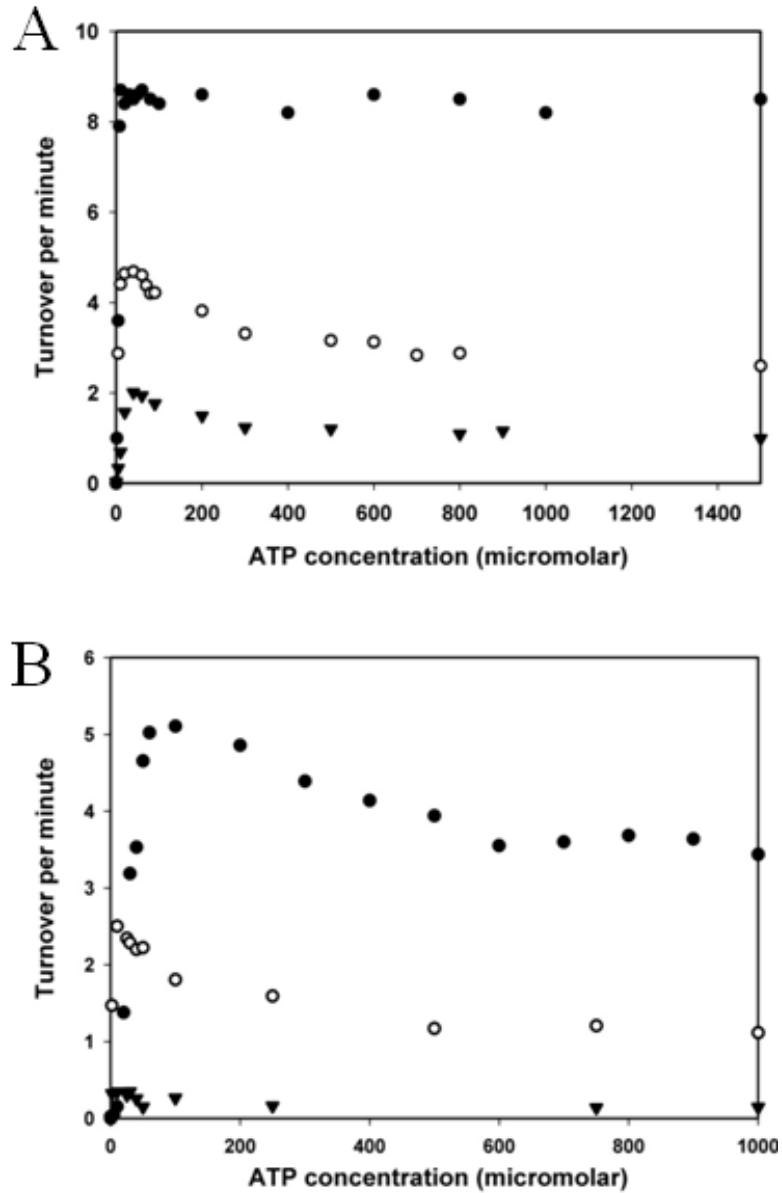
Figure 25: Rate of ATP hydrolysis of WT GroEL compared with EL83A at 100 mM K$^+$. The top shows data for wild type GroEL, and bottom shows data for GroEL$_{D83A}$. ATPase rates were measured in the presence of ATP (open circles), ATP and ES (black triangles), as well as ATP, ES and SP (black circles). Addition of GroES to the EL83A mutant almost completely halts turnover, whereas the turnover rate of WT GroEL is decelerated to about 1 turnover per minute. Upon addition SP, the turnover of EL83A is rescued to approximately the level of turnover of WT.

3.3.3 Defining GroES residence time on EL$_{D83A}$ in the absence of substrate protein

The rate of ATP consumption by EL$_{D83A}$ is well defined by the work above. Although it is clear that GroES increases the length of the hemicycle, the occupancy time of GroES on the destabilized mutant GroEL remains unclear. To investigate the residence time of GroES on the asymmetric complex, GroES discharge was measured using a TSK-4000 gel filtration HPLC column exploiting the unique elution times of GroES and the GroE complex. Here, the [GroEL$_7$*GroES$_7$*ADP]^{cis}•[GroEL$_7$]^{trans} complex was formed at 30°C using fluorescently labeled GroES and unlabeled GroEL with the same buffers as were used for the stopped-flow experiments.

The complex was challenged with wild type GroES and 1mM ATP, then quenched at set time-points using glucose and hexokinase to deplete residual ATP along with 5 mM ADP to stabilize and remaining GroEL*GroES complexes. The advantage of using this method is that GroES release could be examined over long times because the fluorophores are not continuously excited over the entire course of the experiments, thus eliminating the complicating contribution of photobleaching. Experiments were performed using EL$_{D83A}$, wild type GroEL, and oxidized GroEL$_{IAX}$. A stock solution of each variety of GroE complex was prepared, and aliquots were removed and challenged for a particular duration, then quenched for each time point to stabilize remaining complexes. The samples were run on the HPLC at a rate of 1.5 mL per minute in the presence of 100 mM K$^+$, 50mM Tris pH 7.5, 10 mM MgCl$_2$, DTT, and 15 µM ADP to stabilize the resting state of remaining GroE complexes. The oxidized GroEL$_{IAX}$ was run in the absence of DTT.

3.3.3.1 Quenching with hexokinase, glucose, and ADP stabilizes the asymmetric complex

Preventing slow exchange of GroES after quenching of the sample is essential to the success of this experiment. To ensure that the % occupancy measurement was accurate over the course of the experiment, the method used to quench samples was tested by creating an asymmetric complex as describe above using wild type GroEL and fluorescent GroES. The material was challenged with ATP and GroES as described, immediately quenched, then split into two samples. The first sample was injected onto the TSK-4000 column immediately and the second sample was injected after incubation at 30°C for 40 minutes.

The asymmetric complex co-elutes with uncomplexed GroEL at 16.5 minutes, and GroES alone elutes at 19.5 minutes. The % occupancy of fluorescent GroES at 16.5 minutes was within 2% of the original injection confirming the efficacy of the quenching method used for further HPLC discharge experiments (Figure 26). If the quencher were ineffective, demonstration of complete discharge of fluorescent GroES would be exemplified by a shift of the fluorescence peak retention time to 19.5 minutes.
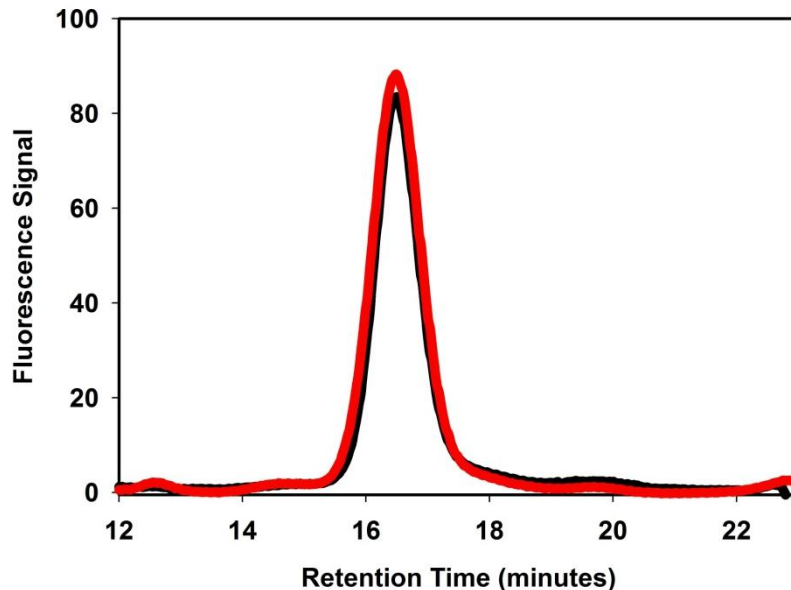
Figure 26: Release of GroES is effectively prevented by addition of hexokinase, glucose, and excess ADP. The red trace was the quenched sample zero minutes after quenching, whereas, the black trace is the same material injected 40 minutes after quenching.

3.3.3.2 The Mean Residence Time (MRT) of GroES can be tuned by manipulation of the D83/K327 intra-subunit salt-bridge.

Destabilization of the intra-subunit salt bridge has severe consequences for the turnover of GroEL in the presence of GroES as demonstrated above. One explanation is that the MRT of GroES on the destabilized mutant is much longer compared to those complexes formed with GroEL$_{wt}$. In the case of wild-type, we propose the *trans* ring exists in equilibrium between the intra-subunit salt-bridge stabilized **T** state, and the **R** state as shown on the left in Figure 27. Manipulation of the salt-bridge allows us to influence the allosteric state of the *trans* ring. Removal of the salt-bridge, as in GroEL$_{D83A}$, reduces sampling of the **T** state, and shifts the *trans* ring equilibrium toward the **R** state, as shown on the right in Figure 27. The *trans* ring can be forced to occupy the **T** state by replacing the salt-bridge residues with cysteines, then covalently cross-linking

56

them as shown in Figure 27, center. If it is mandatory for the *trans* ring to occupy the **T**

state before discharge of GroES from the *cis* ring is possible, a longer MRT is expected

for the destabilized mutant, and a shorter MRT is expected the case of the double cysteine

mutant.
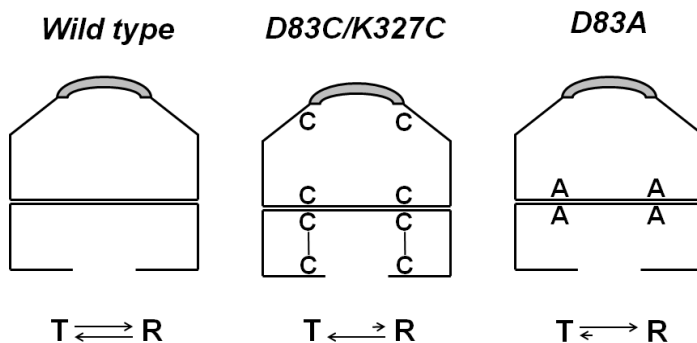
Figure 27: The equilibrium between the T and R allosteric states is changed through modification of the intra-subunit salt bridge. In the absence of nucleotide in the *trans* ring, wild type GroEL shown at left favors the T state. By oxidation of the trans ring cystines of GroELD83C/K327C (center) the ring is mechanically forced to occupy the T state. By destabilizing the *trans* ring by removing the salt bridge using an alanine mutation at position 83, the R state is favored.

Using fluorescently labeled $GroES_{98C}$, three species of asymmetric complexes were

created: $GroEL_{wt}*GroES_{98C}$, $GroELD83A*GroES_{98C}$, and $GroEL_{83C/K327C}*GroES_{98C}$. In the

case of the $GroEL_{83C/K327C}*GroES_{98C}$, the material was oxidized with diamide such that ~

30% of the subunits were oxidized. On average, four of the seven subunits of the *trans*

ring were oxidized, locking the *trans* ring in the T state (30). A non-reducing SDS-

PAGE was run for each sample to confirm cross-linking ratios (Figure 28).

Wild type GroEL discharged GroES with a mean residence time of 52 seconds. This value is comparable to the previously established value of 50 seconds (Figure 29) (33). The oxidized $GroEL_{D83C/K327C}$ mutant discharged GroES much more rapidly. Within 2 seconds, the limit for manual mixing, 59% of the labeled GroES had already discharged from the oxidized $GroEL_{D83C/K327C}$, and only 9% of fluorescent GroES remained bound to GroEL after 45 second. The EL_{D83A} mutant had and initial lag phase followed by slow release with a half-time of ~75 seconds.
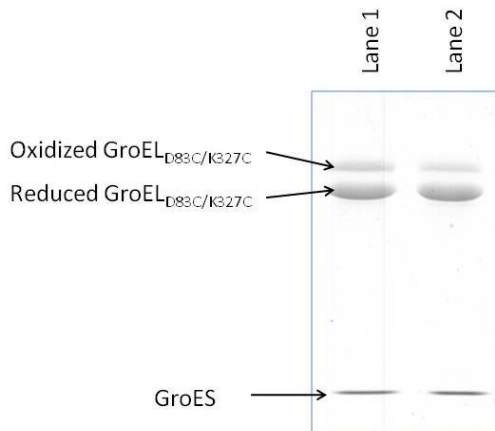
Figure 28: SDS-PAGE of covalently cross-linked double cysteine mutant. SDS-PAGE was used to confirm the oxidation of $GroEL_{D83C/K327C}$ samples. The material in lane 1 is from the time=0 second sample, and lane 2 is from the time=50 seconds sample. The two GroEL bands were compared by measuring the band density with a densitometer. All samples contained approximately 28% oxidized subunits.
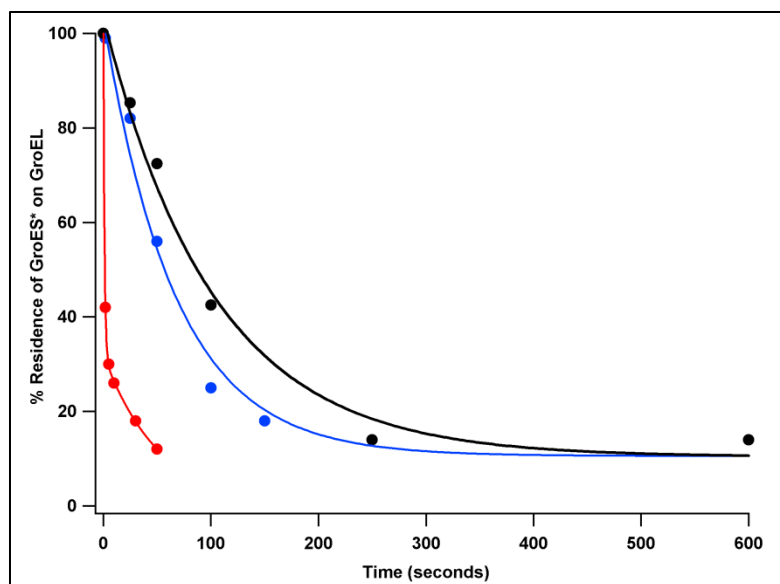
Figure 29: Rate of release of fluorescein labeled GroES from GroEL83A (black), wild type GroEL and oxidized GroEL_{D83C/K327C} (red).

3.4 Discussion and Conclusions

Nested cooperativity posits that GroEL exists in two allosteric states: **T** and **R**. The partitioning between these two states is determined by the concentration of nucleotide in the environment. In the absence of nucleotide, rings occupy the **T** state, whereas increasing concentrations of nucleotide drives the equilibrium to the **R** state. But, according to recent fluorescence correlation spectroscopy experiments using the single ring mutant SR1, even at saturating ATP concentrations, GroEL samples the **T** state ~50% of the time (68). Breaking the interaction between apical and equatorial domains, by eliminating the D83/K327 salt bridge, destabilizes the *trans* ring shifting the equilibrium toward the **R** state (Figure 27). If populating the **T** state of the *trans* ring was not an essential step in the chaperonin cycle, removal of the intra-subunit salt bridge should have minimal effect on the rate of ATP hydrolysis as proposed in scheme 1 of Figure 2. Instead, the destabilized mutant displays only ~1/3 the activity in the absence of SP and GroES, a significant reduction compared with wild type. A recent high-resolution

59

structure shows that the **R** to **T** transition is accompanied by a 22° upward rotation of helix M leading to opening of the nucleotide binding pocket (7). The destabilized mutant is unable to efficiently undergo the necessary structural manipulations required for normal ADP discharge, resulting in a lengthened turnover, particularly in high potassium concentrations where the affinity of the enzyme for nucleotide is high.

The initial **TT** to **TR** transition that lends the sigmoidal character to traces of wild type GroEL at low ATP concentrations is not observed in the destabilized mutant at 100mM K^+ and is interpreted as the rings rapidly accessing the **R** state due to increased affinity for nucleotide. The **TT** state, in this case, is difficult to discern. Moreover, ATPase activity peaks at only 10μM ATP as opposed to 40μM for wild type confirming loss of cooperativity in the **T** to **R** transition. In fact, a destabilized **T** state results in similarities with the single ring mutant, SR1, the most striking of which is loss of cooperativity and a shift of maximal ATP hydrolysis to low ATP concentrations (56).

Also, similar to SR1, the presence of GroES nearly halts the $GroEL_{D83A}$ ATPase activity, whereas wild type exhibits ~0.5 min^{-1} (69). In the case of SR1, the lost ability to discharge GroES is occasioned by the absence of a *trans* ring resulting in a complete lack of negative cooperativity. Although GroES is discharged from $GroEL_{D83A}$ as observed with gel filtration chromatography, the inability to access a stable **T** state hinders discharge of ADP from the nucleotide binding pocket and subsequent discharge of the *cis* ring constituents in the presence of GroES resulting in lost negative cooperativity and a faulty cycle. The artificially stabilized **T** state presented by the D83C/K327C mutant emphasizes the importance of a stable **T** state in the efficacious of discharge GroES from

the *cis* ring. Simply cross-linking the *trans* ring primes the engine prompting rapid dissociation of GroES from the *cis* ring.

The presence of SP has an effect similar to cross-linking of $GroEL_{IAX}$ although to a much less dramatic degree. The hydrophobic SP binding pockets, located on helices H and I of the apical domain, are only exposed in the **T** state, and become buried upon transition to the **R** state. Resumption of $GroEL_{D83A}$ ATPase activity in the presence of SP and GroES suggests that the *trans* ring must sample the **T** state, even when occupied by nucleotide as shown in scheme three in figure 2.

Our experiments manipulated the **T** state to **R** state equilibrium by elimination, in the case of $GroEL_{D83A}$, and covalent cross-linking, in the case of $GroEL_{D83C/K327C}$, of the **T** state stabilizing, intra-subunit salt-bridge. Examination of ATPase activity and GroES discharge of the perturbed mutants clarifies the vital role of the *trans* ring in the turnover of the cycle. The **T** state can be accessed when nucleotide is present in the binding pocket and the presence of SP primes the GroEL engine for rapid release of nucleotide and continuation of the cycle as shown in scheme 3 (Figure 20). We conclude a stable *trans* ring **T** state is essential for turnover of the GroEL:GroES complex, and absence of a stable **T** state severely compromises the GroE cycle.

Chapter 4: Recombining Rings and Subunits of GroEL Using

Acetone and Elevated Temperature

4.1 Introduction

Studying allostery in GroEL is complicated because of the dual seven-fold symmetry of the protein. Investigation into the concerted nature of the ring and the sequential inter-ring communications generated interest in the stoichiometry of interactions between GroEL and its substituents. Mutational manipulation of GroEL seems to be the easiest solution. However, because GroEL is expressed as monomers from a single gene, then assembled post-transcriptionally, genetic manipulation of GroEL to incorporate a subunit or ring with unique characteristic is a challenge. An example of such a desirable species is a ring that has a single monomer with defective ATP hydrolysis. The construction of a fused seven-mer created by connecting seven open reading frames, each encoding a monomer of GroEL, was reported by Farr et al. (1,70). However, since publication in 2000, no other work reported use of the fused seven-mer construct. The aim of this chapter is to identify methods able to create mixed ring and mixed subunit constructs of GroEL from two parent populations.

4.1.1 Theory of Mixing

4.1.1.1 Ring Exchange

Beginning with two unique parent species, termed AA and BB, stochastic pair-wise recombination results in four species: AA, AB, BA and BB. The product of the probability of incorporating a particular species at each position is used to calculate the probability of observing the resultant species. Equations are given in Table 3.

Species	Probability Expression	Calculation	Probability
AA	$p_{AA} = p_A * p_A$	$p_{AA} = 0.5 * 0.5$	0.25
AB	$p_{AB} = p_A * p_B$	$p_{AB} = 0.5 * 0.5$	0.25
BA	$p_{BA} = p_B * p_A$	$p_{BA} = 0.5 * 0.5$	0.25
BB	$p_{BB} = p_B * p_B$	$p_{BA} = 0.5 * 0.5$	0.25

Table 3: Calculating the probability of observing a species by random, pair-wise recombination.

In the case of recombination of GroEL heptamers, species AB and BA are indistinguishable due to the symmetry of the tetradecamer. This means there are only three species observed experimentally: AA, BB, and mixed (AB and BA) Figure 30. The probability of obtaining the mixed species is given by $p_{mixed} = p_{AB} + p_{BA}$, with a resultant probability of 0.5. A probability distribution function for incorporation of species A is shown graphically in Figure 31. Considering the probability distribution function, the observed species are described as 0 subunits incorporated, 7 subunits incorporated, and 14 subunits incorporated.
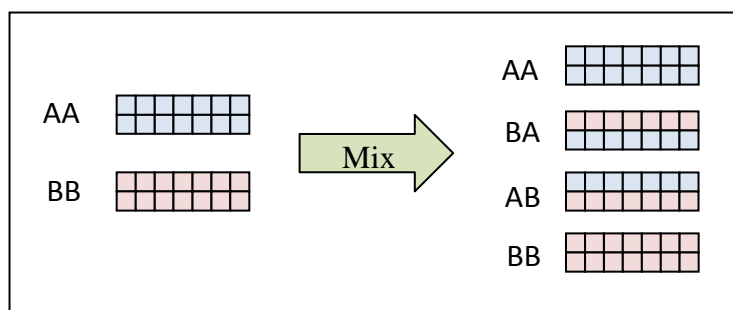
Figure 30: Beginning with the two GroEL parent species on the left (AA and BB), stochastic ring mixing produces four species shown on the right in equal proportions. Each line of seven boxes represents a heptamer.
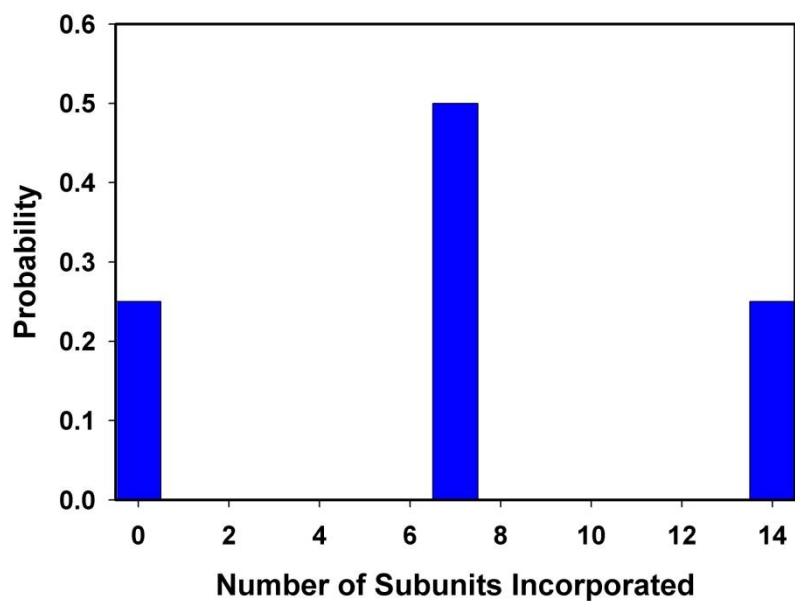
Figure 31: Example expected experimental results when combining rings of GroEL B with GroEL A.   One quarter of the population contains only A (number of subunits incorporated equals 0), half of the population contains one ring of B (number of subunits incorporated equals 7), and a quarter of the population is composed only of B (number of subunits incorporated equals 14).

4.1.1.2 Subunit Mixing

Subunit mixing is more complicated than ring mixing because of the number of mixed species that can be created with the fourteen subunits of GroEL.   For example there are fourteen ways to incorporate a single, unique subunit into a tetradecamer (Figure 32).   Incorporating seven unique subunits can be accomplished 3432 different ways (Table 4).   In fact, there are only 15 unique species that must be considered (when n=0 through 14).   Accounting for redundancies is necessary since no subunit position is unique in GroEL unless one is considering one position in respect to another.
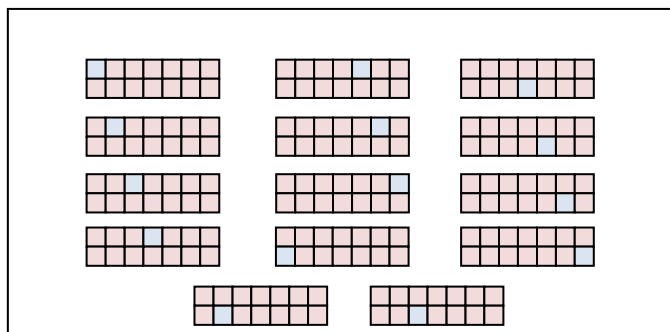
Figure 32: There are fourteen ways to incorporate a single unique subunit, shown in blue, into a tetradecamer. These redundancies must be accounted for when calculating the probability distribution of subunit

n	Possible species
0	1
1	14
2	91
3	364
4	1001
5	2002
6	3003
7	3432
8	3003
9	2002
10	1001
11	364
12	91
13	14
14	1
Total # of Species:	16384

Table 4: A huge variety of species can be created by incorporating n number of a particular subunit into a tetradecamer. However, because of the dual seven-fold symmetry of GroEL, there are actually only 15 unique species, and the rest are redundant.

The expected population for subunit mixing can be calculated with the bionomial

distribution function $P(n, N) = (p^n(1-p)^{N-n}) \left(\frac{N!}{n!(N-n)!} \right)$, where n is the

number of times a particular case occurs, *i.e.* the number of times a mutant subunit is

incorporated into a tetradecamer, and p is the probability of that event occurring.   N is

the number of trials. In this instance N is always 14 because there are 14 subunits.   The

probability distribution is plotted in Figure 33.   Since there is 0.5 probability of

incorporating a monomer from GroEL 'A' and a 0.5 probability of incorporating a

monomer from GroEL 'B', observation of a tetradecamer composed of only one or the

other parent species each carry a probability of 6.1 E^{-5}.
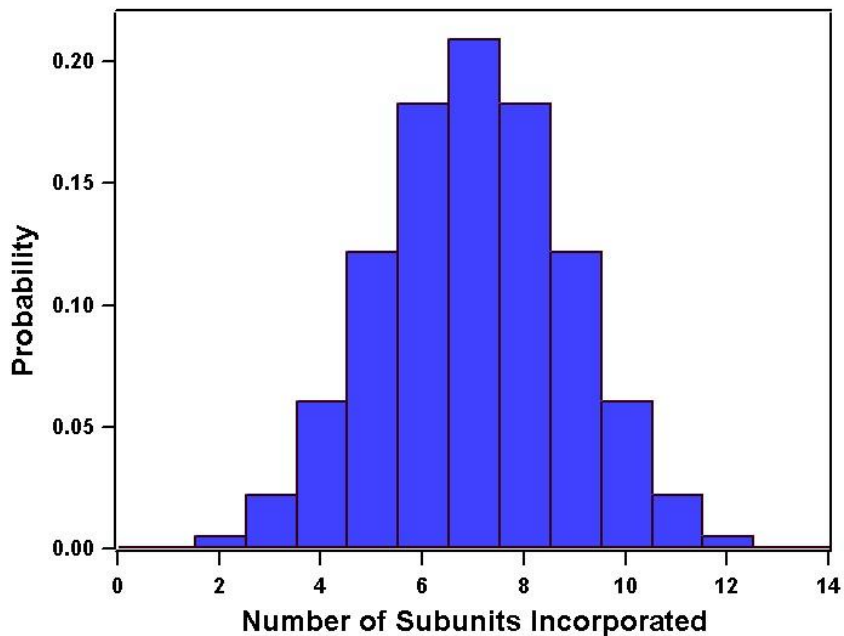
Figure 33: Probability distribution for subunit mixing at equilibrium.

Provided the population is permitted to come to equilibrium, the distribution function

above is expected.   If equilibrium is not reached, determining whether a system is

recombining by subunits, rings, or both becomes more problematic since the parent species are still a large constituent of the population. Experimentally, a partially equilibrated system like the one shown in Figure 34 can appear very similar to that of ring mixing shown in Figure 31.
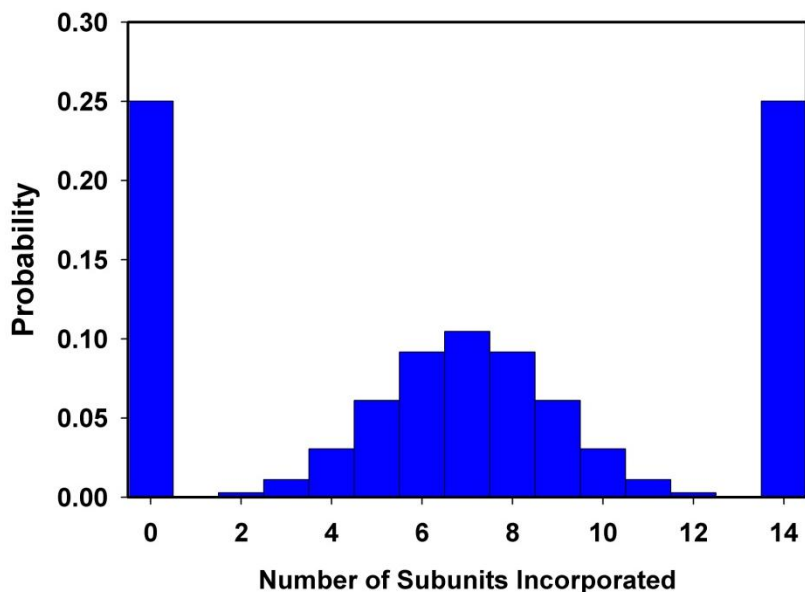
Figure 34: A simulated distribution for subunit mixing that is not permitted to reach equilibrium. Prominent parent species remain, making the system easily mistaken for ring mixing.

4.1.2 Systems for Mixing

The ability to adjust the stoichiometry between types of subunits or rings in a tetradecamer is clearly a valuable tool for future study of GroEL. Methods able to produce consistent mixed rings or subunits must be developed and tested to begin the next phase in understanding GroEL. After scouring the literature, two published mixing systems were identified: Urea treatment, and treatment with a combination of heat and ATP. A third method, acetone exposure, was identified experimentally.

4.1.2.1 Urea

Two mixing methods have been previously reported, one to recombine subunits and the other to recombine rings. The method for scrambling subunits requires treatment with 8M urea to denature and simultaneously break intersubunit interactions of the tetradecamer. Following denaturation, a rapid dilution step is used to reconstitute the material.(71) In the Lorimer laboratory, work with urea has failed to produce an adequate yield of reconstituted material for further experimentation.

4.1.2.2 Heat and ATP

The second published method claims rings are exchanged by incubating tetradecamers in the presence of 50 mM K^+, 5 mM $MgCl_2$, 50 mM Tris pH 7.5 and 5 mM ATP at 42°C for 45 minutes. To demonstrate the efficacy of the ring mixing protocol, Burston et al. used two chromatographically unique species of GroEL: wild type and a mutant they referred to as '3-7-9'. The '3-7-9' mutant contains mutations Y203E, G337S, and I349E. These modifications are claimed to result in the material migrating as a distinct band with delayed migration by SDS-PAGE, and eluting nearly 20 minutes prior to wild type GroEL on a MonoQ 10/10 anion exchange HPLC column (Figure 35).

There are two main points of dispute. First, the claim of resolving these two species by SDS-PAGE is perplexing. Tryptophan, isolucine, and glycine contribute a total of 410.5 Da to the molecular weight of the GroEL monomer, whereas replacement with two glutamic acid residues and serine total 399.3 Da reducing the total molecular weight of the subunit by 11.2 Da. SDS-PAGE lacks the power to resolve a hexa-histidine tagged GroEL from the wild-type, a difference of 931.2 Da (unpublished result). Resolution of subunits with only an 11.2 Da difference in a 57,000 Da protein subunit, a 0.02%

difference in mass, would be surprising even considering the change in dipole moment contributed by the residue change. Assuming resolution between the species is possible with such a small mass difference, it would be expected that the mutant species would migrate further since it is the lighter of the two, the opposite of that reported.
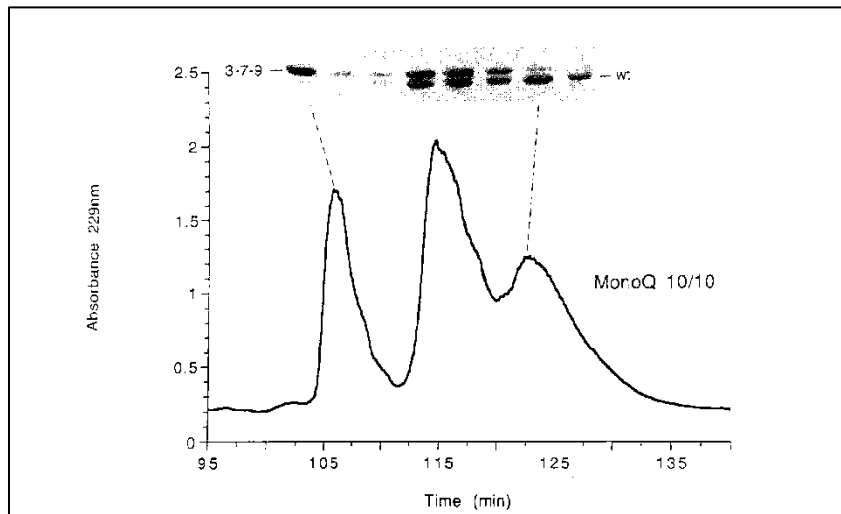
Figure 35: SDS-PAGE and MonoQ 10/10 chromatography of heat and ATP treated material.
Figure from Methods in Enzymology, page 145. (1)A mixture of wild type GroEL and '3-7-9' mutant were treated using the described heat and ATP method, then separated on a MonoQ 10/10 column. An SDS-PAGE was run on fractions eluting from the column, and the resultant band migration is shown above the chromatography.

The second cause for concern is that replacement of two uncharged residues with negatively charged glutamic acid residues resulted in the protein eluting earlier on an the MonoQ 10/10 column. Anion exchange resins such as MonoQ 10/10 work by binding negatively charged protein to a positively charged, resin-immobilized functional group.

The more negative the protein, the more tightly it binds to the resin. Elution of the '3-7-9' species before that of wild-type is counterintuitive, since more negative species are expected to be retained longer by anion exchange columns.

In addition, the quality of the chromatography was quite poor. Between the two parent peaks, an extremely broad, tailing peak containing the mixed species was observed. (72) In the case of ring mixing three peaks would indeed be expected, one for each parent species, and one for the species containing both a mutant ring and a wild type ring. Assuming equal amounts of both species were used in the mixing procedure, one anticipates a 1:1:2 ratio between wild-type, '3-7-9', and the mixed species; however, this was not observed in the example chromatography. The peak corresponding to the mixed species was uneven and unexpectedly broad spanning the entire elution time between the two pure species and containing more the 50% of the total material. Poor resolution between peaks excludes direct comparison of peak areas.

Fractions run on SDS-PAGE were not indicative of ring mixing. By visual inspection, the bands from the mixed species peak do not appear to have a 1:1 ratio of mutant and wild-type monomers throughout the peak as is expected in the case of ring mixing. These observations are more readily interpreted as incomplete subunit mixing, thus more research is needed to understand the true nature of the heat treatment method.

4.1.2.3 Acetone

Interest in ring and subunit exchange was spurred by investigation into how acetone treatment works to strip contaminating protein from GroEL. The acetone treatment method is described in detail in the materials and methods section. An abbreviated

schematic is presented in Figure 36. Briefly, the GroEL solution is brought to 45%

acetone (v/v). At this point, GroEL and protein contaminants precipitate from solution;

however, upon resuspension of the precipitate, GroEL redissolves. SP remains a visible

aggregate that can be removed by centrifugation. Since recovery of GroEL is never

100%, some denatured GroEL also remains in the precipitate of the final centrifugation

step. Acetone treatment is so effective at removing SP, that only 10% of the rings or

fewer retain a contaminant. Although stripping slightly dirty GroEL using this method is

clearly quite effective, how SPs are actually removed remains unclear.
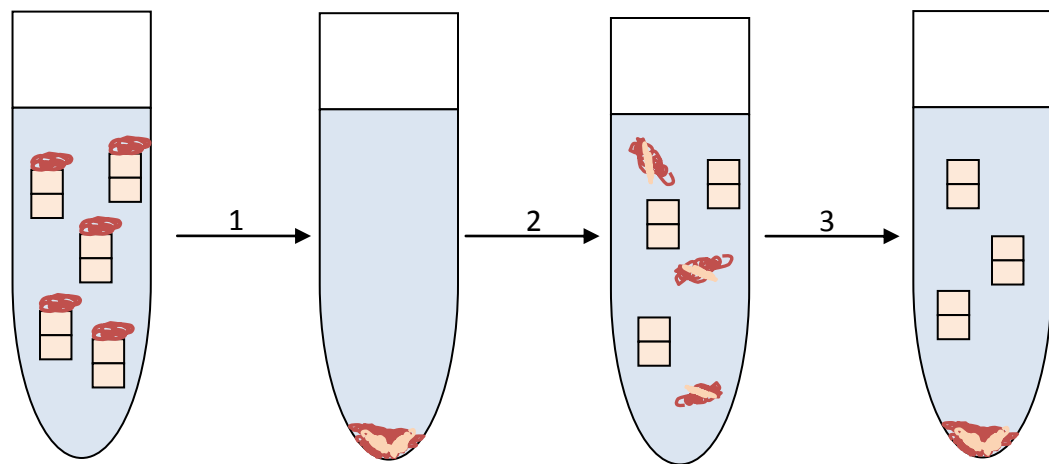
Figure 36: A graphical scheme of the acetone treatment:
On the far left, a preparation of GroEL (orange blocks) is contaminated by substrate protein (red
squiggles). Step 1: The preparation is brought to 45% acetone and then centrifuged. All material
precipitates and the solution is decanted. Step 2: The precipitate is redissolved in buffer. SP and some
GroEL remain aggregated. The reconstituted tetradecamers are stripped of SP. Step 3: The
redissolved material is centrifuged to remove the aggregated proteins. Functional tetradecamer
remains in the supernatant and is collected by decanting.

In exploring acetone treatment, three plausible models for SP removal were

considered. First, the apical domain becomes unstructured while the equatorial domain

remains folded with the subunit and ring interactions remaining in place (Figure 37). Destruction of the hydrophobic SP binding pocket by unfolding helices H and I of the apical domain is expected to cause GroEL to relinquish multivalent binding of SP. Experimental evidence that the GroEL tetradecamer unfolds in a 'top down' manner supports this possibility (73). In this case, no mixed species would be expected.

Second, similar to the claims of the urea treatment method, it is possible the tetradecamer comes apart into individual subunits or small groups (Figure 37). This model also accomplishes release of SP by removing multivalent binding, resulting in exposure of SP to denaturing conditions. In the case that the tetradecamer completely disassembles into monomers, or is in a rapid equilibrium between monomers and some larger structure, it is expected that a binomial distribution of species be observed as in Figure 33. A second way of accomplishing the same situation is a one-in-one-out model in which the tetradecamer loses a single subunit at a time only to have it replaced by another (Figure 37). In this case, the population of monomers in solution during the acetone treatment is minimal. Care must be taken to allow the system to fully equilibrate or confusing data may result.
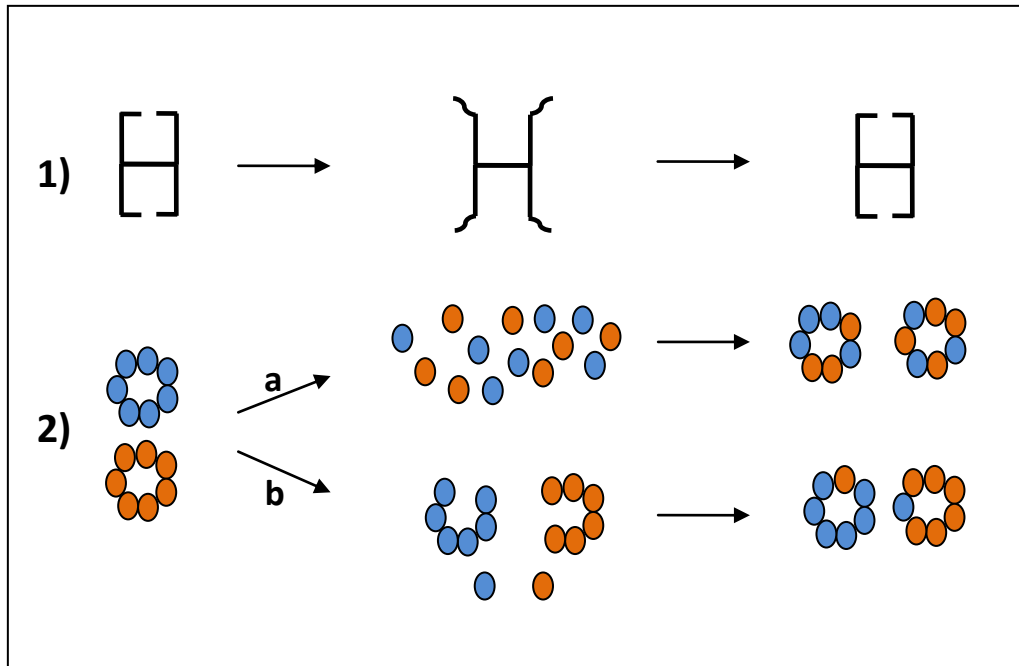
Figure 37: Three possible ways SP may be stripped from GroEL:
In 1) adding acetone to the tetradecamer on the left causes it to unfold in a top down manner. The unstructured apical domains release SP, and at right, refold upon removal of acetone. In 2) the subunits actually come apart to release SP.   Unique species of GroEL are represented as blue and orange seven member rings for ease of illustration. The first possibility is that the rings entirely decompose into subunits as shown in 2a, and then reassemble stochastically upon removal of acetone. The second possibility is a slight variation of 2a. Shown in 2b, rings lose only a single subunit at a time, and replace it with a subunit available in solution. In this situation, the population of independent subunits in the solution is negligible.

Another concern regarding acetone treatment is whether GroEL subunits are being denatured and picked up by intact, functional tetradecamers. Tryptophan fluorescence is used to estimate the extent of contamination since the average protein of 300 to 400 residues contains three to four tryptophan residues. Uniquely, GroEL contains none, making tryptophan a very useful probe to determine contamination. If intact GroEL were able to rescue denatured GroEL monomers, the ability to calculate SP contamination would be undermined by inaccuracy due to seemingly invisible SP.

4.2 Additional Methods

4.2.1 Streptavidin Columns

Streptavidin binds biotin with a dissociation constant (K_d) of 4×10^{-14}M. (74) To exploit the extraordinarily tight binding, GroEL$_{315C}$ was functionalized with biotin maledimide using the same labeling methods as described for fluorescent labels. Labeling efficiency was determined spectrophotometrically using the HABA biotin detection kit from Pierce.

Miniature spin columns were prepared using 500 µL of streptavidin sepharose high performance resin manufactured by GE Healthcare. The columns were equilibrated twice with sample buffer, and then sample was applied and allowed to flow through the column by gravity (Figure 38). The column was centrifuged, and then washed twice with sample buffer. To elute the GroEL bound to the column, a 0.5% SDS (w/v) solution was added to the spin column and allowed to incubate for 10 minutes at room temperature. The column was again centrifuged. Material eluted at each step was collected into separate Eppendorf tubes.
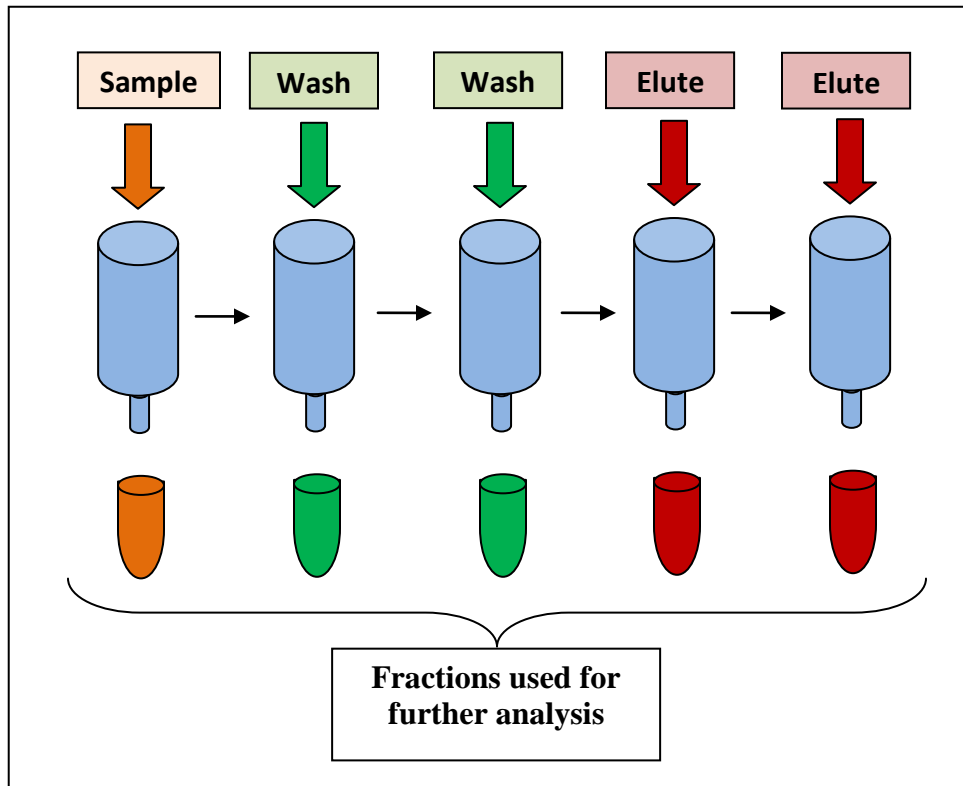
Figure 38: Schematic of streptavidin column experiment.
A mini-spin column shown in blue contains streptavidin sepharose resin. The sample is applied (shown with an orange arrow) and flow through is collected in an eppindorf. Two applications of wash buffer (shown in green) and two applications of elution buffer (shown in red) are sequentially made to the column. The resultant fractions are used in further analysis.

5.2.2 Electrospray Ionization Mass Spectrometry

Electrospray ionization mass spectrometry (ESI-MS) has become an indispensable tool for protein detection because it is able to desolvate protein molecules without disturbing higher order structures of the protein. (75-77) Protein ions are generated in the nano-ESI source by the breaking apart of droplets to form ionized protein species, and dissociation is induced in the ESI interface region of the hybrid quadruple-time-of-flight instrument.

All samples were prepared at the University of Maryland. After treatment of the samples, care was taken to remove solvent components that were added to instigate rearrangement of rings or subunits *via* desalting with PD-10 column into 10 mM Tris pH 7.5, 10 mM $MgCl_2$ storage buffer for shipment at ambient temperature to Amherst. ESI-MS data were collected and analyzed by Rinat Abzalimov of the Kaltashov laboratory at University of Massachusetts, Amherst. Before injection, samples were diluted into 50 mM ammonium acetate buffer, a volatile sample buffer appropriate for mass spectrometry.

4.3 Results

4.3.1 Acetone Treatment

4.3.1.1 Biotinylated GroEL is retained by streptavidin sepharose but biotin free GroEL is not retained

Generating results with confidence in experiments employing streptavidin resin requires confirmation that the resin binds bioinylated species selectively. To demonstrate this, two experiments were performed. In the first control, fluorescently labeled GroEL lacking biotin was applied to a streptavidin column. In the absence of biotin, it is expected that no protein adheres to the column. The fluorescent signal should be observed in the flow through and wash fractions. Native $GroEL_{315C}$ labeled with fluorescein but lacking biotin was applied to the streptavidin resin column, and fractions were collected as described above. A fluorescence spectrum was taken for each collected fraction. All fluorescence was recovered from the resin upon the first wash with 10:10 buffer.
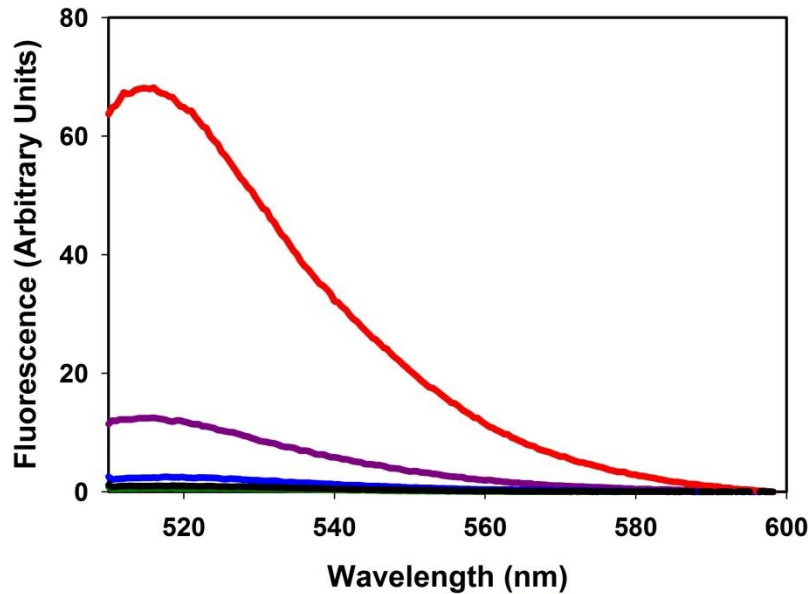
Figure 39: Fluorescence spectra of fluorescein labeled, biotin free GroEL$_{315C}$ streptavidin column fractions. The flow-through (red), first wash and second wash (purple and blue respectively) contained essentially all the fluorescence signal. The elution steps (black and green) showed no appreciable fluorescence.

The second control requires applying only material conjugated with biotin. In this case, the entire fluorescence signal is expected to be retained on the column and eluted in the final two elution steps. Native GroEL$_{315C}$ dually labeled with fluorescein and biotin was applied to the streptavidin resin column, and fractions were collected as described above. A fluorescence spectra was taken for each collected fraction. Flow through and washes with 10:10 buffer failed to remove any appreciable fluorescence from the column. Fluorescence signal was observed in only the elution steps.
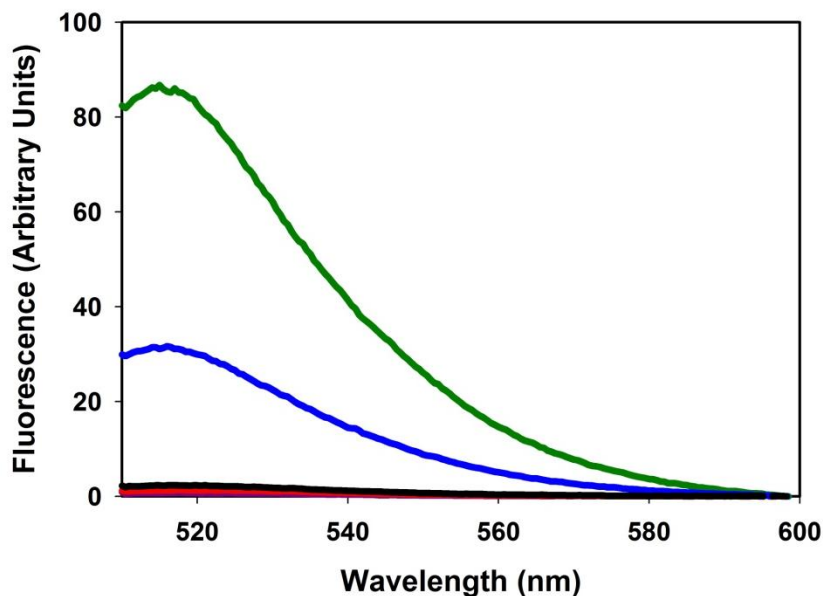
Figure 40: Fluorescence spectra of biotinylated, fluorescein labeled GroEL$_{315C}$. The flow-through and wash steps (black, red, and purple respectively) had no appreciable fluorescence. A large fluorescence signal resulted upon application of the elution buffer.

In order to interpret the fluorescence signals in terms of mixing, almost all of the fluorescence applied to the column must be recovered from the column. Without quantitative recovery, ring and subunit mixing can be difficult to distinguish. Recovery was investigated as follows. Mini-spin columns containing streptavidin resin were prepared. A fluorescence scan was taken of native GroEL$_{315C}$ dually labeled with fluorescein and biotin. The material was then applied to the streptavidin column and fractions were collected as above using a rigorous buffer containing 10% SDS, excess biotin and sodium hydroxide, pH 12 for elution. (74) Fluorescence scans were taken of each collected fraction, and corrected for dilution. The scans from the elution step were corrected for the pH change before comparison. After repeated trials varying both temperature and exposure time to the elution buffer, fluorescence recovery was only 71.7%. Modifying temperature and exposure time did not increase the observed recovery

of fluorescence signal. At less than 75% recovery, the assay is not quantitatively sound, and cannot be used as a stringent test for determining the mode of mixing. However, the assay does offer the ability to confirm mixing is occurring in a particular system. It is in that function the assay is used in the following work.
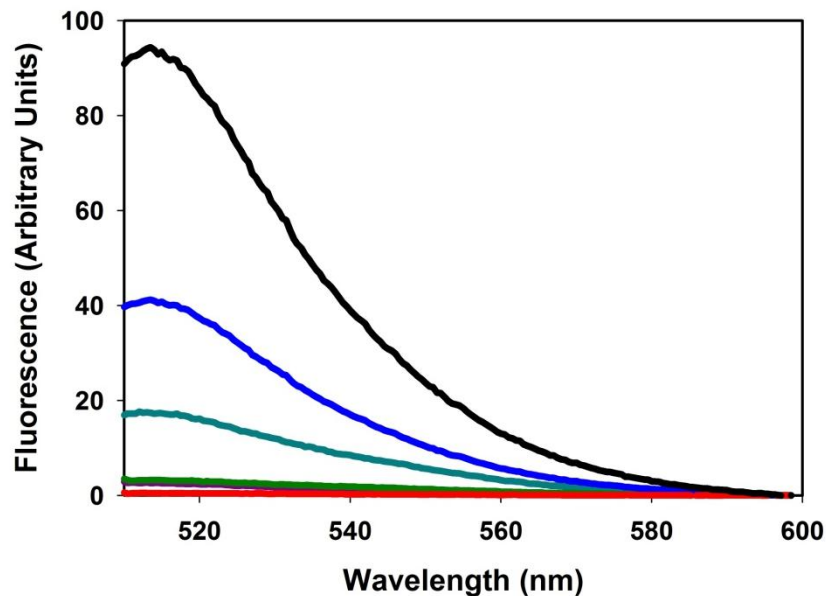
Figure 41: Recovery of GroEL is inadequate to support quantitative analysis of mixing methods. Fluorescence traces were taken of the material before application to the streptavidin column (black), as well as of the fractions collected from the column. The flow-through, first and second wash steps and first and second elution steps (dark green, purple, red, blue and dark cyan respectively) accounted for only 71.7% of the original fluorescence signal.

4.3.1.1 Acetone treated GroEL is retained on Streptavidin resin in a biotin dependent fashion

The predicted population in the case of ring mixing is 1:2:1 with each parent species representing a quarter of the population, but only half of the population carries the fluorescent probe relevant to the assay. In this case, the expected fluorescence signal would be 2:1 where two thirds of the fluorescence signal is retained by the column, and

then eluted with elution buffer due to combination with biotinylated material. One third of the fluorescence signal is expected to pass through the streptavidin column without interaction. These species would be fluorescence material that lacked incorporation of a biotinylated subunit or ring.

Molar equivalents of biotinylated GroEL$_{490C}$ and fluorescein labeled GroEL$_{315C}$ were combined with a final concentration of 11.7μM, and were treated with the standard acetone treatment protocol outlined in the materials and methods. After the final centrifugation step, the material was passed through a 0.22 μm syringe filter, then applied to streptavidin resin miniature spin columns. Flow through, washes, and elution steps were collected as described above. Recovered fluorescence signal from the acetone treated material was entirely observed in the elution step. If mixing were not occurring, fluorescence would not be expected in the elution steps. In the case of ring mixing, some fluorescence is expected to be observed in both the flow-through and wash steps as well as the elution. Since fluorescence material failed to pass through the column with the flow-through and wash steps, it implies subunit mixing is occurring.
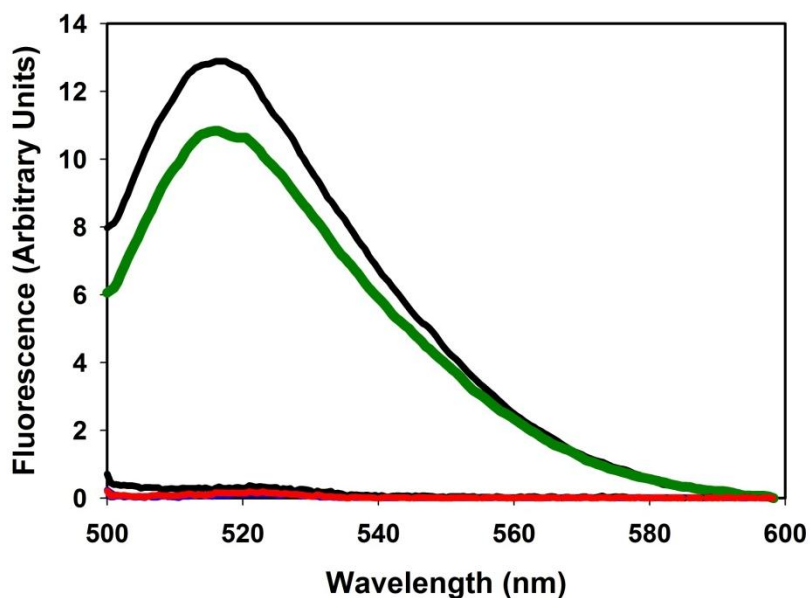
Figure 42: After acetone mixing, fluorescent material was retained by the streptavidin column. The flow-through (black) and wash steps (red and dark pink) showed negligible fluorescence. The majority of the fluorescence signal was observed in the elution steps (black and green).

4.3.1.2 Increased FRET efficiency after acetone treatment of donor only and acceptor only labeled material

FRET between neighboring subunits was also used to detect mixing in $GroEL_{315C}$. The premise of this experiment is that independently labeled donor and acceptor populations are unable to undergo energy transfer unless the two populations have become intermingled on a subunit level since the fluorescent probes would be near enough for ET to occur. In the absence of mixing or in the case of ring mixing, no energy transfer is expected since the fluorescent probes would be on opposite rings or molecules (Figure 43).
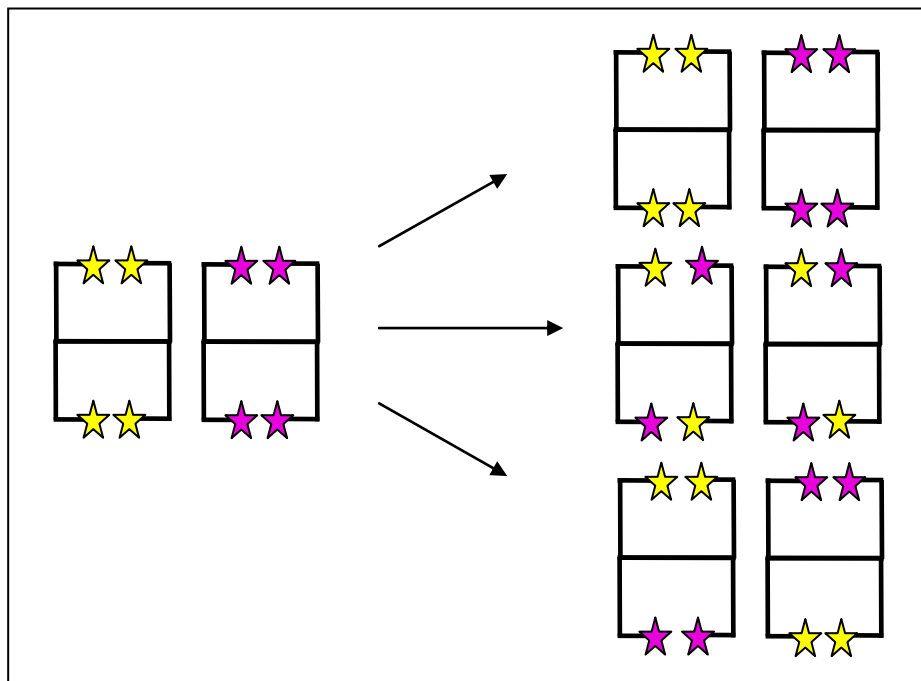
Figure 43: Possible donor and acceptor pairings after recombination.
Combining a donor labeled GroEL (yellow stars demonstrate the position of the donor) with
acceptor labeled GroEL (pink stars) has three possible outcomes shown on the right. In the
case of no mixing (top right) no FRET is expected. If subunits are exchanged (middle right),
the donor and acceptor molecules are near enough for FRET to be observed. FRET is not

Because of the symmetry of the ring, there are three possible ET pairs to consider. Assuming one subunit carries a donor molecule, acceptor molecules could occupy the directly adjacent subunit (labeled 2 in Figure 44), the subunit once removed (labeled 3 in Figure 44) or the subunit twice removed (labeled 4 in Figure 44). Each of these pairs carries a 1/3 probability of being observed assuming stochastic mixing of subunits. To calculate the expected energy transfer (ET), the distance between α-carbons in residue 315 in neighboring subunits was measured in Rasmol using PDB models 1AON and 1KP8, and then plugged into the equation: $ET = \dfrac{1}{1+\left(\frac{r}{R_0}\right)^6}$, where r is the distance

between the dye molecules and R_0 is the Förster distance. In the case of the fluorescein donor and Cy3 acceptor used in this experiment, R_0 is 53 Å. The distance values and expected energy transfer for the T and R state are shown in Table 5.
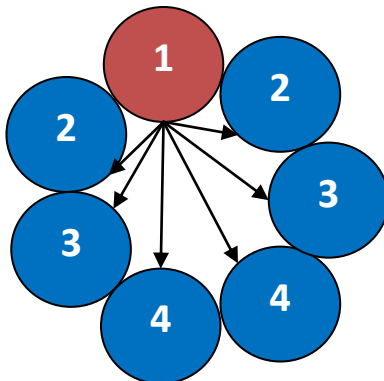
Figure 44: Expected FRET efficiency between neighboring labeled subunits: Expected ET can be calculated from the known distance, R, between the alpha carbon of the labeled residues. Assuming subunit 1 is labeled with donor, there are three FRET pairs that must be considered due to the symmetry of the ring: 1 to 2, 1 to 3, and 1 to 4. If labeled subunits are incorporated stochastically, there is a 1/3 probability of observing each of the

	$r_{T\,state}^{315C}$	$ET_{T\,State}$	$r_{R\,state}^{315C}$	$ET_{R\,State}$
1 to 2	35 Å	0.92	45 Å	0.73
1 to 3	63 Å	0.26	81 Å	0.07
1 to 4	79 Å	0.02	101 Å	0.02
Average ET		0.42		0.27

Table 5: Expected ET between donor and acceptor molecules within a ring of GroEL

is calculated using the distance, r, between the two subunits as shown in Figure 44. Expected ET is shown above for the T state and the R state of GroEL.

To complete this experiment, two populations of fluorescently labeled GroEL were combined in equimolar amounts in the presence of 100mM KCl, 10mM MgCl$_2$, and 50mM Tris, pH 7.5. One population was labeled with the donor, fluorescein, whereas the other population carried the acceptor, Cy3. A fluorescence spectrum was taken using an excitation of 488 nm, and data werre collected between 500nm and 700nm. The solution was then treated with 45% (v/v) acetone. After the final acetone removal step, the material was filtered, and another fluorescence trace was taken in the presence of the same buffer system as above. Finally, the solution was brought to 1mM ATP and rescanned. The scans were normalized with respect to fluorescein emission for the sake of comparison.

Before mixing, no ET was apparent as demonstrated by the lack of Cy3 emission. This scan was treated as the donor only for calculation of energy transfer efficiency. After acetone treatment, the fluorescein/Cy3 pair displayed 6% ET as calculates by the equation $ET = 1 - \frac{F_{DA}}{F_D}$, where F$_D$ is the fluorescence of the donor alone, and F$_{DA}$ is the fluorescence of the donor in the presence of the acceptor. A 3% ET efficiency was observed upon addition of ATP. A decrease in FRET is expected since ATP drives the rotation of the apical domains, thus increasing the distance between residue 315 in neighboring subunits. These results lend credence to the subunit mixing model. However, it is still possible that small aggregates could be contributing the observed ET.
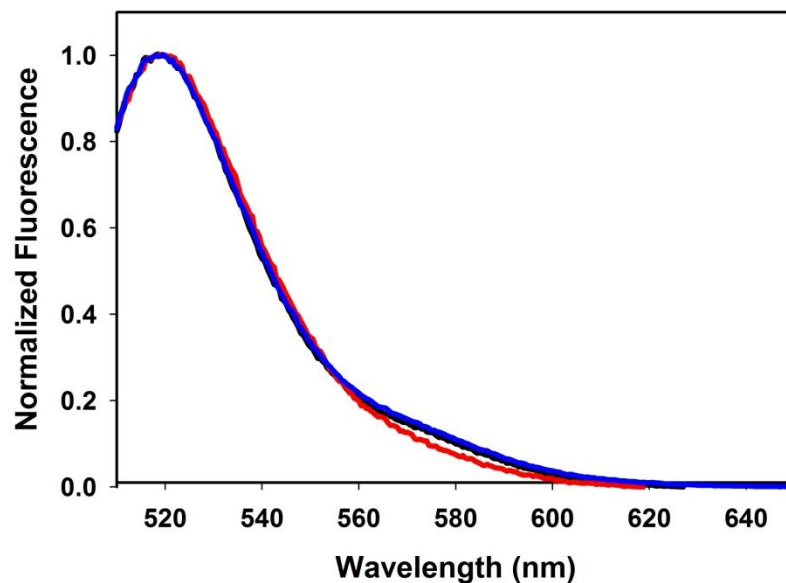
Figure 45: Combining populations of donor-only labeled GroEL$_{315C}$ and acceptor-only labeled GroEL$_{315C}$ results in an increase in ET after acetone treatment. Before acetone treatment (red trace), no ET was observed. After completion of the acetone treatment, 6% ET efficiency was observed (blue trace) notable by the increase in fluorescence at 570 nm. Addition of 1mM ATP resulted in a slight decrease in ET efficiency to 3% (black trace). Fluorescence spectra were normalized to 1 with respect to the donor, fluorescein, for the sake of comparing acceptor emission.

4.3.2 Acetone treatment does not cause simple breakdown into rings or subunits

To better understand the major structural constituents dominating the GroEL population in the presence of acetone, HPLC gel filtration chromatography was performed on fluorescein labeled GroEL$_{315C}$ in the presence of varying concentrations of acetone. Samples were prepared containing 0%, 20%, 25%, 30%, 31% and 35% acetone with a final protein concentration of 29.5 μM. Each sample was injected immediately after a 5 minute incubation period at room temperature onto a TSK-4000 column prequilibrated with buffer containing the corresponding amount of acetone (*i.e.* the sample containing 20% acetone was run on the gel filtration column in the presence of

20% acetone). Samples were monitored by fluorescence at 515 nm using an excitation of 490 nm.

In the absence of acetone, GroEL elutes as a sharp fluorescence peak at 12.5 minutes. As acetone is increased, the fluorescence peak shifts to the right to a position between $GroEL_{14}$ and $GroES_7$ corresponding to smaller sizes, but clearly neither monomer nor tetradecamer. There are three plausible explanations. First, the material is decomposing into rings. Second, the material is in rapid equilibrium between some combination of structures. Third, the composition of the tetradecamer could be maintained with some structural modifications causing a change in retention time. Because the retention times incrementally progress toward smaller sizes as acetone is increased rather than shifting to a particular consistent retention time, it is most likely that the second or third possibilities are valid. This, in combination with the broadening and tailing that occurs as the material is exposed to increasing amounts of acetone support the breakdown of GroEL into substructures as it moves down the size exclusion column.
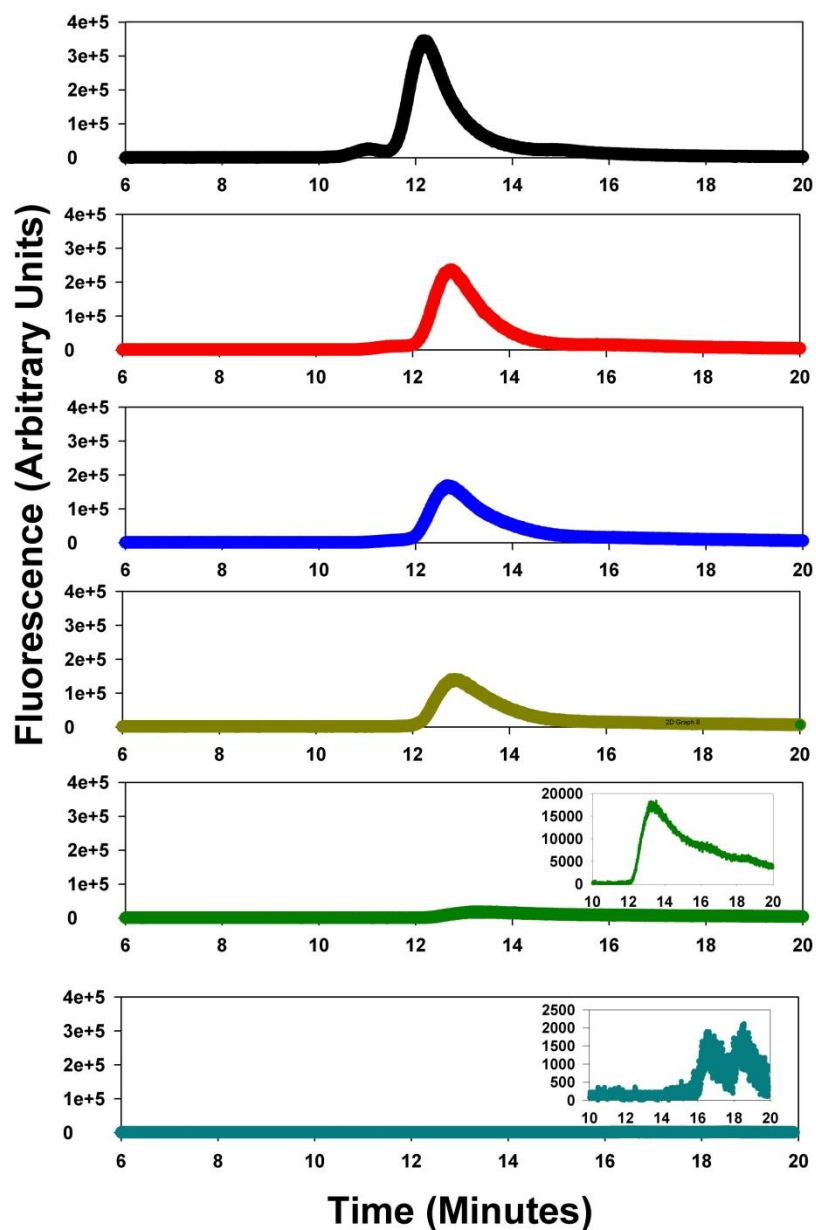
Figure 46: HPLC analysis of fluorescently labeled GroEL in the presence of acetone. In the absence of acetone, GroEL elutes as a sharp peak at about 12 minutes (black trace). As acetone is increased, the peak elutes at later times, broadens, and loses volume. The samples shown here are 0 (black), 20 (red), 25 (blue), 30 (dark yellow), 31 (green), and 35% (cyan) acetone (v/v). An inset is provided for both the 31% and 35% acetone samples for clarity.

The total area of the fluorescence peaks decrease as the volume percent of acetone is increased indicating aggregation is a contributor to the complexity of the acetone system. A critical shift occurs at 31% acetone. At this point, the peak looses much of the fluorescence signal, and exhibits severe tailing indicating the aggregation process has begun to take over. At 35% acetone, only a small amount of fluorescence remains eluting in two peaks at approximately the retention time expected for a monomer. Whether the two peaks correspond to monomers and dimers or perhaps to folded and unfolded monomers is impossible to assert with the given data.

4.3.4 Recombination of GroEL species is accomplished by a 'one-in-one-out' mechanism

The pivotal experiment in understanding the effect of acetone requires the ability to determine the stoichiometry between unique monomers in an acetone treated sample. Using ESI-MS, it is possible analyze stiochiometries of protein complexes; however, two species with unique mass to charge ratios (m/z) are required. The most straightforward method for creating GroEL with a mass difference large enough to be distinguishable from wild-type by mass spec is by using his-tagged GroEL. The addition of six histidine residues results in an additional 931.2 g/mol, or 13,036.8 g/mol for each tetradecamer. Wild type and his-tagged species were initially examined independently to confirm the m/z ratio difference was adequate to warrant further analysis. Even with the large mass difference between the two species, the spectra overlapped remarkably due to the ionization species observed. Because of the poor resolution between the two species, further work with the wild-type and his-tagged GroEL pair was abandoned.

An alternative method for creating a GroEL with a unique mass was devised. Instead, isotopically enriched GroEL was created using ^{13}C and ^{15}N enriched media as described in the materials and methods section. This modification resulted in a heavy tetradecamer (H) with a total mass of 843 kDa as compared to 801 kDa for light (L) GroEL grown in normal LB media. Although the signals overlap in the 10,000 to 13,000 m/z range, the difference is large enough to be discernable by ESI-MS analysis.

The heavy and light species were treated with 45% acetone in a 1:1 ratio. Acetone was removed by PD-10 column, and then the material was diluted into ammonium acetate buffer before injection into the MS under mild ion desolvation conditions. Controlled collisional activation resulted in protein fragments whose masses were used to calculate the stoichiometry of species present in the treated sample (Figure 47). Along with the parent species, recombined species were identified including $L_{13}H_1$, and L_1H_{13}. Since tetradecamers containing a single monomer of the alternate species are present, monomer exchange is unequivocally occurring in the capacity of losing a single subunit or parts of subunits rather than by complete dissociation. The presence of parent species indicates that monomer mixing in the presence of acetone is not a process that reaches equilibrium under feasible treatment conditions.
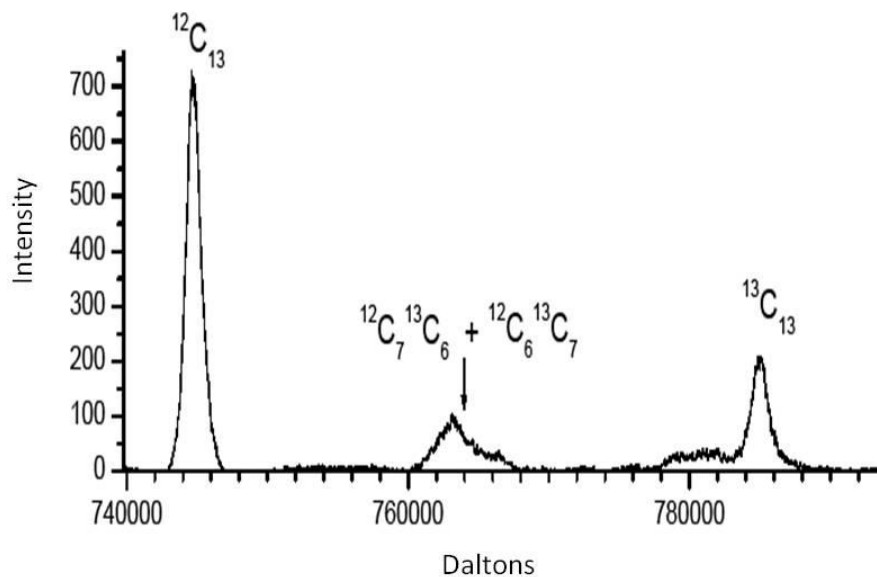
Figure 47: Acetone treated mixture of wild type and isotopically labeled GroEL.

A secondary result of the ESI-MS spectra is that it eliminates concern over rogue monomers being picked up as SP by intact tetradecamers. Acetone instigates denaturation and aggregation of proteins, including GroEL given the proper conditions. Native GroEL is a scavenger for non-native proteins, and as such could very well be picking up aggregated GroEL during the acetone treatment process as discussed in the chapter introduction. Ionization energy was carefully controlled such that protein:protein interactions remained intact, including GroEL:SP interactions. No species were observed that contained subunits in addition to the anticipated fourteen of an intact GroEL.

4.3.2 The Heat and ATP Treatment Method

In 1996, Burston *et. al* reported a method that recombines two parent species to form a unique progeny containing a ring from each parent. See the chapter introduction for a more detailed explanation of the treatment method. Based on the published chromatography, some mode of mixing, either ring or subunit, was occurring. However,

the claim of ring mixing was equivocal because of poor chromatography. In the interest of using the method for future work, experiments were pursued to clarify the impact of heat and ATP on the ring and subunit organization.

Since it was discovered over the course of the acetone experiments with streptavidin columns that quantitative elution was elusive due to the incredibly tight binding between biotin and the immobilized streptavidin, no mixing experiments were performed using streptavidin columns. Instead, ESI-MS was employed to evaluate the effect of heat and ATP.

4.3.2.1 The heat treatment method results in ring exchange

Heavy and light species were combined in equal proportions and treated as described in the chapter introduction. The same ESI-MS experimental techniques used for the acetone treated samples described above were used for analysis of the heat and ATP treatment method. A peak was observed for each parent species. In addition, peaks identified as L_7H_7 species were observed containing 49% of the total area as is expected for ring exchange (Figure 48).
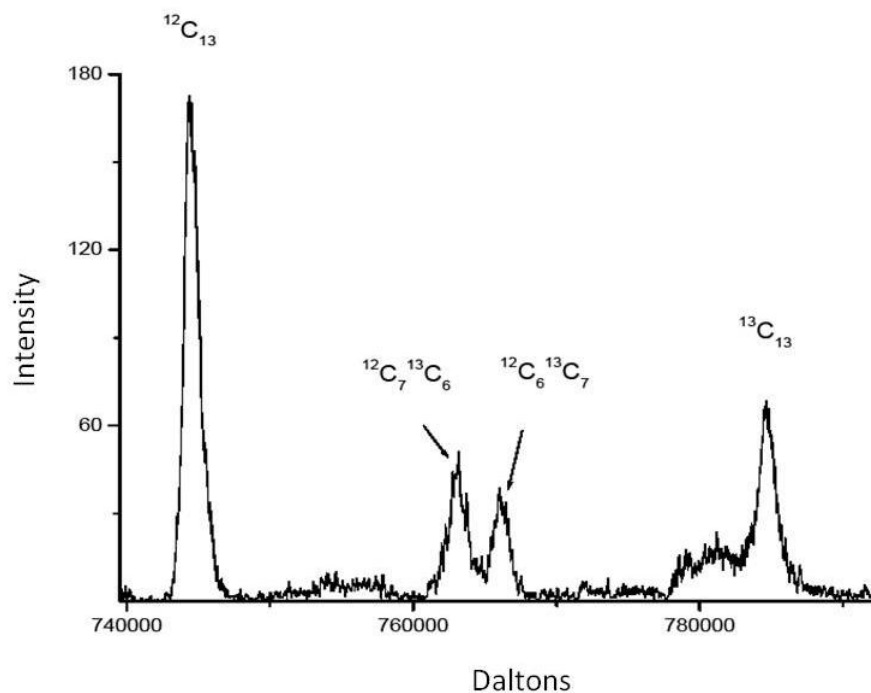
Figure 48: ESI-MS of heat treated mixture of wild type and isotopically labeled GroEL

4.4 Discussion and Conclusions

Methods for mixing subunits and rings are a boon for future work with GroEL. However, identification of reliable methods for accomplishing exchange remains a challenge. The ESI-MS results above confirm that treating GroEL with heat and ATP results in ring mixing, but a predictable method for subunit mixing remains elusive.

Although acetone treatment appeared promising, innate flaws with the method surfaced over the course of the investigation. First, protein loss clearly occurs during acetone treatment. Exposure to acetone resulted in formation of irreversible aggregates that were easily centrifuged or filtered out of solution. Moreover, acetone treating GroEL that is functionalized with hydrophobic dyes proved extremely challenging since fluorescently labeled proteins are infamous for aggregating without an added impetus.

93

The second major flaw with the acetone method is that, although subunit mixing is clearly occurring, the aggregation process takes over before the system reaches equilibrium. When treating material with 45% acetone, aggregation occurs rapidly, confirmed by visual observation of precipitate formation. The effective mixing time in this case is extremely short. Mixing time can be extended by decreasing the amount of acetone or GroEL present, but it is unclear how that impacts the efficiency of subunit exchange.

Although work with the acetone method failed to produce a useful mixing method, it was useful in confirming the efficiency of the method for preparative purposes. ESI-MS analysis demonstrated that acetone treatment produces very clean samples devoid of SP contamination. Also, fears of creating SP from GroEL monomers during the treatment process were assuaged.

Heat and ATP treatment was confirmed to be a successful method for producing exchange by ESI-MS in accordance with the predicted ring exchange model. Assuming transition to individual rings could also take place *in vivo*, it is interesting to consider what role breakdown into rings may play biologically. Might this be nature's method for circumventing the implicit negative cooperativity of the tetradecamer to mobilize a rapid chaperonin response in a cellular emergency? Since turnover of SR1 is halted in the presence of GroES, it is unclear what effect the presence of GroES would have on the dissociated rings of wild type GroEL. If there is a rapid equilibrium between rings and tetradecamer in this environment, wild-type GroEL may be able to circumvent a similar fate. Further work is necessary to assess the biological consequences of elevated temperatures and excess ATP.

Chapter 5: Exploring Aggregation GroEL using Dynamic Light Scattering

5.1 Introduction

Every protein requires a specific quaternary structure to function. When aggregation occurs, this requirement is unsatisfied, resulting in operational consequences for the cell. Aggregation is loosely defined as the association of two or more protein monomers. Here, the term monomer refers to a functional, native oligomer. (78) Protein aggregation *in vivo* has been implicated in a number diseases including Parkinson's, Huntington's, Alzheimer's, ALS, and Scrapie. (79)

Aggregation is often undesirable *in vitro* as well. Biochemists go to great lengths to prevent aggregation that may result in loss of functional protein intended for research or industrial use, but there are some situations in which aggregation is desired. Crystallographic structure determination requires aggregation to produce crystals, and precipitation is sometimes used as a first pass purification or recovery step. (80) The ability to use aggregation as a tool when desired and avoid it when undesired would be beneficial for many biological and industrial applications. Understanding the factors that promote aggregation, and the intermediates involved in aggregate formation is a necessary step in controlling the aggregation process.

Several general mechanisms have been proposed to explain the aggregation. They invoke intermediates in the form of partially or completely unfolded monomers (non-native aggregation), native monomers (native aggregation), globular spheres, or monomers with expanded volume as precursors. The presence of exposed hydrophobic regions in unfolded or non-native species usually results in a greater propensity for aggregation. (78) A reversible aggregate is one that can be recovered to form a functional native monomer, whereas the irreversible aggregates are unable to be recovered to the

functional native state. Amorphous and fibril aggregates are both insoluble and contain secondary structure. However, fibrils have long range order whereas amorphous aggregates do not.

No work has been done to examine the long term stability of GroEL at a biologically relevant temperature. In addition, GroEL presents an interesting model system for studying aggregation. For GroEL to retain function as a protein rescue machine in denaturing circumstances, it must intrinsically favor the native state and resist aggregation. As discussed in the introduction to chapter 4, GroEL forms a reversible aggregate in the presence of acetone. The acetone treatment is a reliable way of stripping the contaminated GroEL of SP since the SP forms irreversible, insoluble aggregates. Acetone, CH_3COCH_3, is the most basic ketone. It is a polar, aprotic solvent that is completely miscible with water. Physical properties of acetone are given in Table 6.

	Acetone
Dipole Moment	2.88 Debye
Boiling Point	56 °C
Dielectric Constant	20.7
Density	0.786 g/mL

Table 6: Physical properties of Acetone

The ability to control the aggregation process to optimize protein yield begins with understanding the aggregation process. In the following work, dynamic light scattering (DLS) was used to establish the long term stability of GroEL as well as to investigate the aggregation of GroEL in the presence of acetone.   Aggregation kinetics were examined while varying both acetone concentration and GroEL concentration.

5.2 Additional Methods

5.2.1 Refractometry

Input of the refractive index of the solvent is required to calculate hydrodynamic radius from the correlation functions obtained from DLS measurements Values for acetone and water mixtures were unavailable in the literature, and were instead determined experimentally using an Abbe refractometer. The temperature of the sample block was maintained at 37 °C by a circulating water bath attached to the instrument. Samples were prepared at the desired acetone to water compositions and pre-incubated at 37 °C in sealed glass sample tubes lacking headspace. Samples were dispensed onto the sample plate and measured immediately. Each acetone and water solution was measured in triplicate and the average was used for calculations.

5.2.2 Dynamic Light Scattering

Dynamic light scattering (DLS) is used to determine the size of suspended particles, and is highly applicable to the study of proteins. (81) DLS measurements to investigate the size distribution of GroEL in a variety of environments were performed in collaboration with Kirt Linegar the Anisimov laboratory of the University of Maryland using a custom-made PhotoCor spectrometer equipped with a 633 nm 10 mW laser as the incident light source. (82) The instrument was equipped with dual Hamamatsu photomultipliers for cross-correlations of two separate signals to increase precision and eliminate afterpulses.   The correlation functions were acquired with a universal PhotoCor-FC correlator with an ALV-5000/E correlator.

To reduce background noise caused by stray light, the sample cell was immerged in decaline which shares the same refractive index as the glass sample cell. Additionally, all sample buffers were filtered using a 0.2 μm filter. An electronic thermostat was used to maintain the sample cell to within ±0.1°C of the desired temperature. Analysis of the correlation functions was performed using both ALV-5000 and DynaLS (Alango/PhotoCor) software.

Correlation functions are defined as $g_2 t - 1 = Ae^{(2\Gamma t)}$, where A is the amplitude, t is time, and Γ is the relaxation rate defined as $\frac{1}{\tau}$. The relaxation time probability distribution function and particle size distribution were calculated using the proprietary NTSVD algorithm of DynaLS (Alango, Israel). Additionally, particle size was calculated by fitting the correlation functions to single exponential decays. Particle size can be calculated using the Stokes-Einstein equation, $D = \frac{k_B T}{6\pi\eta R_h}$, where D is the diffusion coefficient, k_B is Boltzman's constant, T is temperature, η is the shear velocity of the solvent, and R_h is the hydrodynamic radius of the particle.

5.3 Results

5.3.1 The long term stability of GroEL

DLS was used as an alternative method to examine the dynamics of GroEL with exposure to acetone. Because acetone treated samples were observed over long times, the stability of GroEL in buffer in the absence of acetone was tested. A solution of 3.5 μM GroEL in the presence of 10 mM Tris pH 7.5 and 10 mM $MgCl_2$ was continually incubated at 37 °C. The correlation function was measured daily, for 30 days. Dynamic

correlation functions of GroEL in sterile buffer solutions as well as fits to single exponentials on the first and thirtieth days are shown in Figure 49.

5.3.2 Finding the hydrodynamic radius of GroEL and approximating the hydrodynamic radius of substituent particles

An R_h of 9.4±0.1 nm was consistently obtained from the first to the final day of these measurements with no broadening or distortion of the size distribution of the tetradecamer, and without the appearance of additional scatters, as exemplified by the correlation functions given in Figure 49 (a and b).

In addition to determining the R_h of native GroEL, measurements of two additional proteins were made that correspond to substructures of GroEL. Those include SR1, and Bovine Serum Albumin (BSA) which approximates the size of a GroEL monomer. Measurements were made at 22 °C and 37 °C in 10 mM Tris pH 7.5, 10 mM MgOAc buffer. Again, the correlation functions fit well to a single exponential. The R_h of SR1 and BSA are 6.8 nm and 4.1 nm, respectively (Figure 49c and d). The difference between the radii of GroEL measured at 22 °C and 37 °C, 9.5 nm and 9.4 nm respectively, are within the error of the analysis.
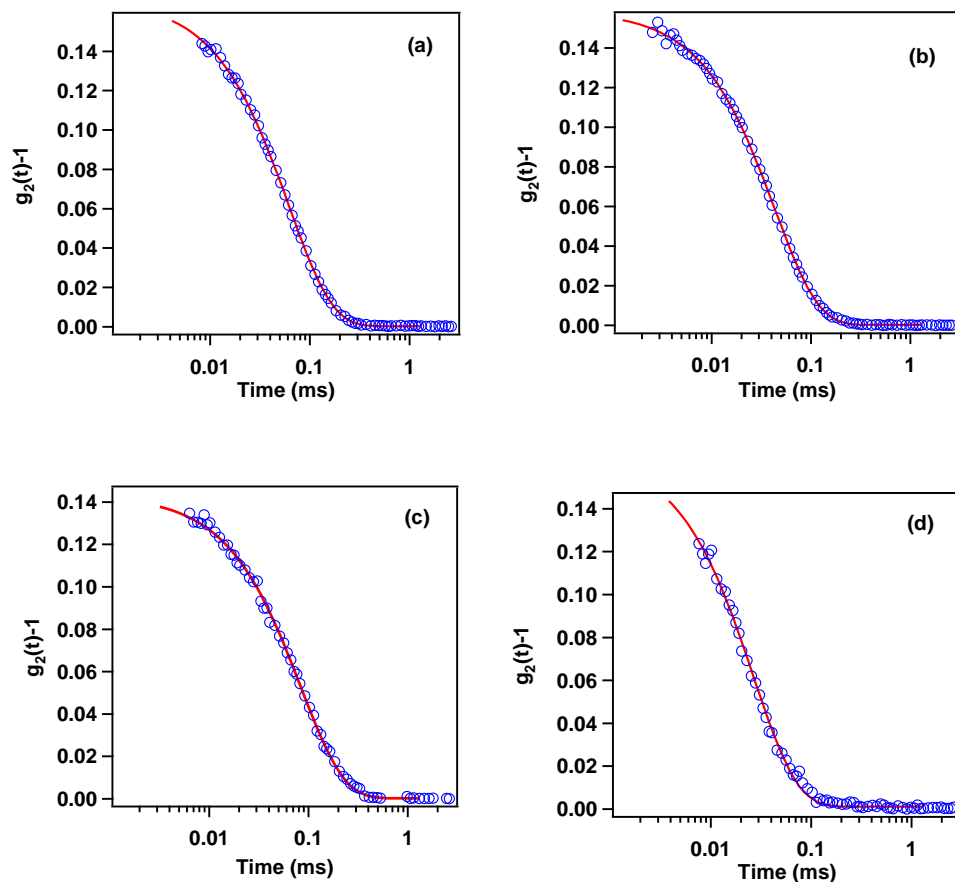
Figure 49: Correlation functions fitted to a single exponential. (a) and (b) are correlation functions for wild-type GroEL incubated at 37°C on days 1 and 30 respectively. (c) and (d) are correlation functions of SR1 and BSA respectively measured at 22°C. Blue open circles are the experimental data points, and the red line is the fit to single exponential.

5.3.3 Aggregation kinetics

Addition of acetone to an aqueous GroEL solution at concentrations as low as 5% (v/v) almost immediately results in the formation of relatively stable colloid-size aggregates of ~100-200 nm as well as an increase in the intensity of scattered light and larger standard deviation of the R_h of the tetradecamer. By calculating the volume of a large order spherical aggregate with a hydrodynamic radius of 100 nm, the number of GroEL tetradecamers needed to form the aggregate can be approximated. Assuming the measured R_h of 9.4nm, 1204 GroEL tetradecamer spheres are needed to form the large

order aggregate. The aggregates coexist with the "basic" aggregates of about 10 nm size. The presence of the intermediate colloid-size aggregates persists and dominates the scattering even over several days of continued measurement. Irreversible super-aggregates (>10 micron) are formed in the presence of 15% (v/v) acetone or more. These aggregates remain detectable after many hours of incubation in the absence of stirring.

Figure 50 demonstrates the evolution of the size distribution for 3.5 μM GroEL in the presence of 20% (v/v) acetone. The relative height of the distribution columns characterize the contribution of different sizes into the intensity of light scattering. After one hour of incubation, intermediate aggregates of ∼150 nm are formed at the expense of the initial "basic" aggregates. Hence the relative contribution of the "basic" aggregates to the light-scattering intensity becomes negligible. Intermediate aggregates persist in solution even after 16 hours.

The dominance of the intermediate aggregates in this solution coincides with the maximum slope (inflection point) in the light scattering intensity as a function of incubation time at 50 min. (Figure 51). The onset of super-aggregates and visible precipitation coincides with the intensity maximum about one hour after the start of the measurement. With further precipitation of GroEL, the solution becomes much more dilute and scatters light very poorly.
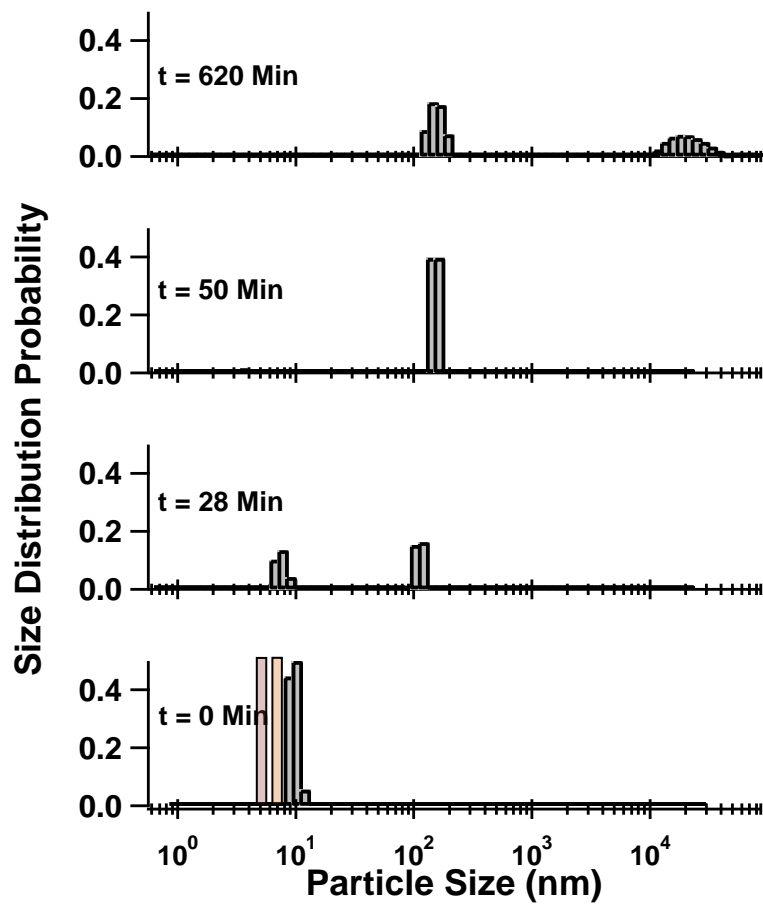
Figure 50: Probability distribution histogram for 3.5 μM GroEL in 20% acetone at 37°C for 620 minutes in the absence of stirring. Stable intermediate aggregates of 100 nm R_h are present for long times before the appearance of irreversible aggregates. For comparison, bars showing the position of BSA (red) and SR1 (orange) were added to the 0 minute trace.
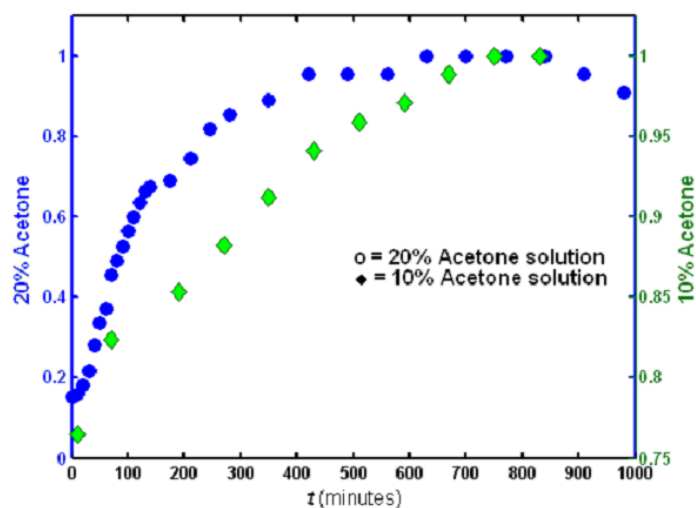
Figure 51: Increasing light scattering intensity over time in the presence of acetone: 20% v/v acetone (blue circles) and 10% v/v acetone (green triangles) Used with permission from Kirtland Linegar. (82)

For 10% (v/v) acetone the intensity of light scattering as a function of time is quite different. While the time required to reach maximum light-scattering intensity is not much different for both acetone concentrations, as long as the initial concentration of GroEL is the same, the 20% acetone sample exhibits a five-fold increase in scattering intensity compared with a 30% increase for the 10% acetone over the course of the measurements. Because the formation of super-aggregates was not observed in the 10% acetone sample, this moderate increase in the scattering intensity is attributable to the formation of kinetically stable colloid-size aggregates which coexist in considerable number with the initial "basic" GroEL particles of about 10 nm radius.

5.3.4 The effect of protein concentration on the rate of aggregate formation

The aggregation process of GroEL is controlled not only by the amount of acetone present, but also the amount of protein in the sample. Although fewer data points are available for the 1.5 μM solution due to the extremely slow kinetics of the sample, the

104

data show the intensity in the 1.5 µM sample requires approximately ten-fold longer time to reach the maximum light scattering intensity when compared to the 3.5 µM sample (Figure 52). This suggests the aggregation rate of GroEL in an acetone-water system is controlled by the ability of a protein to diffuse and interact with other protein molecules in the sample.
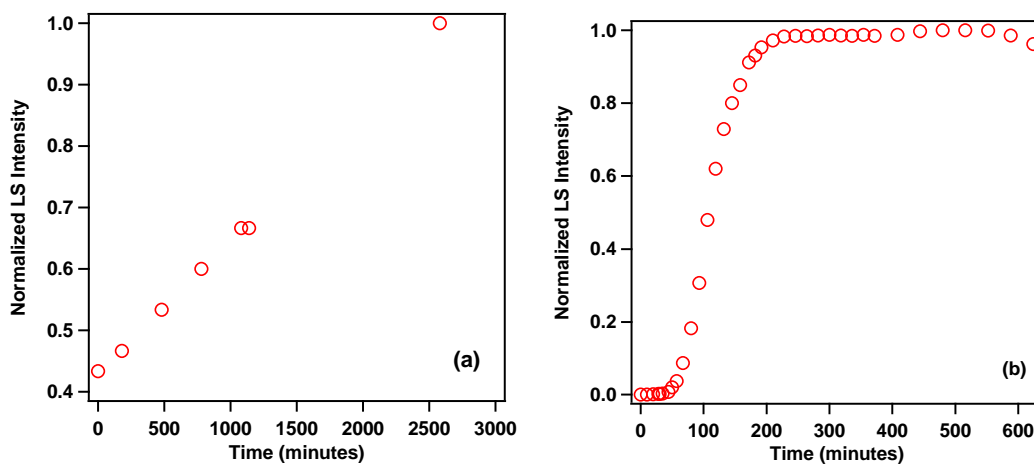
Figure 52: Normalized scattering intensity of 20%(v/v) acetone solution with (a) 1.5 µM and (b) 3.5µM GroEL.

Determining the average GroEL tetradecamer particle size in the presence of acetone rapidly becomes a challenge because the high intensity scattering of the immediately appearing larger aggregates convolutes the correlation function such that the lower intensity scattering contribution of the smaller particles cannot be accurately determined from the single exponential fit. Because of this, it was not possible to reliably determine if unfolding or dissociation of the tetradecamer was contributing to the aggregation.

5.4 Discussion and Conclusions

The DLS studies presented above underline the extraordinary stability of GroEL. First, the hydrodynamic radius of GroEL remains unchanged for over 30 days of incubation at 37 °C in a sterile, buffered solution. The complete lack of aggregation after such a long incubation period, made clear by comparison of the correlation functions on day 0 and day 30, is remarkable. If the same stability is present *in vivo*, the chaperonin clearly has a low aggregation propensity that may benefit the interception of denatured proteins in stressed cells.

Protein aggregation in acetone is a complex process as exemplified by the DLS data presented above. The rate of aggregation is modulated by both the concentration of acetone and the concentration of GroEL. By increasing the protein concentration from 1.5μM to 3.5μM, the time required to reach half of the maximal light scattering intensity was increase 15 times.

Adjusting the acetone concentration had a slightly different effect. At both 10% and 20% acetone, the light scattering intensity reached a maximum at about the same incubation time, but the rate at which the maximum scattering intensity was reached varied between the two sample conditions. At 20% acetone, the signal at time zero already had significant aggregation present demonstrated by the light scattering intensity, however when exposed to 10% acetone, the aggregation increased slowly over the course of the measurement.

Perhaps the most interesting observation from this work was the partitioning of unique aggregate sizes over an extended observation time of 620 minutes. The fact that

colloidal sized aggregates remain in solution over hours of observation before macromolecular aggregates appear and precipitate is remarkable. A similar tendency to partition into larger sizes was observed in studies of tobacco mosaic virus, however, the observation time required before the material precipitated from solution was significantly less than for GroEL. (81)

Chapter 6: Summary and Concluding Remarks

At ~800 KDa, GroEL is a massive protein, with dual seven fold symmetry, and a propensity for binding to denatured proteins. Nevertheless, it has been useful as a model protein in exploring allostery and protein folding for many experimentalists and theoreticians. This dissertation explored three areas pertinent to our expanding knowledge of GroEL, as outlined below.

6.1 The trans ring must access the T state to discharge GroES from the cis ring

It was previously suggested that the addition of SP facilitates turnover of the ring by stabilizing the *trans* ring in the **T** state, and that this stabilization is required to facilitate release of ligands from the opposing ring, however further work was needed (30). We addressed this hypothesis by creating $GroEL_{D83A}$ to remove the **T**-state-stabilizing inter-domain salt-bridge. Recall that the rigid-body movement of the apical domain in the **R** state forces the salt-bridge to break as the residues move apart.

The ATPase activity of $GroEL_{D83A}$ is diminished and exhibits reduced sigmoidocity of the first transition compared to wild-type at all ATP concentrations, in the presence of both 100mM K^+ and 1mM K^+, demonstrating the essential nature of the stabilizing salt-bridge to the continuation of the GroEL cycle. Addition of GroES almost halted turnover of the destabilized mutant, but the presence of SP rejuvenated turnover. SP functions as a stabilizing entity in lieu of the salt-bridge shifting the equilibrium of the *trans* ring toward the **T** state and permitting more rapid discharge of GroES, SP, and ADP from the *cis* ring. Taken together, with the GroES discharge experiments contrasting a forced **T** state *trans* ring versus the destabilized **T** state *trans* ring, we conclude a stable *trans* ring is a necessary step in the GroEL cycle.

6.2 Creating Mutant GroEL Assemblies with Subunit and Ring Recombination Techniques

GroEL is composed of two rings, each of seven sequence identical subunits. Identifying a reliable method to recombine rings or subunits opens up many experimental opportunities to further investigate the negative cooperativity between rings. ESI-MS was used to analyze isotopically labeled GroEL and wild-type GroEL combinations that were treated with either acetone or with incubation at 42°C in the presence of 5mM ATP.

Acetone treatment causes one-in-one-out subunit exchange, however the competing aggregation process prevents the mixing of subunits to reach equilibrium limiting the effectiveness of this method for experimental purposes. Treatment with heat and ATP results recombination of rings in a 1:2:1 ratio. Further work to find a method of subunit recombination is necessary for further study of the allostery of individual rings. Possible modes of recombination to investigate include urea and acid denaturation.

6.3 Aggregation and Stability of GroEL

Stripping the tetradecamer of contaminating substrate protein is an essential step in the purification process, since the presence of SP greatly accelerates the release of GroES. However, a significant volume of the experimental literature were performed using GroEL that was not acetone treated meaning kinetic data gleaned from the experiments are useless. Before now, it was only clear that aggregation played some role in the acetone treatment, and after the treatment, only 10% of the rings or less remained contaminated with SP. Acetone induced aggregation and stability of GroEL were investigated by HPLC and DLS.

It was determined that GroEL is extraordinarily stable maintaining a constant hydrodynamic radius of 9.5nm ±0.3nm for over thirty days at biological temperature. In addition, the population is strikingly homogeneous. Such stability is extremely helpful for the experimentalist, simplifying protein purification and handling, as well as experimental setup.

GroEL is somewhat resistant to macroscopic aggregation induced by acetone. Gel filtration chromatography showed a broadening of the GroEL peak, a shift to longer retention times, and a loss of peak area. These observations are the hallmark of a protein in rapid equilibrium with smaller protein components. This observation inspired further work attempting to recombine unique GroEL species to form mutant assemblies composed of differing rings or subunits as described in chapter 4 and summarized above in section 6.2. The significant loss of peak area only at 30% (v/v) acetone and above demonstrates that the tetradecamer of GroEL is surprisingly resilient during exposure to large volumes of acetone.

DLS experiments showed small order aggregates with R_h=100nm remained in solution for over 650 minutes in the presence of 1.5μM GroEL and 20% (v/v) acetone before the light scattering signal was dominated by macroscopic aggregates. The rate of aggregation was shown to be dependent upon both protein concentration and acetone concentration. This stability and resistance to aggregation underlines the essential role of the chaperonin in rescuing compromised proteins (SP).

Appendix to Materials and Methods

Purification of GroEL

Typically, a fresh transformation of *E. coli* JM105 cells containing the pGEL1 plasmid DNA of interest was plated overnight on an LB-ampicilin medium. A starter culture was grown at 37°C while shaking at 200 revolutions per minute (rpm) in the presence of ampicilin until visibly cloudy, at which point, 100 µL of the starter culture was inoculated into each of four 1.5 liter LB-ampicilin cultures contained in 4 liter flasks. The 1.5 liter cultures were grown at 37°C shaking at 225 rpm until an optical density at 600 nm (OD_{600}) of 0.7 was reached. The cells were induced with 1.5mL of 1M IPTG and allowed to grow overnight at 30°C shaking at 225 rpm.

The cells were harvested by centrifugation at 10,000 relative centrifugal force (RCF) for 15 minutes, then resuspended in a buffer containing 50mM Tris pH 8, 1mM EDTA, 1mM DTT, and 2 'Complete Protease Inhibitor' tablets purchased from Roche. In this and all subsequent steps, 10mM DTT was used for any cysteine mutants. The cells were lysed by sonication, and contaminating cell matter was removed by centrifugation at 32,500 RCF for 15 minutes. The resulting supernatant was decanted and treated drop-wise with Streptomycin Sulfate then incubated in its presence for 10 minutes to remove nucleotide contamination. Precipitated nucleotide was remove by centrifugation at 32,000 RCF for 35 minutes

The DEAE resin packed XK26/40 column was charged with a solution of 200mM Tris pH8 followed by equilibration with buffer containing 50mM Tris pH 8, 5mM MgCl2, 1mM EDTA, and 1mM DTT. The post-streptomycin sulfate material was

filtered with 0.45μm syringe filters and loaded on the DEAE column. Flow through was collected. Protein was eluted with a linear gradient over a volume of two liters against buffer containing 50mM Tris pH 8, 5mM MgCl2, 1mM EDTA, 1mM DTT, and 1M NaCl. Fractions containing GroEL were identified by SDS-PAGE, pooled and brought to 65% ammonium sulfate.

The ammonium sulfate treated protein was allowed to precipitate for at least 30 minutes, and then was collected by centrifugation at 10,000 RCF for 30 minutes. The supernatant was decanted and the tube wiped with a moistened cotton swab to remove residual ammonium sulfate. After redissolving the precipitate in a buffer of 50mM Tris pH 7.5 and 10mM $MgCl_2$ it was desalted on an XK26/40 column packed with S-300 resin equilibrated in the same buffer. Fractions containing EL were identified by SDS-PAGE and pooled. Pooled fractions were concentrated to between 5 mg/mL and 10 mg/mL in preparation for removal of contaminating substrate protein by acetone treatment previously described. (83)

Acetone was added to the concentrated protein solution to bring it to 45% (v/v) while rapidly stirring in a glass centrifuge tube. The material was allowed to incubate in the presence of the acetone for 10 minutes at room temperature followed by centrifugation at 10,000 RCF for 10 minutes. The acetone supernatant was discarded, and a very gentle stream of nitrogen was blown down the side of the tube to help remove residual. A buffer of 10 mM Tris pH 7.5, 10 mM $MgCl_2$, and 2 mM DTT was used to resuspend the GroEL and the contaminants. Once fully resuspended, the cloudy solution was again centrifuged as above. This time, the contaminating proteins remain insoluble while GroEL is recovered in the supernatant. The supernatant was decanted and filtered with a

0.22 µm filter, then concentrated to about 1000 µM monomers. Residual acetone was

removed by PD-10 equilibrated with 10mM Tris pH 7.5, 10mM $MgCl_2$ storage buffer.

At this point, the material was quick frozen in a bath of methanol and dry ice, followed

by storage at -80°C for further use.

Purification of GroES

pGES1 plasmids encoding the GroES of interest were transformed into BL21

competent cells, plated on an LB-ampicilin plate, and grown overnight at 37°C. A starter

culture was prepared from a single colony inoculated into 20 mL of LB-apicilin broth and

grown until cloudy at 37°C shaking at 200 rpm. A total of 4.5 L of LB broth was

inoculated with the starter culture in the presence of ampicilin. The cells were grown at

37°C until they reached an OD_{600} between 0.6 and 0.8. The cultures were inoculated

with 1.5mM of 1M IPTG and grown overnight shaking at 225 rpm and 30°C. The cells

were harvested by centrifugation at 10,000 RCF, and cells were lysed by sonication in a

buffer containing 10 mM Tris pH 7.5, 0.1 mM EDTA, 0.1 mM DTT, and two Complete

Protease Inhibitor Cocktail tablets (Roche). Cellular debris was removed by

centrifugation and DNA was precipitated by treating the supernatant with streptomycin

sulfate followed by centrifugation as described for GroEL. Using an 80°C water bath,

the lysate was brought to 70°C with constant stirring, and was maintained at that

temperature for 10 minutes to denature and aggregate contaminating protein.

Centrifugation removed the denatured material. The supernatant was precipitated with

65% (v/v) saturated ammonium sulfate. After centrifugation the precipitate was

resuspended in 10 mM Tris pH 7.5, 0.1 mM EDTA and 0.1 mM DTT. The supernatant

was then loaded onto a G25 resin packed XK16/40 column and desalted with a buffer of

10 mM Tris pH 7.5, 0.1 mM EDTA and 0.1 mM DTT. The eluent from the G25 column was brought to ~pH 5 by rapid addition of approximately 80 mL of 50 mM sodium acetate (NaOAc) while rapidly stirring. This material was loaded onto an SP Sepharose HP packed XK 16/20 column (Buffer A: 50mM NaOAc pH 5, 0.1 mM EDTA, 0.1 mM DTT; Buffer B: 50 mM NaOAc pH 5, 0.1 mM EDTA, 0.1 mM DTT, 1 M NaCl) and separated with a gradient of 0% to 20% buffer B over 700mL.   Fractions containing GroES were identified by SDS-PAGE and pooled. The pooled volume was precipitated with 65% (v/v) saturated ammonium sulfate. The precipitate was isolated by centrifugation and resuspended in 10 mM Tris pH 7.5, 10 mM MgCl$_2$. The material was concentrated and run through a PD-10 column to remove traces of ammonium sulfate. If necessary, the material was concentrated to 500 µM using a centrifugal filter with a 10 kDa cutoff. The material was then dispensed in small volumes, quick frozen, and stored at -80°C until further use.

Mutagenesis

Briefly, sense and nonsense primers were designed with melting temperatures of greater than 78°C that contain the mutation of interest as well as a restriction site change whenever possible using the QuikChange[®] Primer Design Program available at www.stratagene.com. All primer sequences used were confirmed to lack formation of secondary structure using the same program. Polymerase chain reaction (PCR) was used to create plasmid DNA containing the mutation of interest by setting up reactions containing 5µL reaction buffer provided with the kit, 125 ng of each of the sense and nonsense primers, 1µL dNTP mixture, 30 ng of the parent plasmid DNA, and 1µL of *Pfu* Turbo DNA polymerase. All mutagenesis reactions had a final volume of 50 µL.

Samples were treated in a thermocycler with a heated top assembly according to the parameters in Table 7. If necessary, the extension time and number of cycles were optimized for particular mutants. Parent DNA was digested by mixing 1μL of *Dpn* I with the reaction mixture, and incubating at 37°C for 1 hour. Transformation of BL21 cells with the resultant mutant DNA proceeded as outlined in the section below on transformation.

Program Segment	Number of Cycles	Temperature	Time
1	1	95°C	30 seconds
2	17	95°C	30 seconds
		55°C	1 minute
		68°C	17 minutes
3	1	4°C	>2 minutes

Table 7: Standard thermocycler program for PCR mutagenesis of GroEL and GroES.

Transformation and Harvesting of Mutant DNA

Useful amounts of mutant plasmid DNA were obtained by inoculating a single colony of the transformed cells into LB-ampicilin broth and growing overnight at 37°C with shaking at 200 rpm. The cells were harvested and treated according the QIAfilter Midiprep (or Miniprep when appropriate) Plasmid Purification Kit (Qiagen) with the provided buffers according to the purification protocol outlined by the company without modifications. The kit works by alkaline chemical lysis of the cells, removal of contaminating cellular material by filtration, followed by binding and elution of plasmid DNA from an anion exchange resin using low salt and low pH conditions. If needed, the DNA can be concentrated with an ethanol or isopropyl alcohol precipitation step followed by suspension in autoclaved ddH$_2$O. Efficacy of mutagenesis was confirmed first by agarose gel of the isolated plasmid digested with the appropriate restriction

enzyme that was either added or removed from the plasmid during primer design. After observing the expected band pattern on the agarose gel, the mutant plasmid was sent to the University of Maryland Center for Biosystems Research DNA Sequencing Facility for sequencing.

References

1.   LORIMER, G. H., BALDWIN, T.O. (ED) (1998) *MOLECULAR CHAPERONES*, VOL. 290, ACADEMIC PRESS, NEW YORK

2.   HORWICH, A. L., FENTON, W. A., CHAPMAN, E., AND FARR, G. W. (2007) TWO FAMILIES OF CHAPERONIN: PHYSIOLOGY AND MECHANISM. *ANNUAL REVIEW OF CELL AND DEVELOPMENTAL BIOLOGY* **23**, 115-145

3.   FENTON, W. A., KASHI, Y., FURTAK, K., AND HORWICH, A.L. (1994) RESIDUES IN CHAPERONIN GROEL REQUIRED FOR POLYPEPTIDE BINDING AND RELEASE. *NATURE* **371**, 614-619

4.   WANG, J., BOISVERT, D.C. (2003) STRUCTURAL BASIS FOR GROEL-ASSISTED PROTEIN FOLDING FROM THE CRYSTAL STRUCTURE OF (GROEL-KMGATP)14 AT 2.0A RESOLUTION. *J. MOL. BIOL* **327**, 843-855

5.   MURZIN, A., BRENNER, S.E., HUBBARD, T.J.P., AND CHOTHIA, C. (1995) SCOP: A STRUCTURAL CLASSIFICATION OF PROTEINS DATABASE FOR INVESTIGATION OF SEQUENCES AND STRUCTURES. *JOURNAL OF MOLECULAR BIOLOGY* **247**, 536-540

6.   BROCCHIERI, L., AND KARLIN, S. (2000) CONSERVATION AMONG HSP60 SEQUENCES IN RELATION TO STRUCTURE, FUNCTION, AND EVOLUTION. *PROTEIN SCI* **9**, 476-486

7.   FEI, X., YANG, D., LARONDE-LEBLANC, N., AND LORIMER, G. H. (2013) CRYSTAL STRUCTURE OF A GROEL-ADP COMPLEX IN THE RELAXED ALLOSTERIC STATE AT 2.7 Å RESOLUTION. *PROCEEDINGS OF THE NATIONAL ACADEMY OF SCIENCES* **110**, E2958-E2966

8.   ROSEMAN, A. M., RANSON, N.A., GOWAN, B., FULLER, S.D., SABIL, H. (2001) STRUCTURES OF UNLIGANDED AND ATP-BOUND STATES OF THE ESCHERICHIA COLI CHAPERONIN GROEL BY CRYOELECTRON MICROSCOPY. *J. STRUCT. BIOL.* **135**, 115-125

9.   XU, Z. H., HORWICH, A. L., AND SIGLER, P. B. (1997) THE CRYSTAL STRUCTURE OF THE ASYMMETRIC GROEL-GROES-(ADP)(7) CHAPERONIN COMPLEX. *NATURE* **388**, 741-750

10.   HUNT, L. F., WEAVER, A.J., LANDRY, S.J., GIERACH, L., DEISENHOFER, J. (1996) THE CRYSTAL STRUCTURE OF THE GROES CO-CHAPERONIN AT 2.8 ⊕ RESOLUTION. *NATURE* **379**, 37-45

11.   ZONDLO, J., FISHER, K. E., LIN, Z., DUCOTE, K. R., AND EISENSTEIN, E. (1995) MONOMER-HEPTAMER EQUILIBRIUM OF THE ESCHERICHIA COLI CHAPERONIN GROES. *BIOCHEMISTRY* **34**, 10334-10339

12.   LORIMER, G. H. (1996) A QUANTITATIVE ASSESSMENT OF THE ROLE OF THE CHAPERONIN PROTEINS IN PROTEIN FOLDING IN VIVO. *FASEB J.* **10**, 5-9

13.   SHEWMAKER, F., MASKOS, K., SIMMERLING, C., AND LANDRY, S. J. (2001) THE DISORDERED MOBILE LOOP OF GROES FOLDS INTO A DEFINED BETA -HAIRPIN UPON BINDING GROEL. *J. BIOL. CHEM.* **276**, 31257-31264

14.   NOJIMA, T., MURAYAMA, S., YOSHIDA, M., AND MOTOJIMA, F. (2008) DETERMINATION OF THE NUMBER OF ACTIVE GROES SUBUNITS IN THE FUSED HEPTAMER GROES REQUIRED FOR INTERACTIONS WITH GROEL. *J. BIOL. CHEM.* **283**, 18385-18392

15.   SAIBIL, H. R., AND RANSON, N. A. (2002) THE CHAPERONIN FOLDING MACHINE. *TRENDS IN BIOCHEMICAL SCIENCES* **27**, 627-632

16.   BETANCOURT, M. R., THIRUMALAI, D. (1999) EXPLORING THE KINETIC REQUIREMENTS FOR ENHANCEMENT OF PROTEIN FOLDING RATES IN THE GROEL CAVITY. *J MOL BIOL* **287**, 627-644

17.   THIRUMALAI, D., AND LORIMER, G. H. (2001) CHAPERONIN-MEDIATED PROTEIN FOLDING. *ANNUAL REVIEW OF BIOPHYSICS AND BIOMOLECULAR STRUCTURE* **30**, 245-269

18.   MOU, J., SHENG, S., HO, R., SHAO, Z. (1996) CHAPERONINS GROEL AND GROES: VIEWS FROM ATOMIC FORCE MICROSCOPY. *BIOPHYSICAL JOURNAL* **71**, 2213-2221

19.   MACHIDA, K., KONO-OKADA, A., HONGO, K., MIZOBATA, T., AND KAWATA, Y. (2008) HYDROPHILIC RESIDUES 526KNDAAD531 IN THE FLEXIBLE C-TERMINAL REGION OF THE CHAPERONIN GROEL ARE CRITICAL FOR SUBSTRATE PROTEIN FOLDING WITHIN THE CENTRAL CAVITY. *J. BIOL. CHEM.* **283**, 6886-6896

20.   FARR, G. W., FENTON, W. A., AND HORWICH, A. L. (2007) PERTURBED ATPASE ACTIVITY AND NOT "CLOSE CONFINEMENT" OF SUBSTRATE IN THE CIS CAVITY AFFECTS RATES OF FOLDING BY TAIL-MULTIPLIED GROEL. *PROCEEDINGS OF THE NATIONAL ACADEMY OF SCIENCES* **104**, 5342-5347

21.   BEN-ZVI, A. P., AND GOLOUBINOFF, P. (2001) REVIEW: MECHANISMS OF DISAGGREGATION AND REFOLDING OF STABLE PROTEIN AGGREGATES BY MOLECULAR CHAPERONES. *JOURNAL OF STRUCTURAL BIOLOGY* **135**, 84-93

22.   ANFINSEN, C. B. (1973) PRINCIPLES THAT GOVERN THE FOLDING OF PROTEIN CHAINS. *SCIENCE* **181**, 223-230

23.   DILL, K. A., CHAN, H.S. (1997) FROM LEVINTHAL TO PATHWAYS TO FUNNELS. *NATURE STRUCTURAL BIOLOGY* **4**

24.   MURPHY, K. P., PRIVALOV, P.L., AND GILL, S.J. (1990) COMMON FEATURES OF PROTEIN FOLDING AND DISSOLUTION OF HYDROPHOBIC COMPOUNDS. *SCIENCE* **247**, 559-561

25.   PRIVALOV, P. L., TIKTOPULO, E.I., VENYAMINOV, S., GRIKO,Y., MAKHATADZE, G.I., AND KHECHINASHVILI, N.N. (1989) HEAT CAPACITY AND CONFORMATION OF PROTEINS IN THE DENATURED STATE. *J MOL BIOL* **205**, 737-750

26.   SHTILERMAN, M., LORIMER, G. H., AND WALTER ENGLANDER, S. (1999) CHAPERONIN FUNCTION: FOLDING BY FORCED UNFOLDING. *SCIENCE* **284**, 822-825

27.   RYE, H. S., BURSTON, S. G., FENTON, W. A., BEECHEM, J. M., XU, Z. H., SIGLER, P. B., AND HORWICH, A. L. (1997) DISTINCT ACTIONS OF CIS AND TRANS ATP WITHIN THE DOUBLE RING OF THE CHAPERONIN GROEL. *NATURE* **388**, 792-798

28.   BARTOLUCCIA, C., LAMBAB, D., GRAZULISC, S., MANAKOVAC, E., HEUMANND, H. (2005) CRYSTAL STRUCTURE OF WILD-TYPE CHAPERONIN GROEL *JOURNAL OF MOLECULAR BIOLOGY* **354**, 940-951

29.   SEWELL, B. T., BEST, R. B., CHEN, S., ROSEMAN, A. M., FARR, G. W., HORWICH, A. L., AND SAIBIL, H. R. (2004) A MUTANT CHAPERONIN WITH REARRANGED INTER-RING ELECTROSTATIC CONTACTS AND TEMPERATURE-SENSITIVE DISSOCIATION. *NAT STRUCT MOL BIOL* **11**, 1128-1133

30.   GRASON, J. G., J; LORIMER, G. H. (2002) SETTING THE CHAPERONIN CHRONOMETER: A TWO-STROKE, TWO-SPEED, PROTEIN MACHINE. UNIVERSITY OF MARYLAND, COLLEGE PARK

31.   VIITANEN, P. V., LUBBEN, T.H., REED, J., GOLOUBINOFF, P., O'KEEFE, D.P., AND LORIMER, G.H. (1990) CHAPERONIN-FACILITATED REFOLDING OF RIBULOSEBISPHOSPHATE

CARBOXYLATE AND ATP HYDROLYSIS BY CHAPERONIN 60 (GROEL) ARE K+ DEPENDENT. *BIOCHEMISTRY* **29**, 5665-5671

32. TODD, M. J., VIITANEN, P.V., AND LORIMER, G.H. (1993) HYDROLYSIS OF ADENOSINE 5'-TRIPHOSPHATE BY *ESCHERICHIA COLI* GROEL: EFFECTS OF GROES AND POTASSIUM ION. *BIOCHEMISTRY* **32**, 8560-8567

33. GRASON, J. P., GRESHAM, J. S., AND LORIMER, G. H. (2008) SETTING THE CHAPERONIN TIMER: A TWO-STROKE, TWO-SPEED, PROTEIN MACHINE. *PROCEEDINGS OF THE NATIONAL ACADEMY OF SCIENCES* **105**, 17339-17344

34. GRASON, J. P., GRESHAM, J. S., WIDJAJA, L., WEHRI, S. C., AND LORIMER, G. H. (2008) SETTING THE CHAPERONIN TIMER: THE EFFECTS OF K+ AND SUBSTRATE PROTEIN ON ATP HYDROLYSIS. *PROCEEDINGS OF THE NATIONAL ACADEMY OF SCIENCES* **105**, 17334-17338

35. SAMESHIMA, T., UENO, T., IIZUKA, R., ISHII, N., TERADA, N., OKABE, K., FUNATSU, T. (2009) FOOTBALL- AND BULLET-SHAPED GROEL-GROES COMPLEXES COEXIST DURING THE REACTION CYCLE. *JOURNAL OF BIOLOGICAL CHEMISTRY* **283**, 23765-23773

36. SCHMIDT, M., RUTKAT, K., RACHEL, R., PFEIFER, G., JAENICKE, R., VIITANEN, P., LORIMER, G., AND BUCHNER, J. (1994) SYMMETRIC COMPLEXES OF GROE CHAPERONINS AS PART OF THE FUNCTIONAL CYCLE. *SCIENCE* **265**, 656-659

37. KOIKE-TAKESHITA, A., YOSHIDA, M.; TAGUCHI, H. (2008) REVISITING THE GROEL-GROES REACTION CYCLE VIA THE SYMMETRIC INTERMEDIATE IMPLIED BY NOVEL ASPECTS OF THE GROEL(D398A) MUTANT. *JOURNAL OF BIOLOGICAL CHEMISTRY* **283**, 23774-23781

38. INOBE, T., TAKAHASHI, K., MAKI, K., ENOKI, S., KAMAGATA, K., KADOOKA, A., ARAI, M., AND KUWAJIMA, K. (2008) ASYMMETRY OF THE GROEL-GROES COMPLEX UNDER

PHYSIOLOGICAL CONDITIONS AS REVEALED BY SMALL-ANGLE X-RAY SCATTERING. *BIOPHYS. J.* **94**, 1392-1402

39.   TAKAGI, F., KOGA, N., AND TAKADA, S. (2003) HOW PROTEIN THERMODYNAMICS AND FOLDING MECHANISMS ARE ALTERED BY THE CHAPERONIN CAGE: MOLECULAR SIMULATIONS. *PROCEEDINGS OF THE NATIONAL ACADEMY OF SCIENCES OF THE UNITED STATES OF AMERICA* **100**, 11367-11372

40.   LORIMER, G. (1997) PROTEIN FOLDING. FOLDING WITH A TWO-STROKE MOTOR. *NATURE* **388**, 720-721, 723

41.   CORSEPIUS, N. C., AND LORIMER, G. H. (2013) MEASURING HOW MUCH WORK THE CHAPERONE GROEL

CAN DO. *PROCEEDINGS OF THE NATIONAL ACADEMY OF SCIENCES*

42.   TAGUCHI, H., UENO, T., TADAKUMA, H., YOSHIDA, M., AND FUNATSU, T. (2001) SINGLE-MOLECULE OBSERVATION OF PROTEIN-PROTEIN INTERACTIONS IN THE CHAPERONIN SYSTEM. *NATURE BIOTECHNOLOGY* **19**, 861-865

43.   UENO, T., TAGUCHI, H., TADAKUMA, H., YOSHIDA, M., AND FUNATSU, T. (2004) GROEL MEDIATES PROTEIN FOLDING WITH A TWO SUCCESSIVE TIMER MECHANISM. *MOLECULAR CELL* **14**, 423-434

44.   SAKIKAWA, C., TAGUCHI, H., MAKINO, Y., AND YOSHIDA, M. (1999) ON THE MAXIMUM SIZE OF PROTEINS TO STAY AND FOLD IN THE CAVITY OF GROEL UNDERNEATH GROES. *JOURNAL OF BIOLOGICAL CHEMISTRY* **274**, 21251-21256

45.   CHEN, D.-H., SONG, J.-L., CHUANG, D. T., CHIU, W., AND LUDTKE, S., J. (2006) AN EXPANDED CONFORMATION OF SINGLE-RING GROEL-GROES COMPLEX ENCAPUSLATES AND 86 KDA SUBSTRATE. *STRUCTURE* **14**, 1711-1722

46.   KERNER, M. J., NAYLOR, D.J., ISHIHAMA, Y., MAIER, T., CHANG, H., STINES, A.,
GEORGOPOULOS, C., FRISHMAN, D., HAYER-HARTL, M., MANN, M. (2005) PROTEOME-
WIDE ANALYSIS OF CHAPERONE-DEPENDENT PROTEIN FOLDING IN *ESCHERICHIA COLI*. *CELL*
122, 209-220

47.   VIITANEN, P. V., DONALDSON, G. K., LORIMER, G. H., LUBBEN, T. H., AND GATENBY, A. A.
(1991) COMPLEX INTERACTIONS BETWEEN THE CHAPERONIN 60 MOLECULAR CHAPERONE
AND DIHYDROFOLATE REDUCTASE. *BIOCHEMISTRY* **30**, 9716-9723

48.   WANG, Z., FENG, H.P., LANDRY, S. J., MAXWELL, J., GIERASCH, L. M. (1999) BASIS OF
SUBSTRATE BINDING BY THE CHAPERONIN GROEL. *BIOCHEMISTRY* **38**, 12537-12546

49.   PARENT, K. N., AND TESCHKE, C. M. (2007) GROEL/S SUBSTRATE SPECIFICITY BASED ON
SUBSTRATE UNFOLDING PROPENSITY. *CELL STRESS & CHAPERONES* **12**, 20-32

50.   NOIVIRT-BRIK, O., UNGER, R., AND HOROVITZ, A. (2007) LOW FOLDING PROPENSITY AND
HIGH TRANSLATION EFFICIENCY DISTINGUISH IN VIVO SUBSTRATES OF GROEL FROM OTHER
ESCHERICHIA COLI PROTEINS. *BIOINFORMATICS* **23**, 3276-3279

51.   AOKI, K., MOTOJIMA, F., TAGUCHI, H., YOMO, T., YOSHIDA, M. (2000) GROEL BINDS
ARTIFICIAL PROTEINS WITH RANDOM SEQUENCES. *J BIOL CHEM* **275**, 13755-13758

52.   STAN, G., BROOKS, B. R., LORIMER, G. H., AND THIRUMALAI, D. (2005) IDENTIFYING
NATURAL SUBSTRATES FOR CHAPERONINS USING A SEQUENCE-BASED APPROACH. *PROTEIN
SCI* **14**, 193-201

53.   STAN, G., BROOKS, B. R., LORIMER, G. H., AND THIRUMALAI, D. (2006) RESIDUES IN
SUBSTRATE PROTEINS THAT INTERACT WITH GROEL IN THE CAPTURE PROCESS ARE BURIED
IN THE NATIVE STATE. *PROCEEDINGS OF THE NATIONAL ACADEMY OF SCIENCES OF THE
UNITED STATES OF AMERICA* **103**, 4433-4438

54. YIFRACH, O., AND HOROVITZ, A. (1995) NESTED COOPERATIVITY IN THE ATPASE

    ACTIVITY OF THE OLIGOMERIC CHAPERONIN GROEL. *BIOCHEMISTRY* **34**, 5303-5308

55. YIFRACH, O., AND HOROVITZ, A. (2000) COUPLING BETWEEN PROTEIN FOLDING AND

    ALLOSTERY IN THE GROE CHAPERONIN SYSTEM. *PROCEEDINGS OF THE NATIONAL ACADEMY*

    OF SCIENCES **97**, 1521-1524

56. GRESHAM, J. S. (2004) *ALLOSTERY AND GROEL: EXPLORING THE TENENTS OF NESTED*

    COOPERATIVITY. DOCTOR OF PHILOSOPHY, UNIVERSITY OF MARYLAND

57. CREIGHTON, T. E., AND EWBANK, J. J. (1994) DISULFIDE-REARRANGED MOLTEN

    GLOBULE STATE OF .ALPHA.-LACTALBUMIN. *BIOCHEMISTRY* **33**, 1534-1538

58. SAMBROOK, J., FRITSCH, E.F., AND MANIATIS, T. (1989) *MOLECULAR CLONING, A*

    LABORATORY MANUAL, SECOND ED., COLD HARBOR LABORATORY PRESS

59. LAEMMLI, U. K. (1970) CLEAVAGE OF PROTEINS DURING THE ASSEMBLY OF THE HEAD OF

    BACTERIOPHAGE T4. *NATURE* **227**, 680-685

60. KOSOWER, N. S., KOSOWER, E.M., WERTHEIM, B., CORREA, W.S. (1969) DIAMIDE, A NEW

    REAGENT FOR THE INTRACELLULAR OXIDATION OF GLUTATHIONE TO THE DISULFIDE

    BIOCHEMICAL AND BIOPHYSICAL RESEARCH COMMUNICATIONS **37**, 593-596

61. PROBES, M. (2008) THE HANDBOOK--A GUIDE TO FLUORESCENT PROBES AND LABELING

    TECHNOLOGIES. 10TH ED., INVITROGEN

62. HOROVITZ, A., FRIDMANN, Y., KAFRI, G., AND YIFRACH, O. (2001) REVIEW: ALLOSTERY IN

    CHAPERONINS. *JOURNAL OF STRUCTURAL BIOLOGY* **135**, 104-114

63. LIN, Z., AND RYE, H. S. (2006) GROEL-MEDIATED PROTEIN FOLDING: MAKING THE

    IMPOSSIBLE, POSSIBLE. *CRITICAL REVIEWS IN BIOCHEMISTRY AND MOLECULAR BIOLOGY* **41**,

    211 - 239

64. Sameshima, T., Iizuka, R., Ueno, T., and Funatsu, T. (2010) Denatured proteins facilitate the formation of the football-shaped GroEL-(GroES)$_2$ complex. *Biochem J.* **427**, 247-254

65. Sameshima, T., Ueno, T., Iizuka, R., Ishii, N., Terada, N., Okabe, K., Funatsu, T. (2008) Football-and-bullet-shaped GroEL-GroES complexes coexist during the reaction cycle. *J Biol Chem* **283**, 23765-23773

66. Murai, N., Makino, Y., and Yoshida, M. (1996) GroEL Locked in a Closed Conformation by an Interdomain Cross-link Can Bind ATP and Polypeptide but Cannot Process Further Reaction Steps. *J. Biol. Chem.* **271**, 28229-28234

67. Gutfreund, H. (1995) *Kinetics for the Life Sciences*, Press Syndicate of the University of Cambridge, New York

68. Frank, G. A., Goomanovsky, M., Davidi, A., Ziv, G., Horovitz, A., and Haran, G. (2010) Out-of-equilibrium conformational cycling of GroEL under saturating ATP concentrations. *Proc Natl Acad Sci U S A* **107**, 11793-11798

69. Chatellier, J., Hill, F., Foster, N. W., Goloubinoff, P., and Fersht, A. (2000) From minichaperone to GroEL 3: properties of an active single-ring mutant of GroEL. *J Mol Biol* **304**, 897-910

70. Farr, G. W. F., K; Rowland, M.B.; Ranson, N.A.; Sabil, H.R.; Kirchhausen, T; Horwich, A. (2000) Multivalent binding of non-native substrate proteins by the chaperonin GroEL. *Cell* **100**, 561-573

71. Gorovits, B. M. S., J.W.; Horowitz, P.M. (1995) Residual structure in urea-denatured chaperonin GroEL. *Biochemistry* **34**, 13928-13933

72. BURSTON, S. G., WEISSMAN, J. S., FARR, G. W., FENTON, W. A., AND NORWICH, A. L. (1996) RELEASE OF BOTH NATIVE AND NON-NATIVE PROTEINS FROM A CIS-ONLY GROEL TERNARY COMPLEX. *NATURE* **383**, 96-99

73. CHEN, J., AND SMITH, D. L. (2000) UNFOLDING AND DISASSEMBLY OF THE CHAPERONIN GROEL OCCURS VIA A TETRADECAMERIC INTERMEDIATE WITH A FOLDED EQUATORIAL DOMAIN. *BIOCHEMISTRY* **39**, 4250-4258

74. RYBAK, J.-N., SCHEURER, S. B., NERI, D., AND ELIA, G. (2004) PURIFICATION OF BIOTINYLATED PROTEINS ON STREPTAVIDIN RESIN: A PROTOCOL FOR QUANTITATIVE ELUTION. *PROTEOMICS* **4**, 2296-2299

75. ROBINSON, C. V. (2005) WATCHING AND WEIGHTING-CHAPERONIN COMPLEXES IN ACTION. *NATURE METHODS* **2**, 331-332

76. VAN DUIJN, E., SIMMONS, D.A., VAN DEN HEUVEL, R.H.H., BAKKES, P.J., VAN HEERIKHUIZEN, H., HEEREN, R.M.A., ROBINSON, C.V., VAN DER VIES, S.M., HECK, A.J.R. (2006) TANDEM MASS SPECTROMETRY OF INTACT GROEL-SUBSTRATE COMPLEXES REVEALS SUBSTRATE-SPECIFIC CONFORMATIONAL CHANGES IN THE TRANS RING. *JOURNAL OF THE AMERICAN CHEMICAL SOCIETY* **128**, 4694-4702

77. CATALINA, M. I., VAN DEN HEUVEL, R.H.H., VAN DUIJN, E., HECK, A.J.R. (2005) DECHARGING OF GLOBULAR PROTEINS AND PROTEIN COMPLEXES IN ELECTROSPRAY. *CHEM. EUR. J* **11**, 960-968

78. ROBERTS, C. J. (2007) NON-NATIVE PROTEIN AGGREGATION KINETICS. *BIOTECHNOLOGY AND BIOENGINEERING* **98**, 927-938

79. RIEGER, T. R., MORIMOTO, R. I., AND HATZIMANIKATIS, V. (2006) BISTABILITY EXPLAINS THRESHOLD PHENOMENA IN PROTEIN AGGREGATION BOTH IN VITRO AND IN VIVO. *BIOPHYS. J.* **90**, 886-895

80. LI, S. X., D.; LI, J. (2004) DYNANMIC LIGHT SCATTERING APPLICATION TO STUDY PROTEIN INTERACTIONS IN ELECTROLYTE SOLUTIONS. *JOURNAL OF BIOLOGICAL PHYSICS* **30**, 313-324

81. PANYUKOV, Y., YUDIN, I, DRACHEV, V, DOBROV, E, DURGANOV, B. (2007) THE STUDY OF AMORPHOUS AGGREGATION OF TOBACCO MOSAIC VIRUS COAT PROTEIN BY DYNAMIC LIGHT SCATTERING. *BIOPHYSICAL CHEMISTRY* **127**, 9-18

82. LINEGAR, K. L. (2008) *APPLICATION OF DYNAMIC LIGHT SCATTERING TO CHEMICAL AND BIOMOLECULAR ENGINEERING: POLYMERS, PROTEINS, AND LIQUID CRYSTALS.* MASTER OF SCIENCE MASTER, UNIVERSITY OF MARYLAND

83. VOZIYAN, P. A., FISHER, M. T. (2000) CHAPERONIN-ASSISTED FOLDING OF GLUTAMINE SYNTHETASE UNDER NONPERMISSIVE CONDITIONS: OFF-PATHWAY AGGREGATION PROPENSITY DOES NOT DETERMINE THE CO-CHAPERONIN REQUIREMENT. *PROTEIN SCIENCE* **9**, 2405-2412